A Novel Device for the Treatment of Obstructive Sleep Apnea

by

Qiyun Gao

B.S. Mechanical Engineering
Massachusetts Institute of Technology, 2021

SUBMITTED TO THE DEPARTMENT OF MECHANICAL ENGINEERING IN PARTIAL FULFILLMENT OF THE REQUIREMENTS FOR THE DEGREE OF

MASTER OF SCIENCE IN MECHANICAL ENGINEERING

AT THE
MASSACHUSETTS INSTITUTE OF TECHNOLOGY

JUNE 2023

Authored by: Qiyun Gao
Department of Mechanical Engineering
May 12, 2023

Certified by: Ellen T. Roche
Associate Professor of Mechanical Engineering and Institute for Medical Engineering & Science
Thesis supervisor

Accepted by: Nicolas Hadjiconstantinou
Chairman, Committee on Graduate Students

A Novel Device for the Treatment of Obstructive Sleep Apnea

by

Qiyun Gao

Submitted to The Department of Mechanical Engineering on May 16, 2023 in Partial Fulfillment of the Requirements for the Degree of Master of Science in Mechanical Engineering

ABSTRACT

In this thesis, a novel device for the treatment of Obstructive Sleep Apnea (OSA) is developed and tested. This device uses intra-oral suction to stabilize tongue and/or soft palate in a position that does not obstruct the airway, thus reduce apnea episodes. The treatment device consists of a patient-specific oral device and a non-patient-specific pump unit. Patients wear the oral device on their upper palate that directs suction towards tongue and/or soft palate. A length of tubing connects the oral device to the pump unit, which is placed bedside and is envisioned to be a wearable device in further iterations.

Experimental results from a small-scale clinical trial verified that the device performs its intended function of stabilizing the tongue, and does not cause increase in Apnea Hypopnea Index (AHI) in healthy volunteers. MRI Imaging on volunteers wearing the device proved the device does enlarge the airway by 60% - 80%. A finite element model of the tongue, soft palate and airway, with muscle fiber direction derived from Diffusion Tensor MRI, is implemented as a proof of concept that the device can treat OSA. The estimation of the level of vacuum required to stabilize the tongue by a finite element (FE) model is consistent with experimental results.

Thesis Supervisor: Ellen T. Roche

Title: Latham Family Career Development Professor

Associate Professor, Mechanical Engineering and Institute for Medical Engineering & Science, Massachusetts Institute of Technology

Acknowledgements

This research would truly not have been possible without the support, advice and inspiration that I received from numerous individuals throughout the project.

I would like to deliver special thanks to my advisor Prof. Ellen Roche for taking me into her lab; spending a great deal of time and effort supporting my research with her advice and her many resources, and ensuring my survival in graduate school.

I would like to thank Dr. Tarsha Ward and Dr. Ravi Rasalingam for keeping the project going in every aspect, helping us get funding and publicity, and provide advice from the clinical and business viewpoint. I would like to thank Prof. Jonghye Woo at MGH for letting me join his cohort, scanning our subjects and teaching me everything about the human tongue. I would like to thank Dr. Debkalpa Goswami for initially bringing me into the project when I was an undergraduate, providing guidance on how to thrive in graduate school and introducing me into the 'paper business'. I would like to thank Dr. Nevan Hanumara for leading the clinical trial and teaching me how to do clinical trial properly, for his passion in maintaining an organized lab space without bench-clutter, and his clear view on what should be done by researcher versus being outsourced.

I would like to thank my UROPs Frank Ozello, Jessica Wang and Keenan Fronhofer for building these oral devices, pump units and anything we designed with quality and on time, with special thanks to Frank for staying in lab late with me. I would like to thank previous UROPs Christina Patterson, Andre Rodriguez, Mulan Jiang, Joshen Patel, Kaleb Blake, Quentin Thernize, Roberto Bolli, Jonathan Tagoe, Andie Maloney and Alex Doran; visiting scholars David Van Story and Erwin Franz for working with me building the project step-by-step or laying groundwork before I joined. I would like to thank Catherine Ricciardi and Tatiana Urman in Clinical Research Center for keeping the clinical trial going and advising on how to get what we want while adhering to code and keeping patients safe. I would like to thank Dr. David Vaknin for teaching us how to scan patients and let us practice scanning on himself.

I would like to thank members of Roche Group (TTDD Lab) for exposing me to the world of biomechanics and medical devices. Especially Caglar and Yiling who helped me on the finite element model of bio tissue when I had zero experience modeling previously. Jonathan worked on

this project as a UROP then joined our lab, and we bang thoughts off each other. In the lab I am always able to find help when needed and do feel the community here. This is a happy place I'm staying.

I owe a lot to my family who have always supported my endeavors and have been a secure place for me to worry less about life to pursue my dreams. My family kept reassuring me "medical device is big money and is high tech" when I wanted quit until I got back together, and yes what they said is correct.

Finally, I would like to extend my special thanks to my partner Nan that I can lean on when I was going through ups and downs. She laughs at me when I demonstrated my bad mathematical skills and careless experimental design through stupid mistakes and helped with my math, statistics and data crunching. She kept my strain finite so I will always converge even under increasingly larger stress. Here this thesis is done and I'm ready for the next one.

This research was supported by Deshpande Center, MIT Catalyst, Tufts CTSI and an Acorn grant.

Contents

List of Figures

List of Tables

Nomenclature

Letters

P	Pressure
Q	Flow rate
T	Time
η	Percentage of time the treatment is successfully delivered

Abbreviations

AASM	American Academy of Sleep Medicine
AHI	Apnea Hypopnea Index
CPAP	Continuous Positive Airway Pressure
DTI	Diffusion Tensor Imaging, synonym of DT-MRI
DT-MRI	Diffusion Tensor Magnetic Resonance Imaging
HNS	Hypoglossal Nerve Stimulation
MAD	Mandibular Advancement Device
MIT	Massachusetts Institute of Technology
MRI	Magnetic Resonance Imaging
OPT	Oral Pressure Therapy
OSA	Obstructive Sleep Apnea
PM	Portable Monitor
RI	Risk Indicator
TRD	Tongue Retention Device

Glossary

Apnea	Cessation of airflow for at least 10 seconds
Hypopnea	Reduction in airflow by at least 30% for at least 10 seconds
Latched	Tongue is stabilized by the oral device in the treatment position
Unlatched	Tongue disengaged from the oral device

1 Introduction

1.1 Background and Motivation

Obstructive sleep apnea (OSA) is a chronic health condition affecting 34% of men and 17% of women in the U.S.[1]. OSA patients experience repetitive collapse of throat muscles which cause obstruction of breathing during sleep, known as apnea and hypopnea events [2]. (Figure 1-1). The most common muscle involved in the obstruction is the tongue [3]. Although treatment options currently exist to prevent these obstructions, most patients do not use them as they are painful, cumbersome and uncomfortable [4]–[8] (Figure 1-2).

Untreated OSA can lead to long term health consequences including an increase in risk of heart disease, metabolic disorders and cognitive impairment. Symptoms of OSA includes excessive daytime sleepiness, fatigue, headache and memory loss. These symptoms can lead to loss of productivity, motor vehicle accidents, and general increased risk of injury and fatality [2]. New approaches to treat OSA are therefore required.

1.2 Definition and Evaluation of Obstructive Sleep Apnea

1.2.1 Apnea, Hypopnea and Apnea Hypopnea Index

As defined by American Academy of Sleep Medicine (AASM), an apnea event is the cessation of airflow for at least 10 seconds, and a hypopnea event is the reduction in airflow by at least 30% for at least 10 seconds with decrease in oxygen saturation. The metric of severity of OSA is apnea hypopnea index (AHI), defined as the number of apnea and hypopnea events per hour of sleep. The severity of OSA is defined in Table 1-1. [9], [10]. According to the AASM clinical guideline [11], AHI is the most important deciding factor when diagnosing OSA. Treatment is prescribed if a patient has an AHI greater than 15.

Mild OSA	$5 \leq AHI < 15$
Moderate OSA	$15 \leq AHI < 30$
Severe OSA	$AHI \geq 30$

Table 1-1: AASM Definition of severity of OSA

Furthermore, AHI is the most important metric when evaluating the efficacy of OSA treatments. When continuous positive airway pressure therapy (CPAP, see Section 1.3) is prescribed, it is common that a split-night study is performed: patients have their AHI measured during the first half of the night. Then the patient is administered CPAP and have their AHI measured again to confirm the efficacy immediately [12].

1.2.2 Methods of OSA Evaluation

The current golden standard of evaluation of OSA is in-lab polysomnography (PSG) [11]. PSG records electroencephalogram (EEG), electrooculogram (EOG), chin electromyogram, airflow, oxygen saturation, respiratory effort, and electrocardiogram (ECG) or heart rate [11]. PSG data is interpreted by trained personnel according to AASM Apnea Scoring Manual [9] and the AHI is reported.

PSG is not the only option to evaluate OSA. Portable monitors (PM), also known as "Type-3 polysomnography"[13], are popular sleep study devices that are widely used for OSA screening [11] , diagnosis [14], and evaluation of efficacy of treatment devices [15], [16]. PMs have lower specificity and sensitivity than PSG since it monitors only airflow, effort and oxygen saturation [17] One study by Berry et al shows 92% sensitivity and 80% selectivity compared to PSG [18]. AASM clinical guidelines claims PMs tend to underestimate the severity of OSA [11]. These drawbacks are partially attributed to the standard data analysis algorithm that reports AHI without a doctor looking at the data [17]. Despite that, PMs can still diagnose OSA with certainty if the measured AHI is high enough [11].

1.3 Current Treatments for Obstructive Sleep Apnea

The current first-line treatment is Continuous Positive Airway Pressure (CPAP) shown in Figure 1-2a. CPAP use positive air pressure to force air through the obstruction thus improve aspiration [19]. AASM clinical guideline recommend clinicians to offer CPAP to patients first, and turn to 'alternative therapies' only if the patient declines CPAP [11]. However, it requires a tight-fitting mask, large diameter tubing and loud bedside pumps. 25-50% of patients prescribed CPAP cannot tolerate it, leading to poor compliance [4].

Mandibular Advancement Device (MAD) is another widely used treatment in addition to CPAP[8]. As shown in Figure 1-2b, it uses a hinge to advance the lower jaw forward, thus indirectly advancing the tongue and preventing it from obstructing the airway [20]. Unfortunately, this treatment is uncomfortable and has side effect of jaw problems, and approximately 45% of patients prescribed MAD cannot tolerate it [5], [8].

The Tongue Retention Device (TRD) shown in Figure 1-2c employs a bubble shaped passive suction chamber to keep the tongue protruding out of patient's mouth overnight. Approximately 50% of patients prescribed TRD cannot tolerate it [6][8].

Hypoglossal Nerve Stimulation (HNS) is a surgical option shown in Figure 1-2d, that implants electrodes to stimulate the hypoglossal nerve and keep muscles from collapsing. It is adjustable and customizable in term of stimulation. However, the device requires surgery to implant, not all patients respond, (one third of patients responded to the surgery [21], [22]) and has a strong contraindication of soft palate collapse – targeting muscle alone does not move the soft palate out of the way. Furthermore, there around one third of patients are non-responders after surgery, and there are currently no formal predictors of the success rate of the surgery [7], [23] [24].

Finally, there are Oral Pressure Therapy (OPT) devices that use intra-oral suction to keep the tongue and soft palate from obstructing the airway. There are a number of active oral devices available on market. Winx and iNAP are similar devices (as deemed by FDA [25]) that use intraoral negative pressure applied to the whole mouth to stabilize the tongue and soft palate . Figure 1-2e shows the Winx device and the location of Winx oral appliance in patient's mouth. In a sample of 337 patients from 6 studies (all sponsored by ApniCure), 79% of patient had an AHI reduction of > 50% from baseline with residual AHI < 20. 25% of patients have met the AASM definition of successful OSA treatment by having residual AHI < 10. [26]. Figure 1-2f shows the iNAP device and the location of iNAP oral appliance in patient's mouth. For the iNAP device, approximately 50% of the patient responded out of 353 patients in a hospital-sponsored study [27]. The study was conducted with their iNAP set to -150mmHg which is sufficient to cause blisters in long-term use [28].

1.4 Thesis Aims

Currently available treatments for OSA have their own drawbacks, contraindications and non-compliant patient groups. We envision that there is a niche for a comfortable, effective and personalized approach to treat obstructive sleep apnea.

In this thesis, we leverage a variety of mechanical design, electronics engineering and computational modeling methods in combination with clinical knowledge and biomechanics methods to help design, manufacture and evaluate a novel device for the treatment of obstructive sleep apnea. This device uses localized intra-oral suction applied directly to tongue and tongue only, in order to stabilize tongue in a position that does not obstruct the airway, thus reducing apnea and hypopnea events. This thesis is in pursue of the following aims:

1. Devise a protocol to reliably design and manufacture patient-specific oral devices that performs adequately for every patient we take in, with vision of automate the process in the future.
2. Design and manufacture pump units that provide configurable suction to the oral device. The pump units must have extensive datalogging capabilities to facilitate clinical trials.
3. Develop a computational model to aid in the design and optimization of oral devices.
4. Evaluate the treatment system in clinical trials with onboard datalogging, portable sleep monitors, and medical imaging for safety, comfort, mechanism and efficacy.

The work in this thesis is important in the advancement of the field of sleep medicine, biomechanics, dental appliances and medical devices. More importantly, the commercialization of the treatment system devised in this thesis will benefit millions of people suffering from untreated OSA. Everyone deserves a better night of sleep. I hope this thesis brings us one step closer.

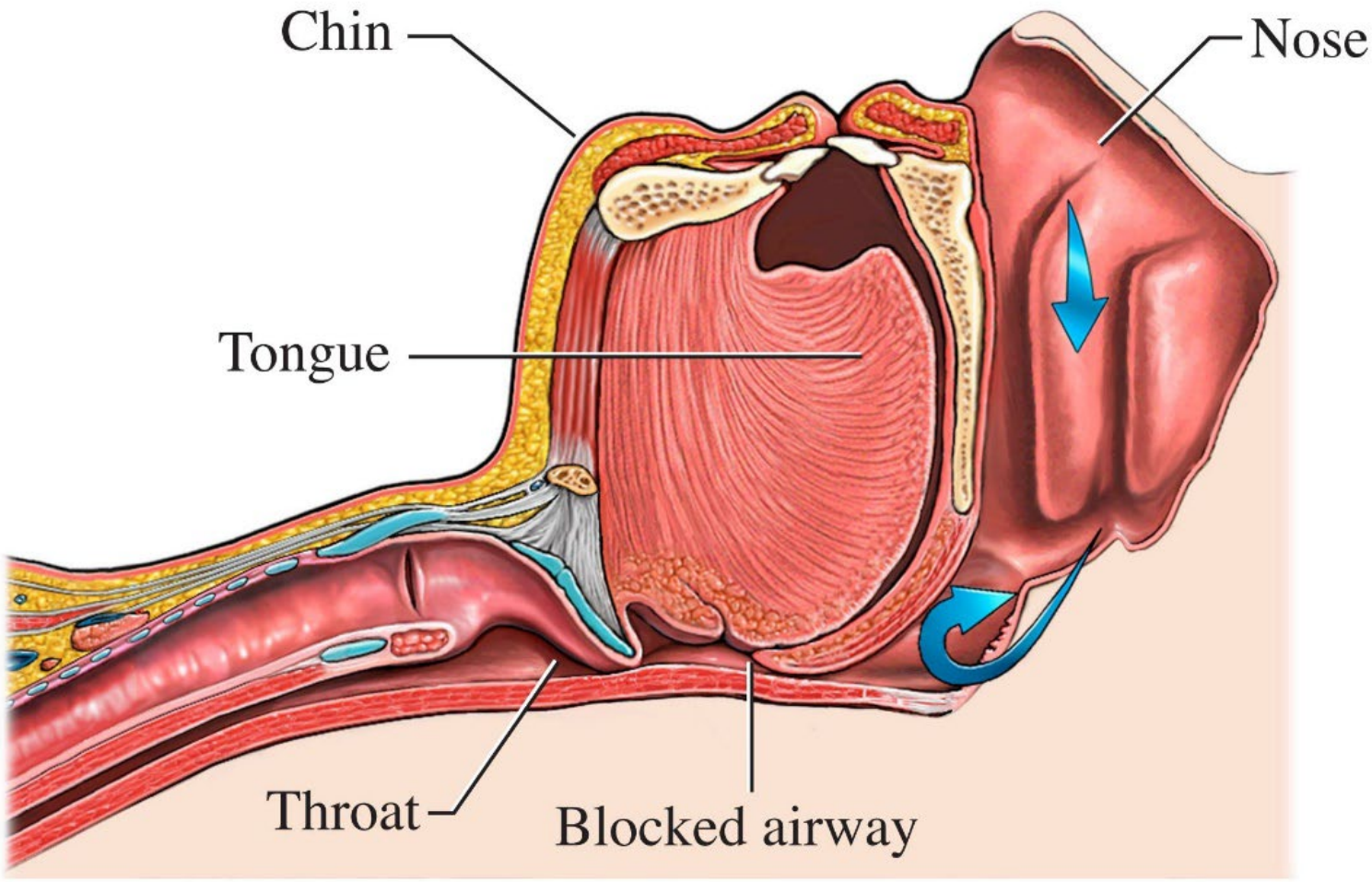

Figure 1-1: Illustration of Obstructive Sleep Apnea (OSA) [29]

(a)
Continous Positive Airway Pressure
(CPAP)

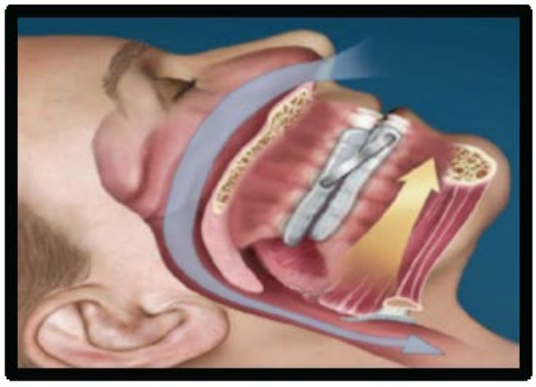

(b)
Mandibular Advancement Device
(MAD)

(c)
Tongue Retention Device
(TRD)

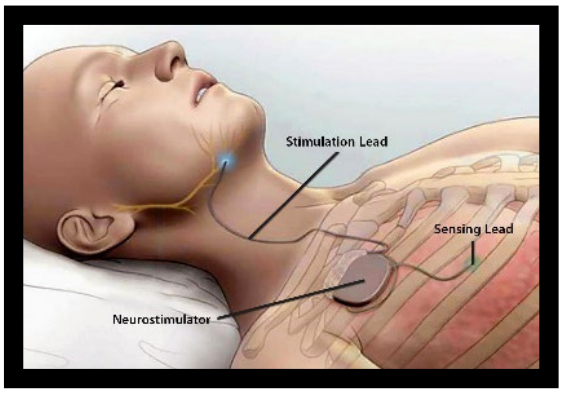

(d)
Hypoglossal Nerve Stimulation
(HNS)

Figure 1-2: Current treatment options for OSA (Continues to the next page)

(e) ApniCure Winx Sleep Therapy System

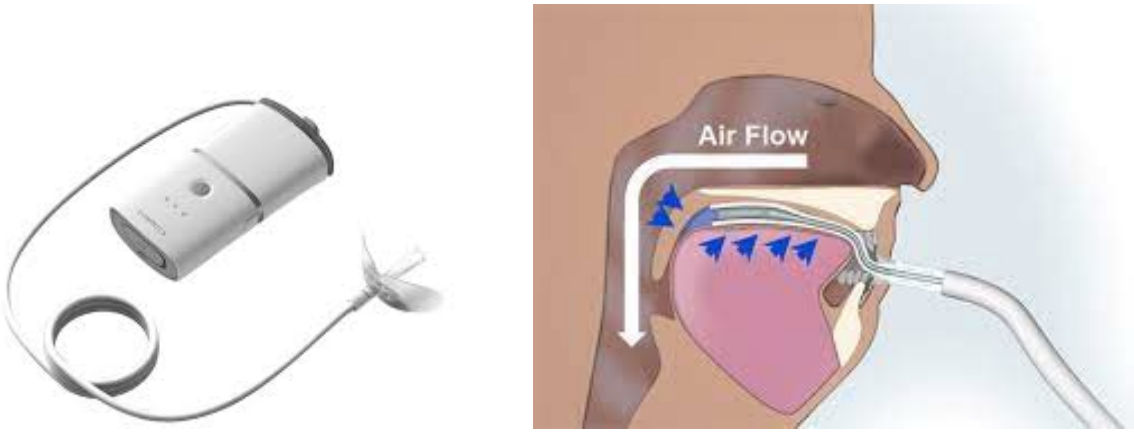

(f) iNAP Sleep Therapy System

Figure 1-2: Current treatment options for OSA

2 Device Overview

The treatment device uses intra-oral suction to stabilize tongue and/or soft palate in a position that does not obstruct the airway, thus reducing apneic episodes. This device also features extensive measurement and data-logging capabilities that enables the accurate recording of duration and quality of treatment. The following sections describes the form, construction and operation of the treatment device.

A diagram of the full treatment device is shown in Figure 2-1. The treatment device consists of a patient-specific oral device and a non-patient-specific pump unit. Patients wear the oral device on their upper palate that directs suction towards tongue and/or soft palate. A length of tubing connects the oral device to the pump unit, which is placed by the bedside and is envisioned to be redesigned as a wearable device in future iterations as illustrated in Figure 2-2.

Renderings and a photograph of the oral device are shown in Figure 2-3. the oral device consists of a dental interface and a perforated layer. the oral device can be manufactured with dental interface and perforated layer as one body or as an assembly. Currently, the oral device is printed as one monolithic body.

The dental interface takes the form of a dental device such as nightguard, retainer or aligner. the dental interface affixes the oral device to patient's upper palate (maxillary arch) and could serving dental purposes such as preventing damage from bruxism, or aligning teeth.

The perforated layer directs externally provided suction towards tongue and/or soft palate through a number of opening at various locations to stabilize the tongue and/or soft palate to prevent them from obstructing the airway. the form and location of perforated layer might vary from patient to patient based on patient condition, oral geometry, and required intensity of treatment.

A suction tube and a sensing tube are connected to the perforated layer, routed out of patient's mouth, and connected to the pump unit. Separate suction and sensing tubes are used in order to measure the pressure within the perforated layer without being affected by the pressure drop in the length of tubing.

The hollow perforated layer and the socket for tubing is clearly visible in the cross-sectional view of an oral device in Figure 2-4. The location of the oral device in its treatment position is shown in Figure 2-5.

Unlike Winx and iNAP (Section 1.3) that apply a general vacuum to the oral cavity then create a seal by having the posterior of tongue contact the soft palate [27], our device apply localized suction directly towards the tongue through a mesh that provides both superior-inferior localization and anterior-posterior traction, thus stabilize the tongue in the natural position. A detailed description of the design and manufacture of the oral device can be found in Appendix A.

Figure 2-6 shows a photograph of the pump unit. The purpose of the pump unit is to provide a configurable level of suction to the oral device, and to log treatment data and events. A block diagram of the treatment system is shown in Figure 2-7. A detailed description of the design and functionality of the pump unit can be found in Appendix B. A copy of user's manual of the treatment device can be found in Appendix C.

The device and pump were produced in small batches in-house and issued to volunteers to conduct the clinical trial.

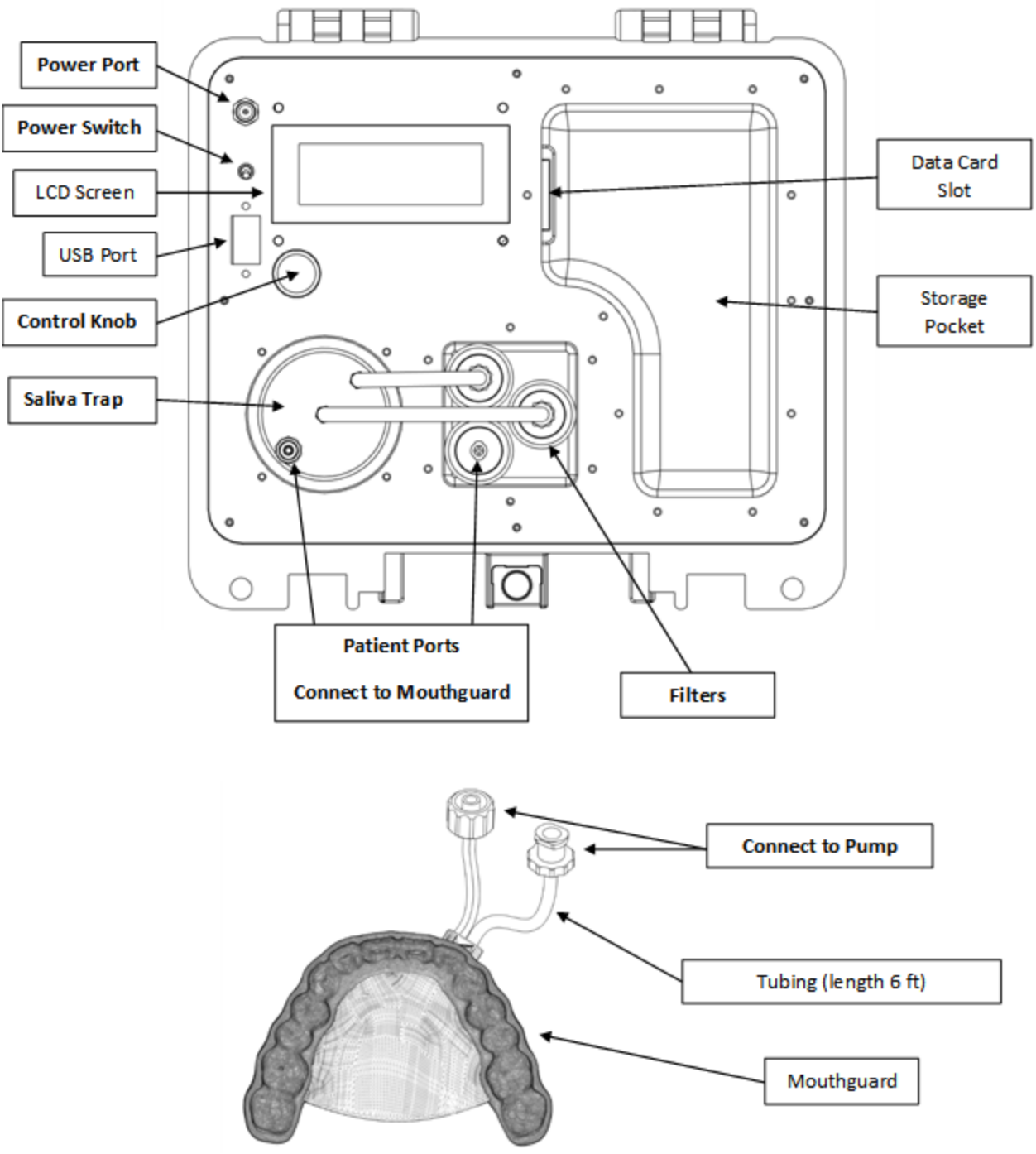

Figure 2-1: Diagram of pump unit and oral device from user manual

Figure 2-2: Envisioned miniaturized pump unit in future iterations.

(Apple iPhone 13 Pro Max Shown as Size Reference)

Figure 2-3: Renderings and photograph of the oral device

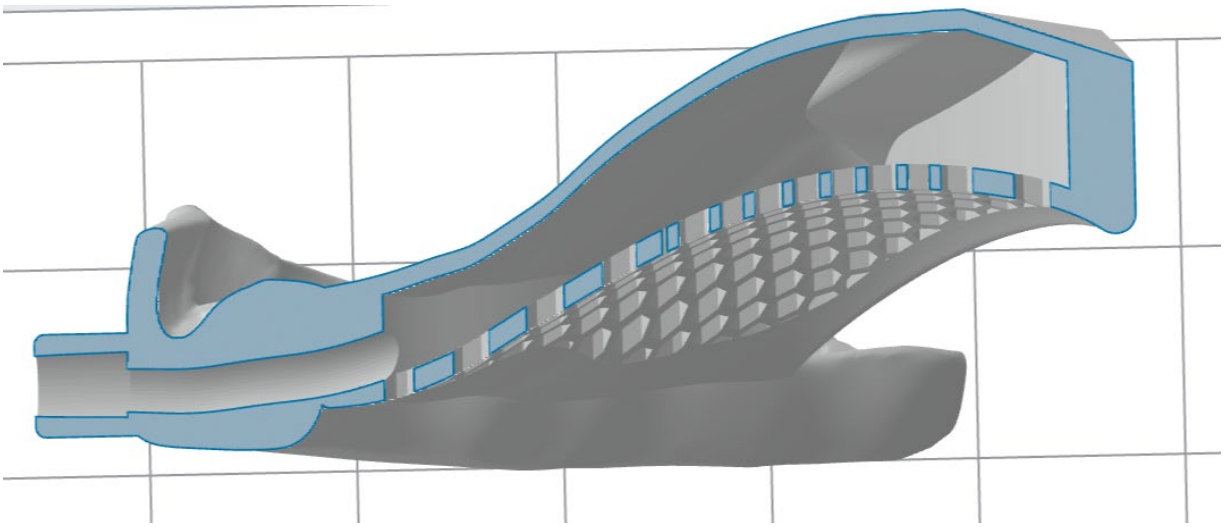

Figure 2-4: Photograph and center-sagittal cross-section of the oral device

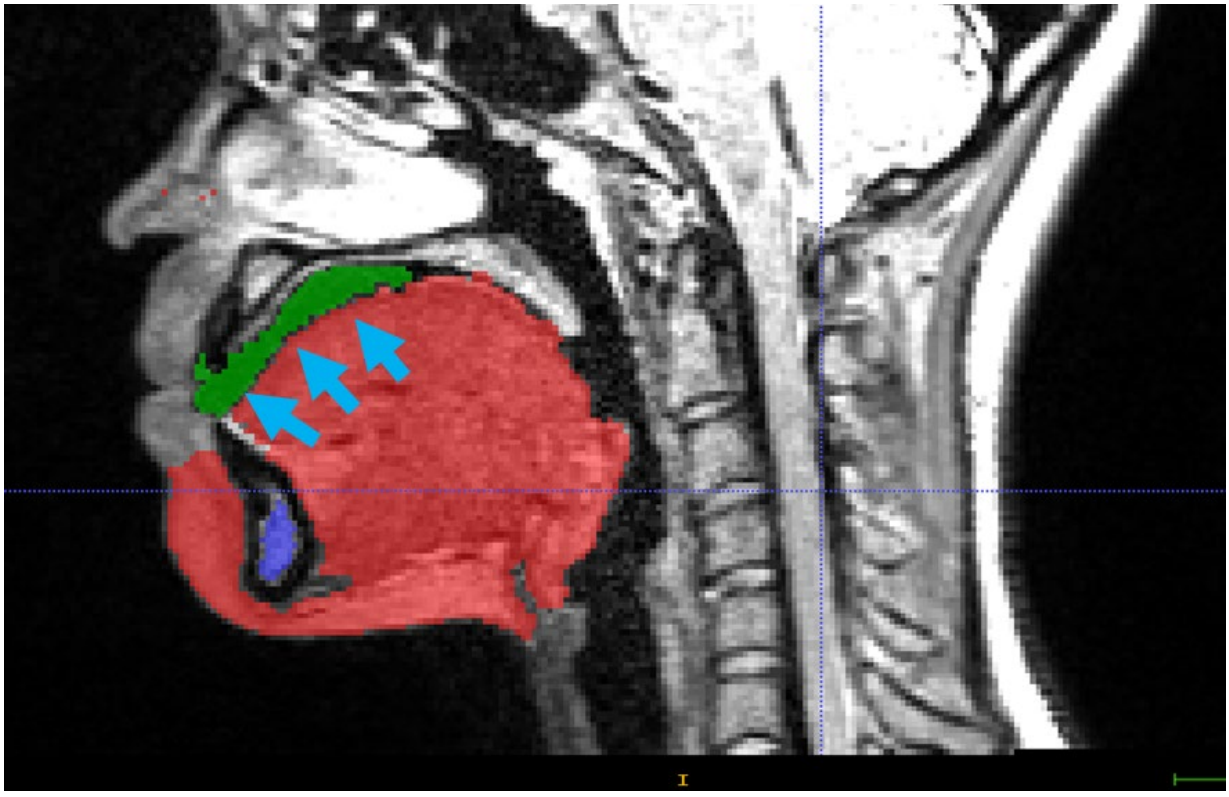

Figure 2-5: Segmented MRI Image of a study participant wearing the oral device shown in green, with suction applied to the tongue.

Figure 2-6: Photograph of the pump unit

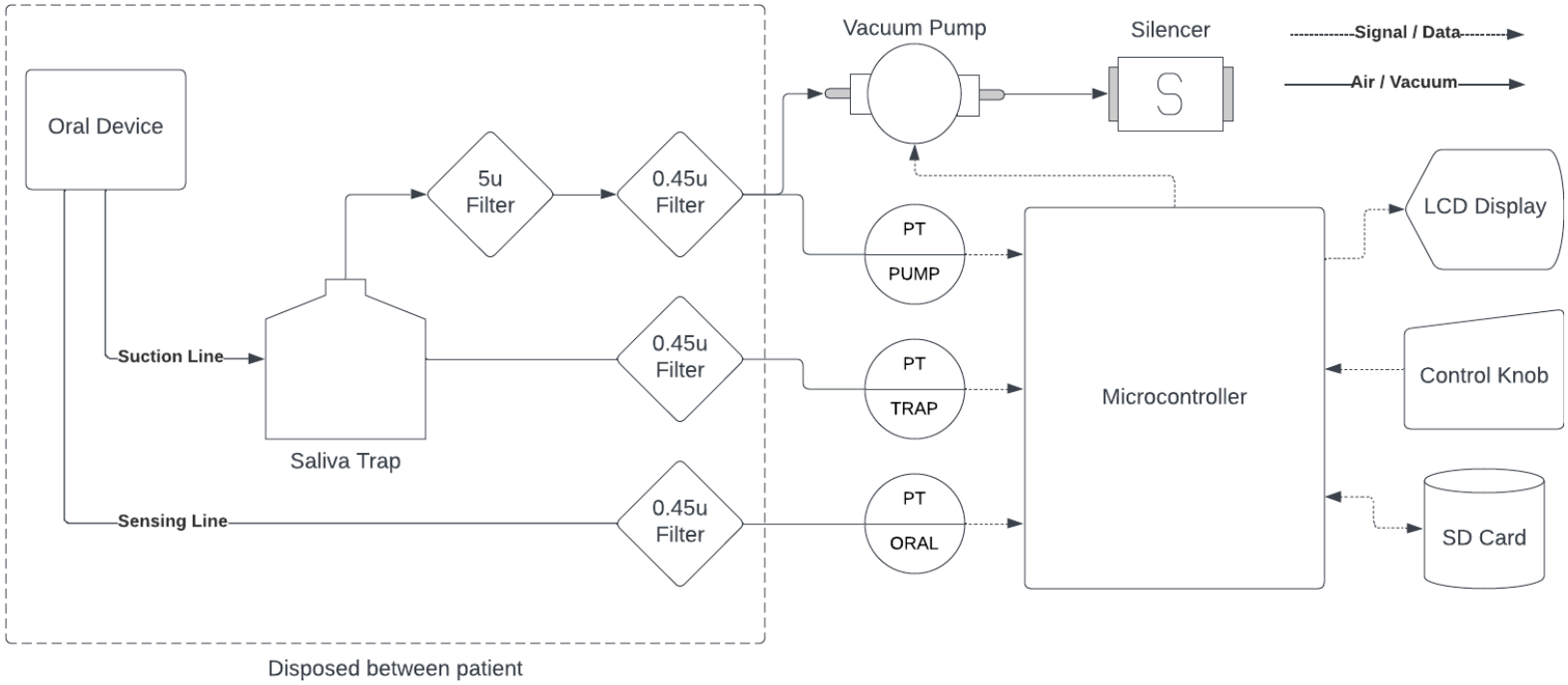

Figure 2-7: Block diagram for the treatment system.

3 Clinical Trial

To evaluate the safety, comfort and efficacy of our device, a small-scale clinical trial was conducted with healthy subjects. Two sub-studies were conducted:

1. Therapy delivery test: collect data with onboard datalogger of the pump unit to determine the percentage of time the therapy is being successfully delivered. i.e., the tongue is being stabilized in the treatment position that would not obstruct airway.
2. Home sleep study: collect data with portable sleep monitor to determine whether our treatment device cause a significant change in OSA related measurements including but not limited to apnea hypopnea index (AHI).

3.1 Therapy Delivery Rate

3.1.1 Methods

This study included 5 healthy subjects, (3 female and 2 male, age 30 ± 10 years, recruited in MIT, Harvard and publicly in Cambridge, MA) wearing the treatment device for at least 3 nights each. Data reported here was the duration of treatment session, T, and the percentage of time the therapy is being successfully delivered, η.

Each pump contains an onboard datalogger that logs many streams of data including current time, pressure in the oral device, and status of all components. The sampling rate was 20Hz.

Duration of treatment session, T, is approximated by the time the pump is powered on with the assumption of the subject inserted the oral device prior to, or immediately after the pump is turned on. Similarly, the subject is assumed to remove the oral device immediately before, or right after turning the pump off.

To calculate η, the duration of the tongue being stabilized in the treatment position ('latched'), T_L, is calculated first. T_L is obtained by thresholding the pressure in the oral device, P_o. P_o is directly measurable by the pump unit without being affected by pressure drop (Section 2). The definition of the pressure threshold to determine whether the tongue is latched is the

prescribed treatment pressure + 10 mmHg. If pressure in the oral device is lower than the threshold, the tongue is latched. Then, η is calculated as T_L / T.

The oral device is designed in a way that the vacuum would not be established if the tongue is not in the stabilized position, so the oral pressure can be used as a metric to determine whether the treatment is delivered.

Finally, the data per patient per night is aggregated using two methods:

3.1.1.1 Pooled Treatment Delivery Percentage (η_1)

η_1 is calculated as the sum of T_L across all subject and all nights divided by the sum of T across all subject and all nights. Therefore, η_1 is the actual percentage of time the system is delivering treatment and it is an appropriate metric to evaluate the mechanical performance of the treatment device.

However, η_1 fails to address how well would each subject sleep per night. The summation nature of η_1 makes the output biased towards the η of the subject who slept largest number of hours during the study. To accurately represent the performance of the treatment device from a clinical standpoint, a different metric is required.

3.1.1.2 Per-subject Treatment Delivery Percentage (η_2)

η_2 is calculated by first obtaining the mean and standard deviation of the η across all nights for each patient, then average the resulting means again and propagate the standard deviation from the first average to η_2. η_2 can accurately represent how did the treatment device perform each night on each patient since all steps are unweighted. The unweighted average ensures that each subject contribute to the measurement of performance equally regardless of duration of sleep or number of nights slept.

3.1.2 Results

Of the 5 subjects who were studied, 3 were female and 2 were male. The age ranged from 20 to 40 years. Subjects sleep with our device for mean of 6.19 ± 2.32 hours per night (mean ± standard deviation) and a median of 6.43 hours per night. The per-night averaged percentage of time the treatment is successfully delivered is 95% ± 14% (mean ± standard deviation). The pooled percentage of the time the treatment is successfully delivered is 96%.

Figure 3-1 shows data collected for one night for a participant. When the tongue is unlatched from the device the oral pressure will fall close to zero. When the tongue is latched to the device, the pressure will be fluctuating near the prescribed treatment pressure (labeled as 'set point') due to control loop oscillation. We found that the volunteer's tongue unlatches from the device quite often, but for a very short duration (< 10 seconds), then re-latches to the treatment device.

Figure 3-2 shows the recorded duration and percentage of time the tongue stayed latched to the treatment device (η) for each patient each night. The duration of recording per night varies per patient, but η for most nights stayed close to 100%.

Figure 3-3 shows the pooled and nightly-averaged η per subject across the duration of entire study.

Figure 3-4 shows the comparison between pooled and nightly-averaged η across all subjects in the study.

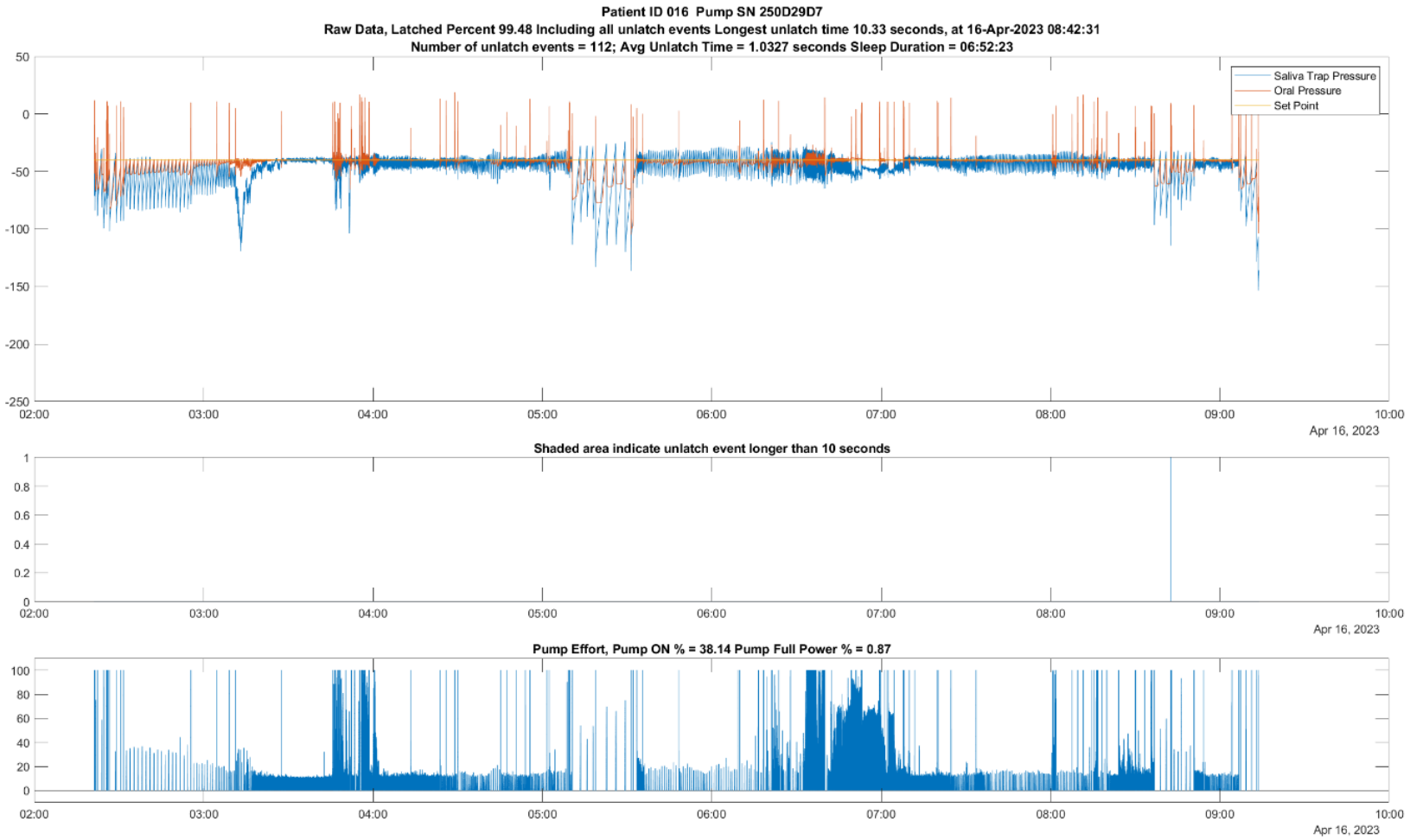

Figure 3-1: data collected from the pump unit from one night of the study.

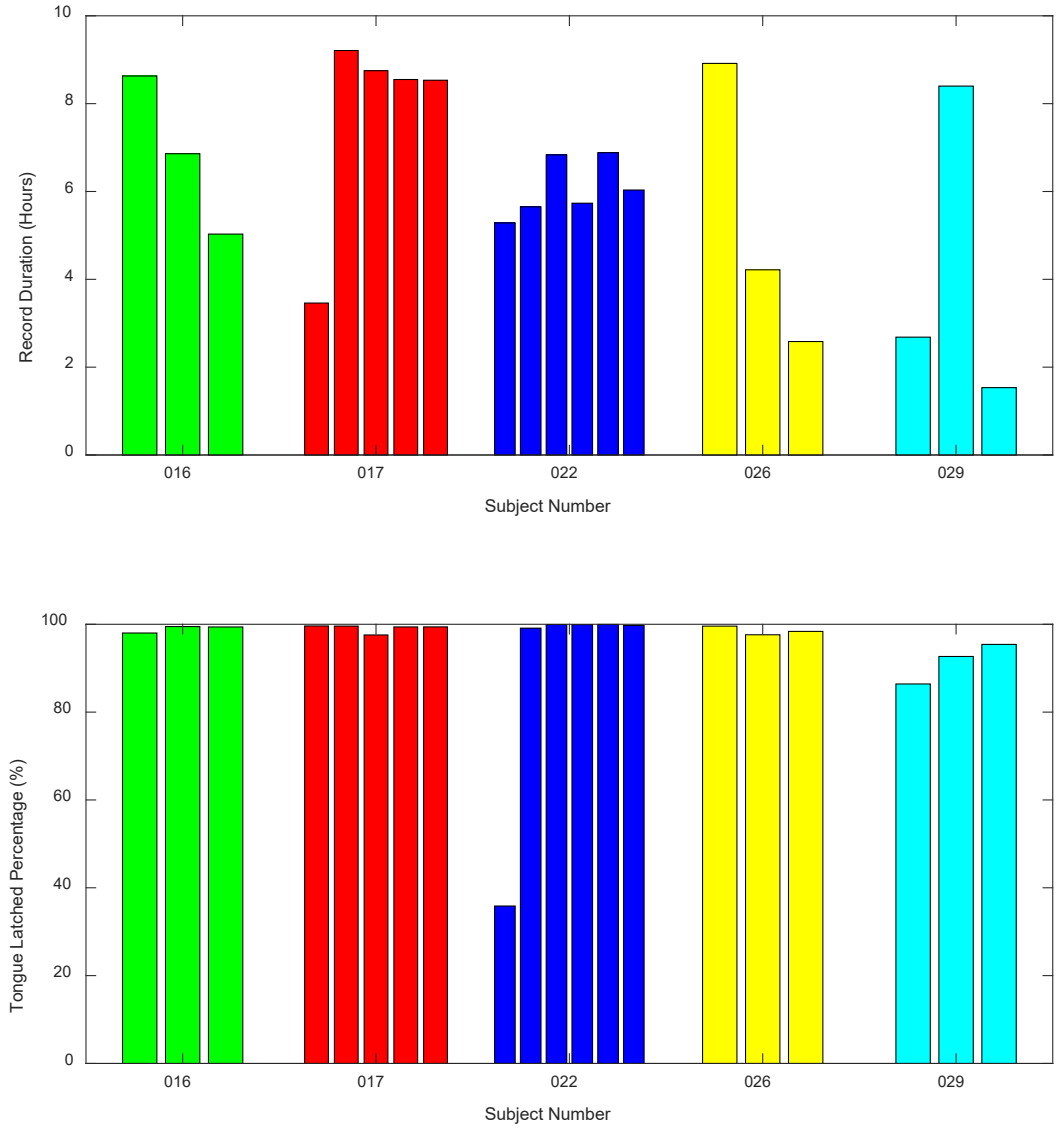

Figure 3-2: Raw data collected from treatment delivery study. Each bar represents data from one night. The top panel plots record duration per night of each patient (roughly corresponds to hour of sleep). The bottom panel plots the percentage of time the tongue is latched

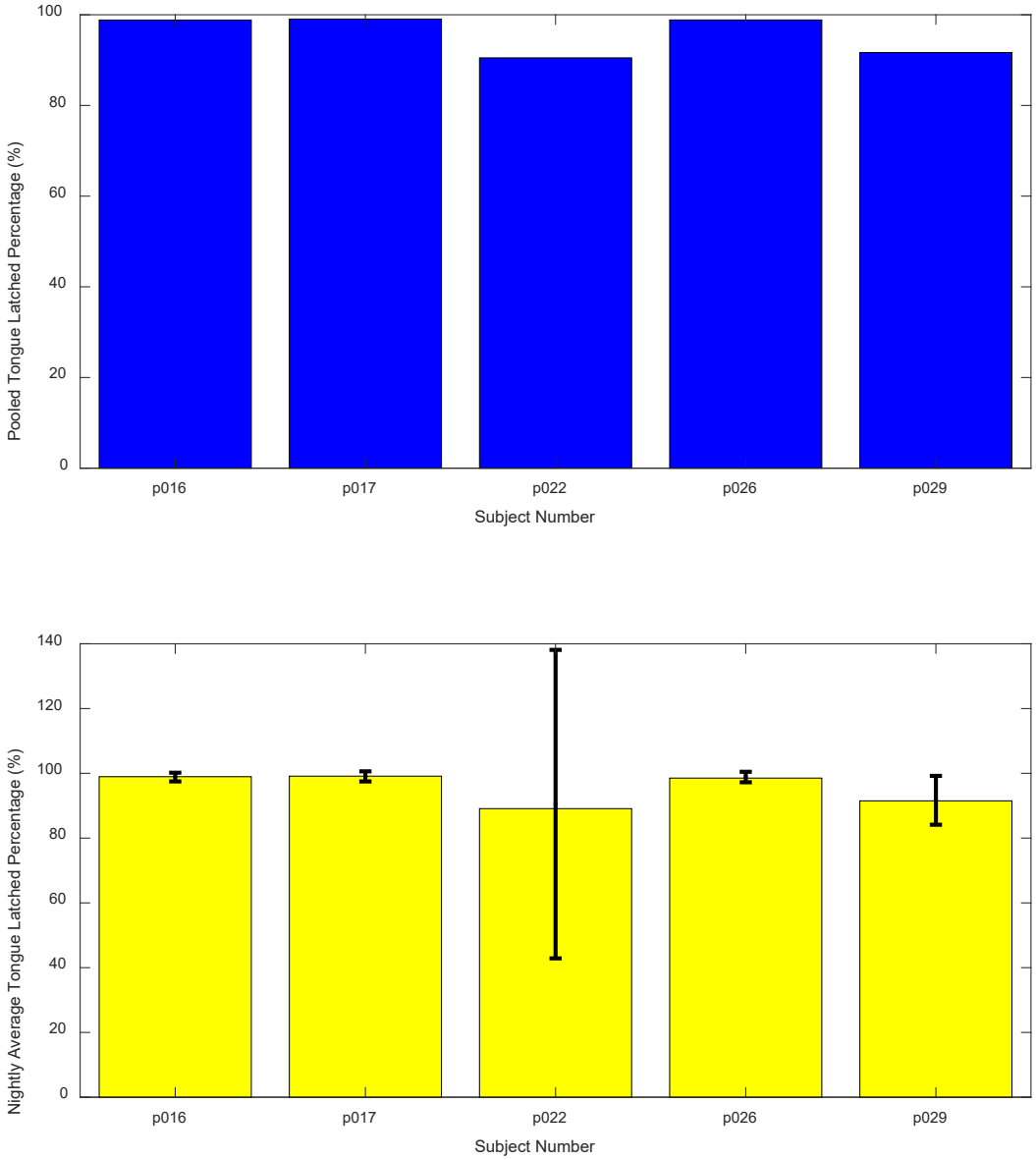

Figure 3-3: Pooled and nightly averaged percentage of time of successful treatment delivery. Error bar represents two standard deviations each side (95% confidence interval).

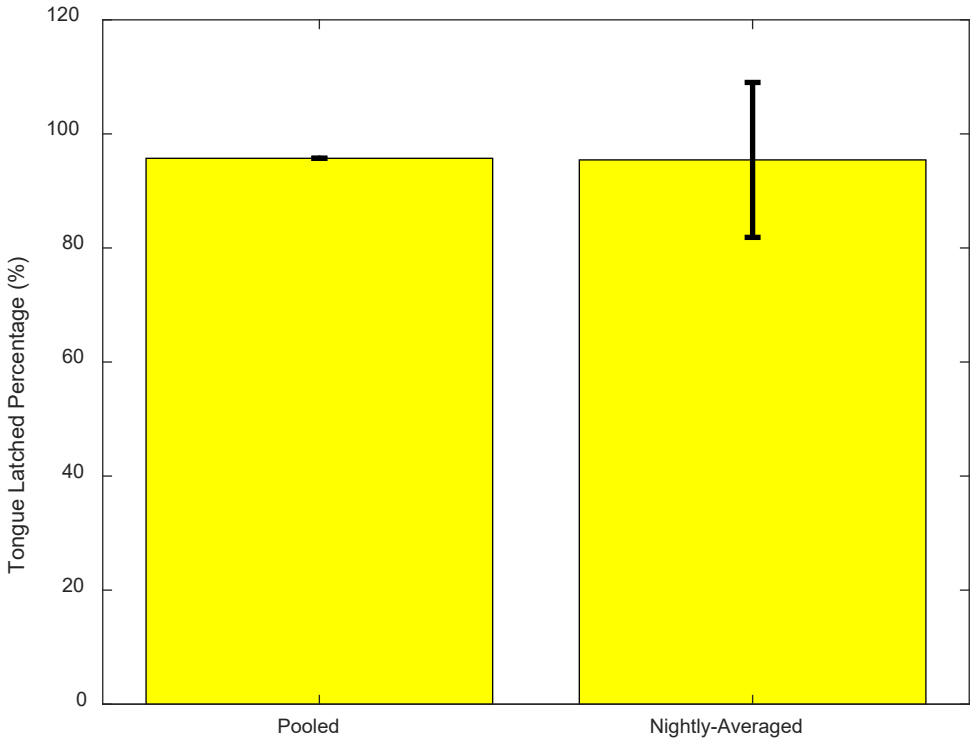

Figure 3-4: Comparison between pooled percentage and nightly averaged percentage of duration of delivery of successful treatments. Error bar represents two standard deviations each side (95% confidence interval).

3.2 Home Sleep Study

3.2.1 Methods

Four of the five healthy subjects (3 female, 1 male, age 30 ± 10 years) that participated in our therapy delivery study (Section 3.1) are also included in the sleep study, where they wore a portable sleep monitor (Figure 3-5) (ResMed ApneaLink Air, ResMed Inc., San Diego, CA) to monitor their sleep for 5 nights – 2 control nights without treatment were recorded as baseline, in addition to 3 nights wearing the oral device connected to the pump unit.

ResMed ApneaLink Air were used in numerous studies to access the efficacy of OSA treatment devices [20], [30], [31]. ApneaLink was validated against in-lab PSG in multiple studies and was approximately 80% agreeable to PSGs, with higher agreeability to PSGs when patient has moderate to severe OSA [18], [32], [33].

ResMed ApneaLink Air records the following signals:

1. Nasal flow rate (flow), measured with nasal cannula
2. Respiratory effort (effort), measured with sensor belt on chest or abdomen
3. Pulse per minute and oxygen saturation (SpO2), measured with pulse oximeter
4. Snoring, measured with onboard accelerometer

The acquired sleep data was analyzed with an automatic scoring software (ApneaLink, ResMed Inc., San Diego, CA) that identifies apnea and hypopnea events following the AASM definition [11] then report apnea hypopnea index (AHI, Section 1.2.1) and risk indicator (RI). RI a sleep score that is specific to the ResMed ApneaLink Air portable sleep monitor. RI takes flow limitation and snore event into account in addition of apnea and hypopnea events. Figure 3-6 shows an excerpt from the clinical manual [34] outlining the calculation of RI. Though RI is not a widely used score in the sleep medicine field, we included this score in our study as an additional metric to evaluate respiratory obstruction.

AHI and RI of each subject each night was averaged across baseline nights and across treatment nights for each subject for a per-subject response. Then paired t-test was performed

to evaluate whether there is a significant difference in AHI and RI between baseline nights and treatment nights.

3.1.2 Results

Of the 4 healthy subjects who were studied, 3 were female and 1 were male. Age ranged from 20 to 40 years. We found that for healthy subjects, there were no statistically significant change in AHI or RI with p-value of 0.66 and 0.63 respectively, which demonstrates that the device is not causing any new obstructions.

Raw data taken from one participant for one night is shown in Figure 3-7 to illustrate the data collected for each subject. Figure 3-8 plots AHI and RI reported by ApneaLink software per participant per night, grouped by baseline and treatment. Per-subject mean and standard deviation of the AHI and RI on baseline nights and treatment nights are plotted in Figure 3-9 for evaluation of outcome of each participant. Finally, two box plots are in Figure 3-10 comparing the AHI and RI on baseline nights and treatment nights.

Figure 3-5: ResMed ApneaLink portable sleep monitor shown in left panel. Photography demonstrating the portable sleep monitor in action. (Photo by ResMed)

Analysis indices

AHI (apnea-hypopnea index): Mean number of all apnea classes (unclassified, central, mixed, obstructive) and hypopneas per hour in the evaluation period. Events are also shown individually in the apnea and hypopnea index fields. If the measured value exceeds the normal range, the value will be displayed "framed".

RI (risk indicator):

The risk indicator (RI) is calculated as follows:

RI = point score as a sum of AHI + score of FL/FS

Points calculated from AHI:

AHI x 1 h = number of points (eg, AHI = 5/h x 1 h= 5 points)

where h is the evaluation period

FL/FS point score:

Number of points = 10 x (0.8 x FL + 1.2 x FS) / If

where:

- AHI = apnea-hypopnea index
- FL = number of flow-limited breaths without snoring
- FS = number of flow-limited breaths with snoring
- If = total number of breaths

If the measured value exceeds the normal range, the value is displayed "framed".

Figure 3-6: Definition of AHI, and RI. Excerpt from ResMed ApneaLink Air Clinical Manual.

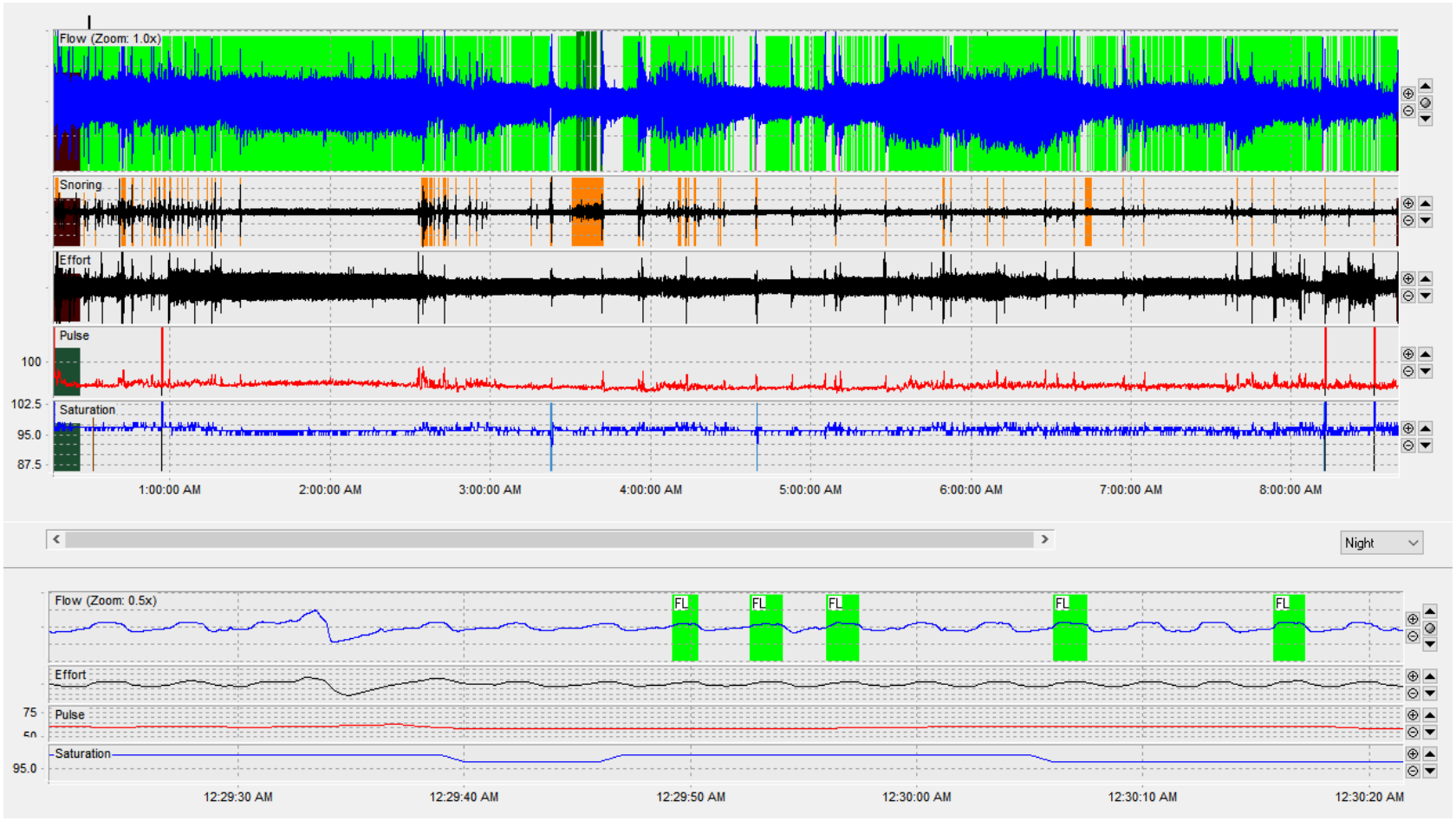

Figure 3-7: Data collected from one night of study from one subject, illustrating the general form of the data. Screen Capture from ApneaLink software. The top panel displays flow, snoring, respiratory effort, pulse and oxygen saturation. The bottom panel display

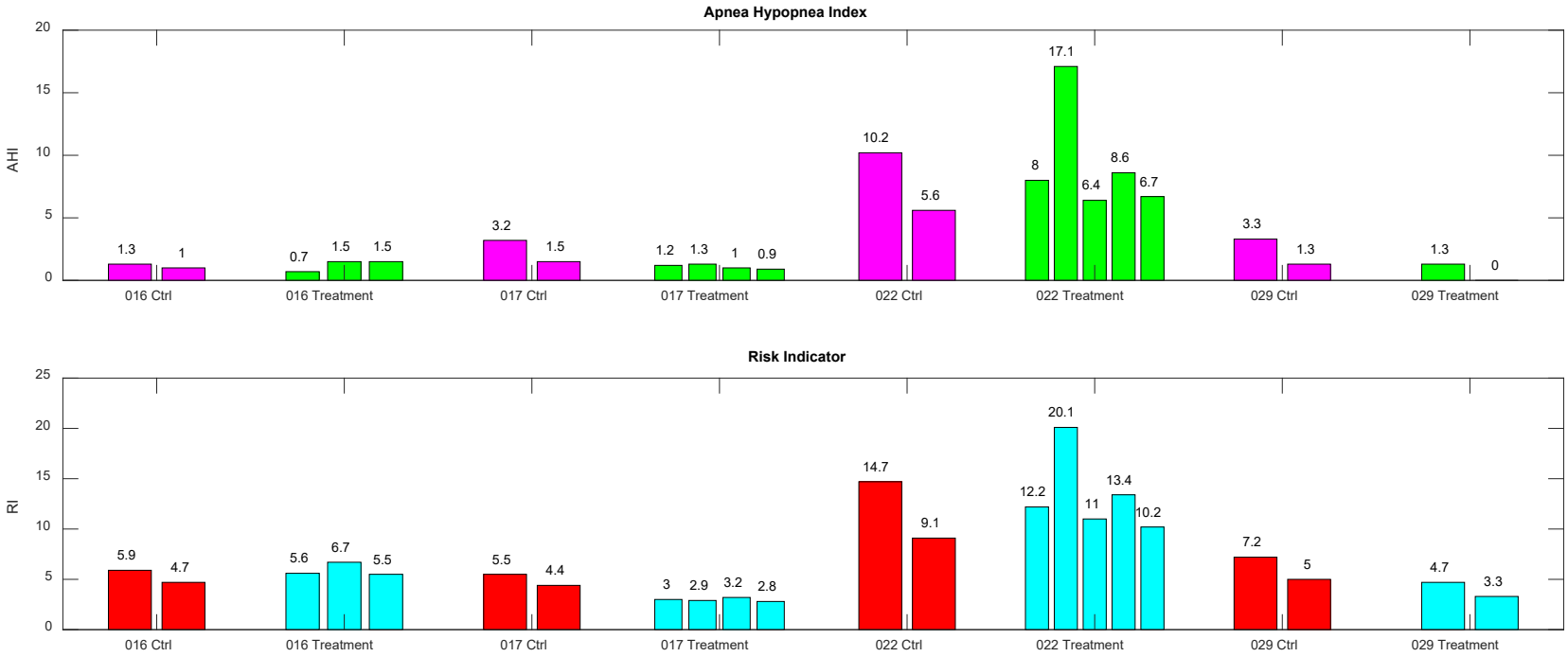

Figure 3-8: Data from ResMed ApneaLink Software plotted per night and grouped per subject. Control is measured without oral device or pump. Treatment is measured with oral device and pump.

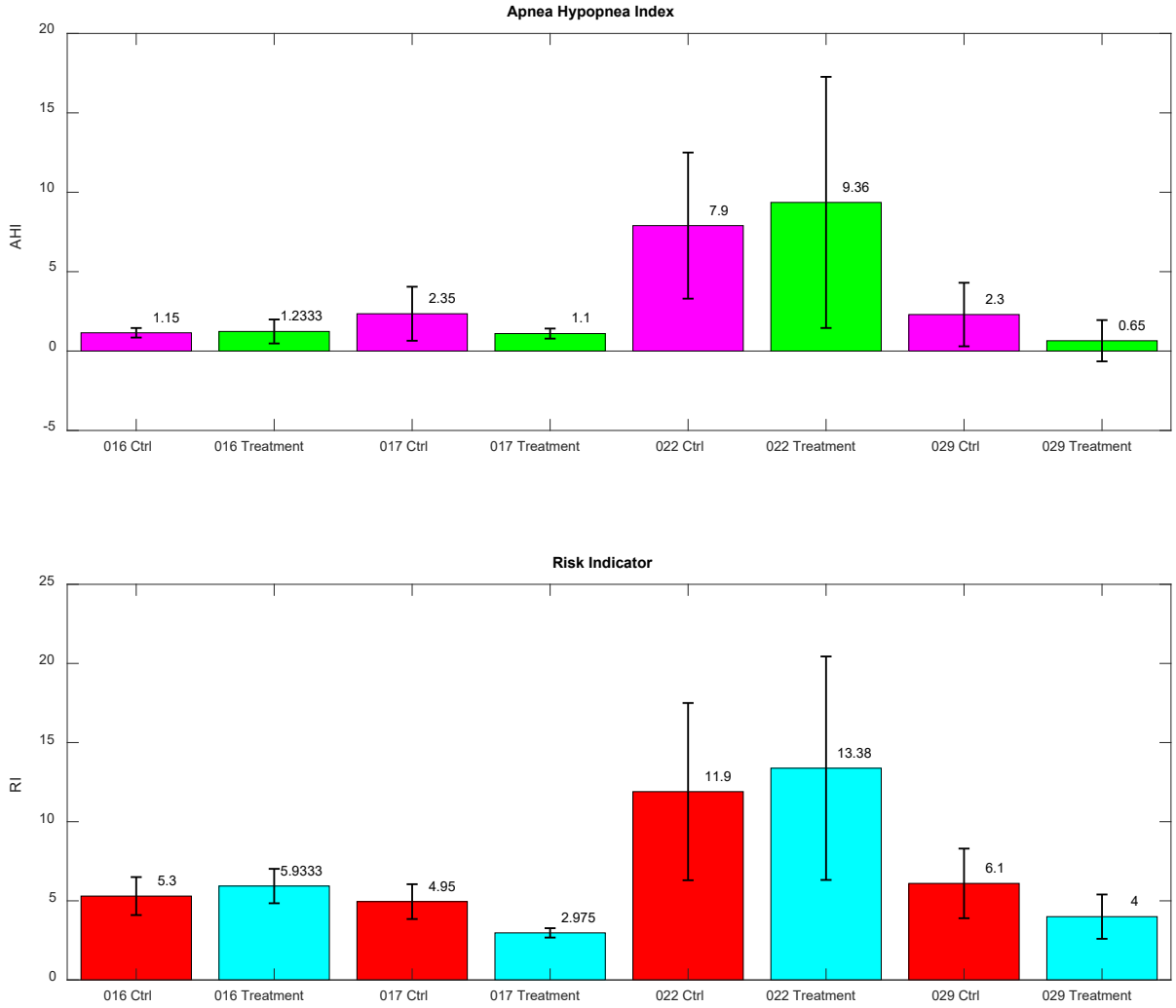

Figure 3-9: per-subject comparison of AHI and RI between baseline and treatment. Error bar represent 95% confidence interval.

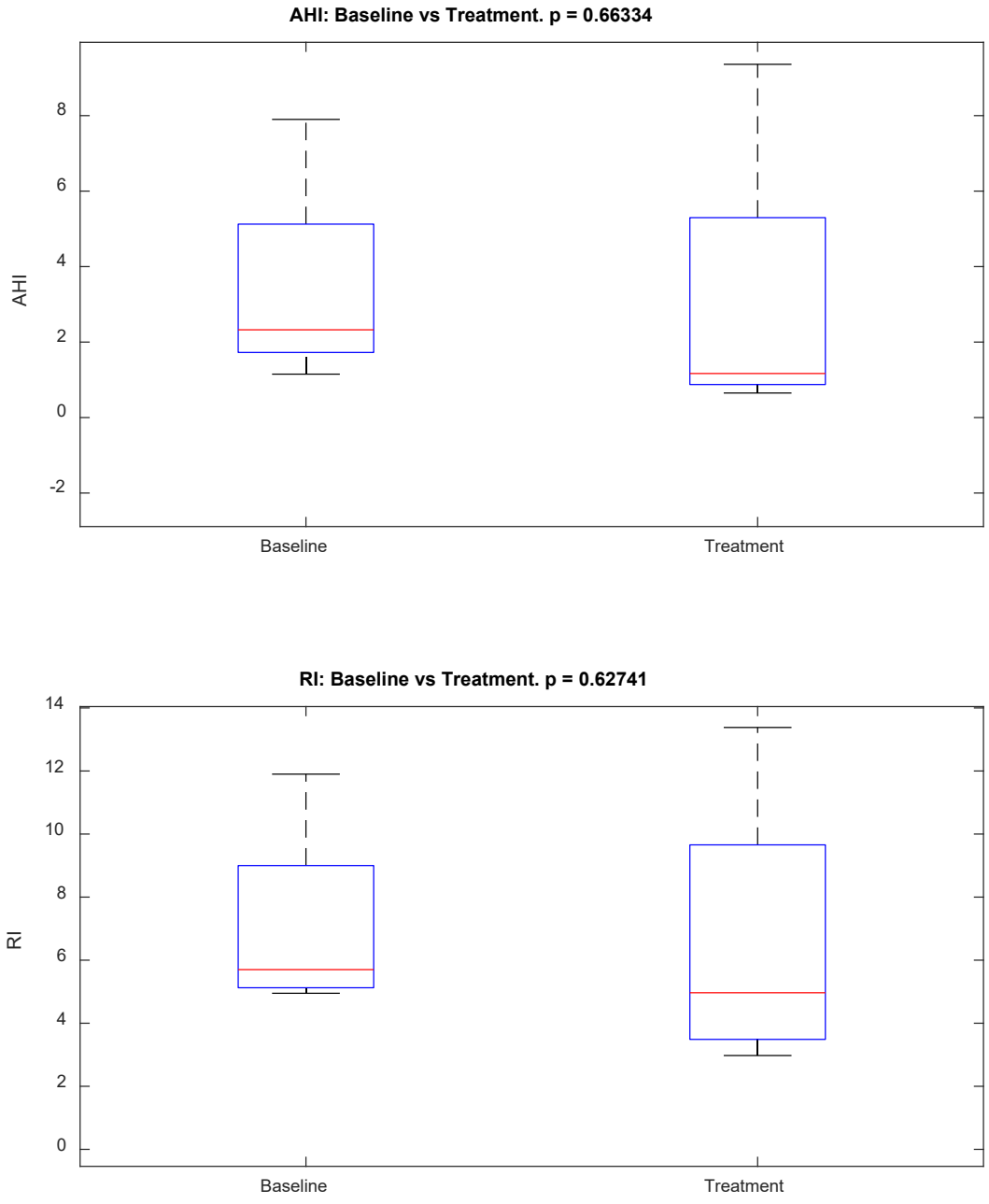

Figure 3-10: Statistically insignificant AHI and RI results from healthy participants.

3.3 MRI Imaging

3.3.1 Methods

This study included two healthy subjects, one female ('participant A'), one male, ('participant B'). Subjects were between 20 and 30 years old. Each subject was imaged awake in supine position. The imaging protocol is listed below:

1. T2 and DTI sequence without any device.
2. T2 sequence with oral device inserted, without suction.
3. T2 and DTI sequence with -100 mmHg of suction applied towards tongue
4. T2 sequence with -100mmHg of suction applied towards tongue and soft palate

The T2 images allows accurate segmentation of tissue, bone, water and airway. The DTI images contain information of muscle fiber orienation. The set of images are used to measure the minimum cross-sectional area of airway as a metric of efficacy of the treatment device; to understand the mechanism of action; and to provide anatomical and fiber orientation information for computational modeling in Section 4.

Application of suction towards tongue was done with the oral device similar to[1] those shown in Figure 2-4. Application of suction towards tongue and soft palate was done with modified oral device featuring two ¼ inch-diameter openings at the posterior of oral appliance near subject's soft palate. Suction was provided by regulated wall vacuum instead of pump unit.

Each image was then segmented with ITK-SNAP semi-automatically using active contour guided segmentation [35] and imported into Autodesk Fusion for visual inspection. The minimum cross-sectional areas of the airway images were found numerically with a MATLAB script. As the airway runs close to the axial direction, the minimal cross section area can be found by identifying the axial slice with the smallest number of labeled voxels and counting the number of voxels. The result is checked by visual inspection before reporting to ensure the algorithm identified the correct local minimum within the airway.

[1] 'Similar' means using the same mechanism but the patient-specific parts are different. The dental inter face, the shape of suction chamber and perforated layer were all customized per subject.

3.3.2 Results

Figure 3-11a and 3-11b shows the axial and sagittal view of T2 images from the female and the male subject in the following four configurations:

(i) Baseline without any device ('Baseline')

(ii) Oral device inserted without suction ('No SX')

(iii) Oral device applying -100mmHg to tongue ('T SX')

(iv) Oral device applying -100mmHg to tongue and soft palate ('T+SP SX')

A segmented image of participant A wearing our oral device with suction applied to tongue is shown in Figure 3-12 to illustrate the location of the tongue and oral device. Figure 3-13 provides an illustration of the size and location of segmented airway. The airway segmentations of participant A and B are shown in Figure 3-14.

The cross-sectional area of the narrowest section of airway was measured for each airway segmentation. The cross-sectional area as a function of axial position for participant A without device, along with the sagittal profile of the airway being measured, is shown in Figure 3-15 to illustrate the process.

Figure 3-16 and 3-17 plots the airway cross-sectional area against axial position. Minimum airway cross-sectional area under the four different configurations is reported in bar plots. The comparisons of airway cross sectional area between baseline and treatment are reported in Table 3-1.

		Airway minimum area comparing to	
Participant	Treatment	Baseline (no device)	Passive device (no SX)
A	No SX	125%	100%
	Tongue SX	186%	149%
	T+SP SX	53%	42%
B	No SX	86%	100%
	Tongue SX	159%	184%
	T+SP SX	60%	68%

Table 3-1: Response of participant A and B to the treatment device measured by comparing minimum airway cross-sectional area against baseline and passive device.

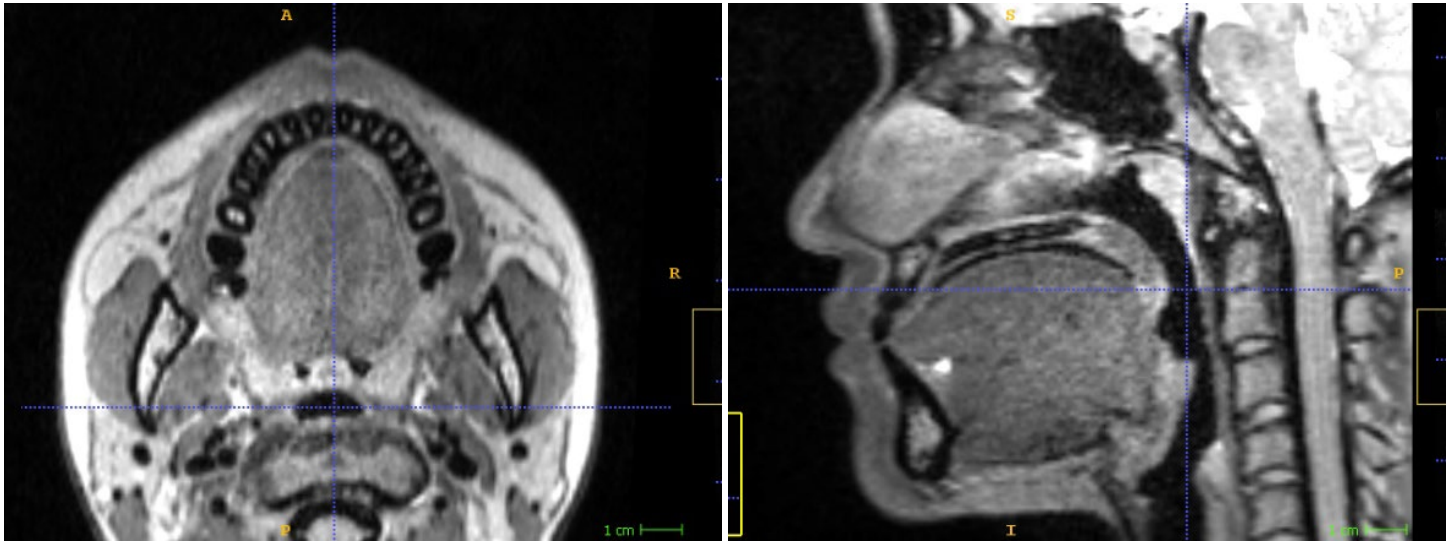

(i) Baseline

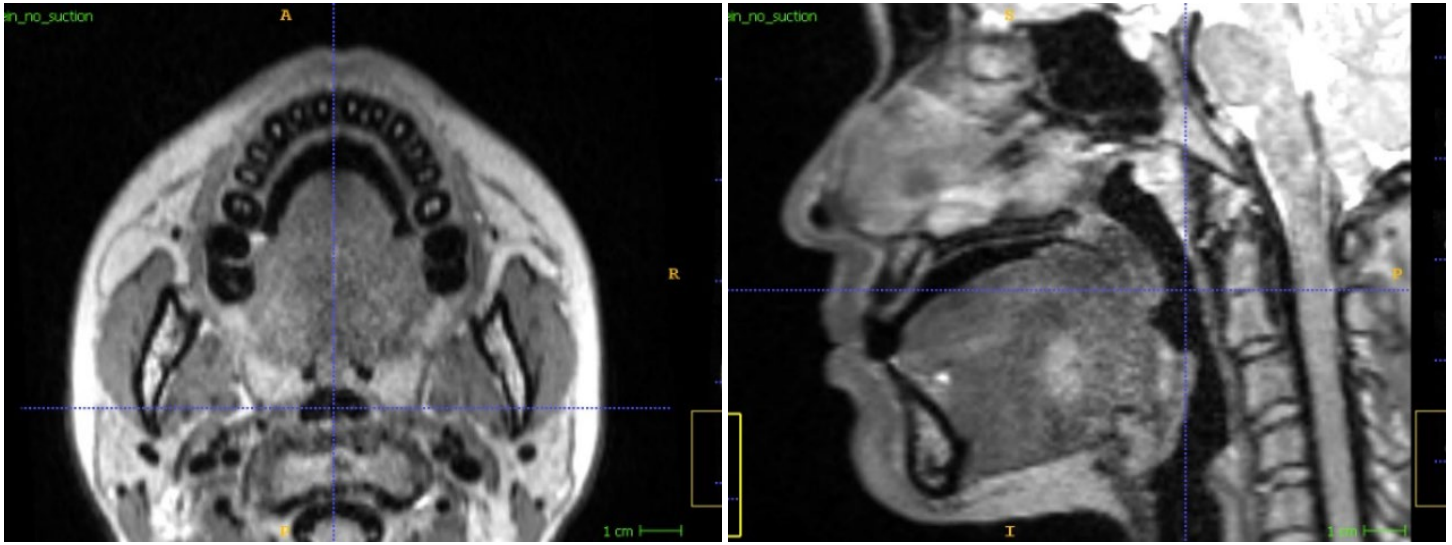

(ii) Device inserted without suction

Figure 3-11a: MRI images of participant A wearing an oral device. (Continues to next page)

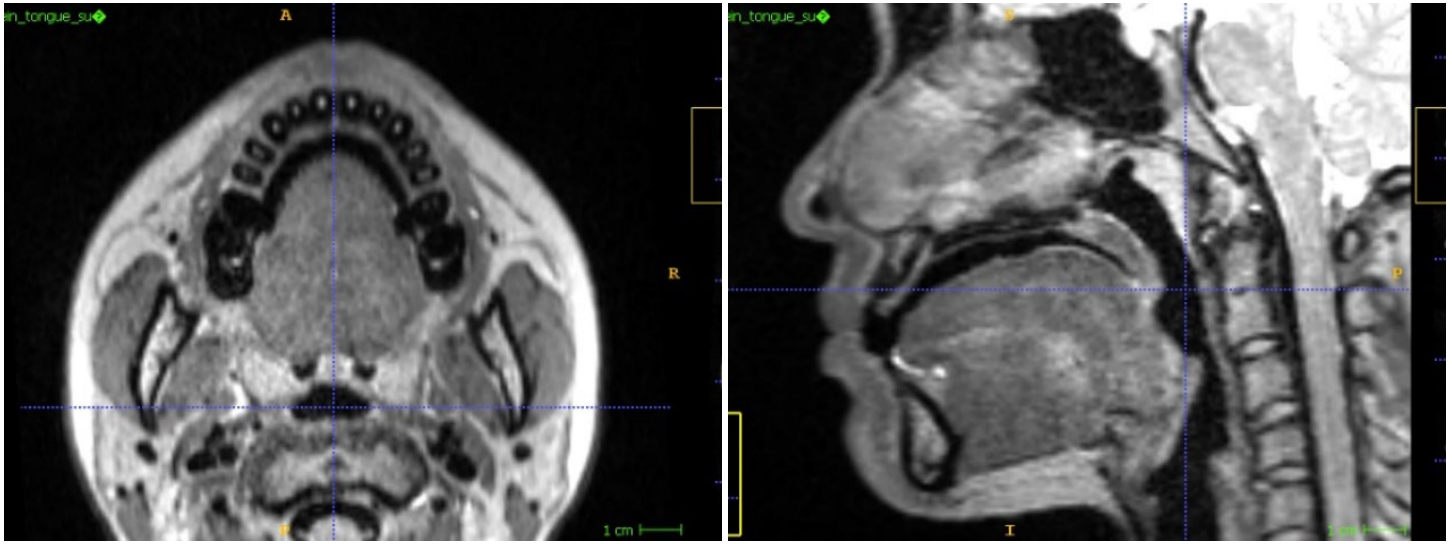

(iii) Applying suction to tongue

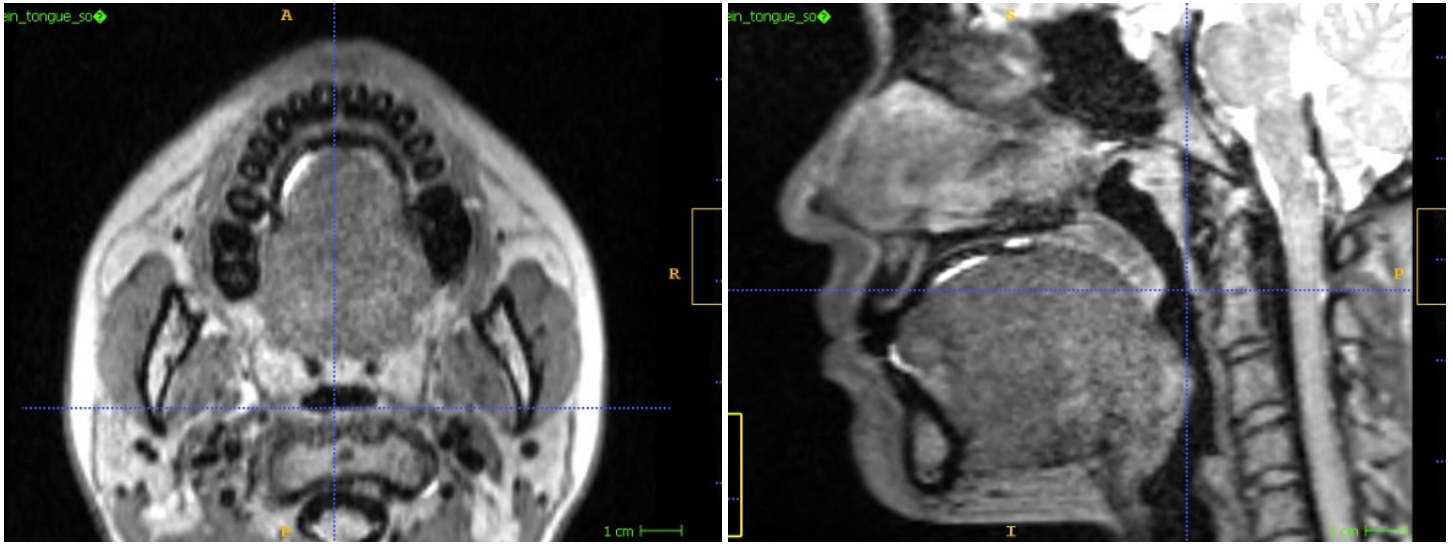

(iv) Applying suction to tongue and soft palate

Figure 3-11a (continued): MRI images of participant A wearing an oral device.

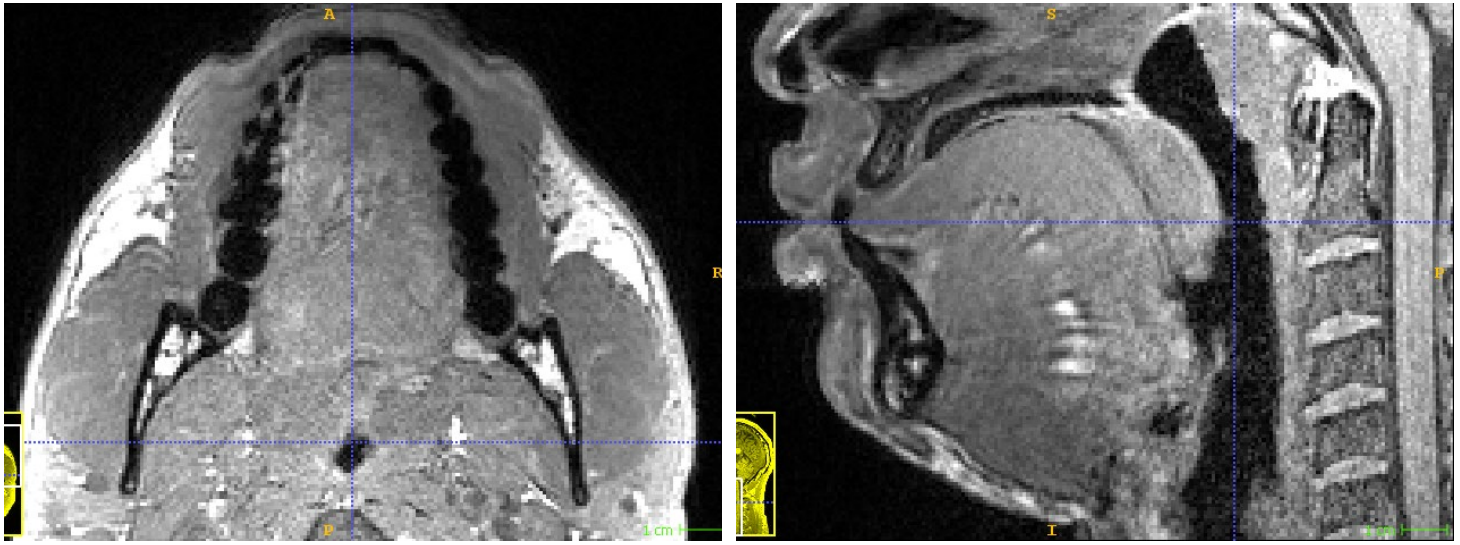

(i) Baseline

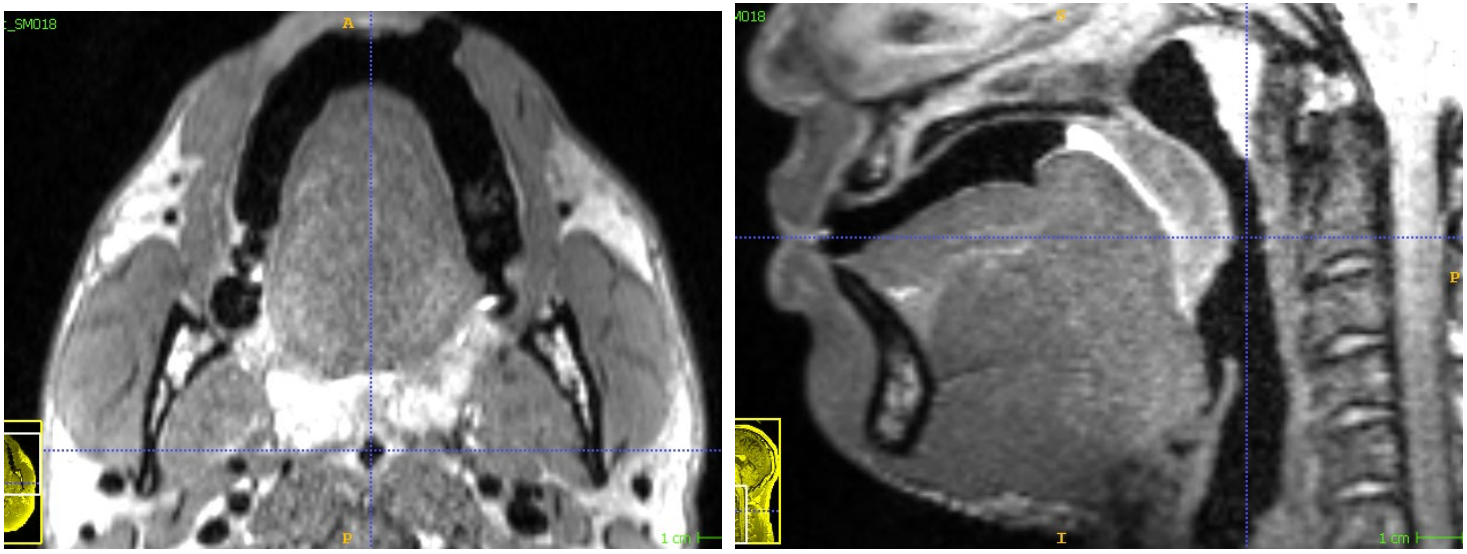

(ii) Device inserted without suction

Figure 3-11b: MRI images of participant B wearing an oral device. (Continues to next page)

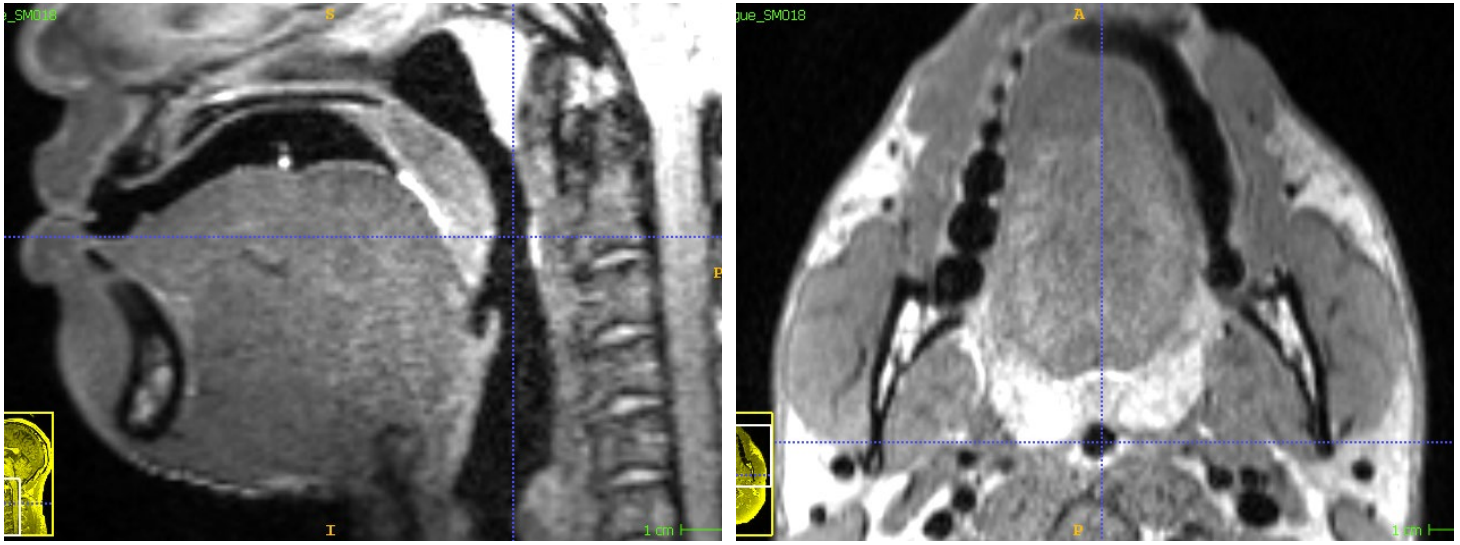

(iii) Applying suction to tongue

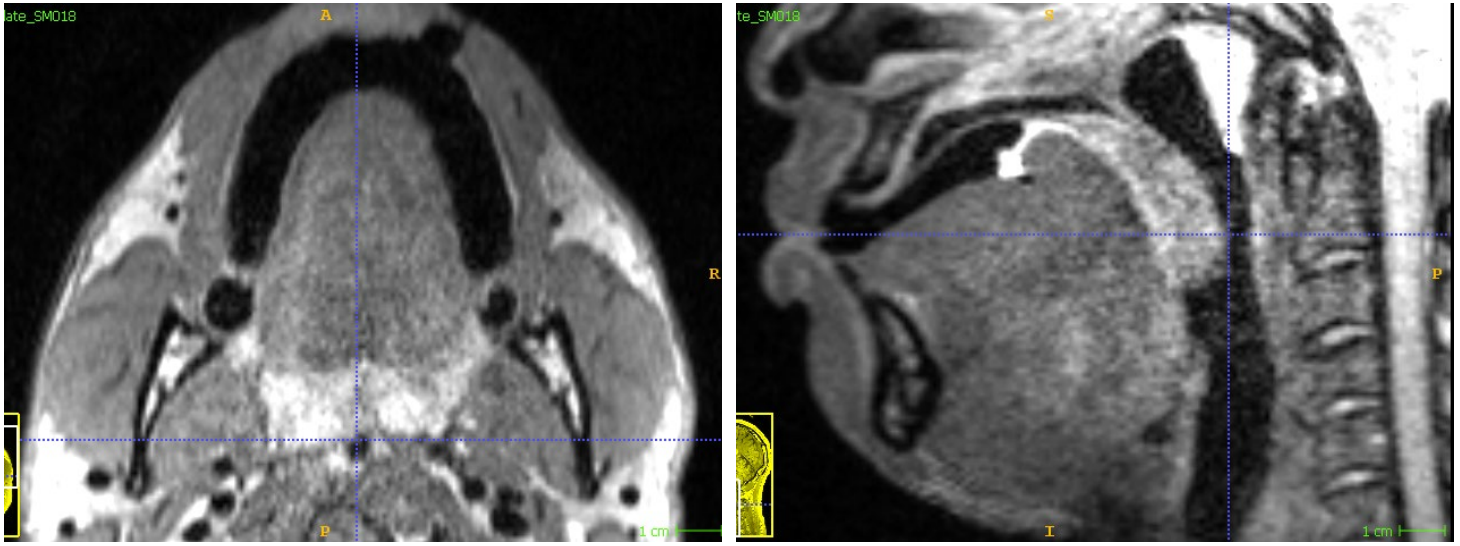

(iv) Applying suction to tongue and soft palate

Figure 3-11b(continued): MRI images of participant B wearing an oral device.

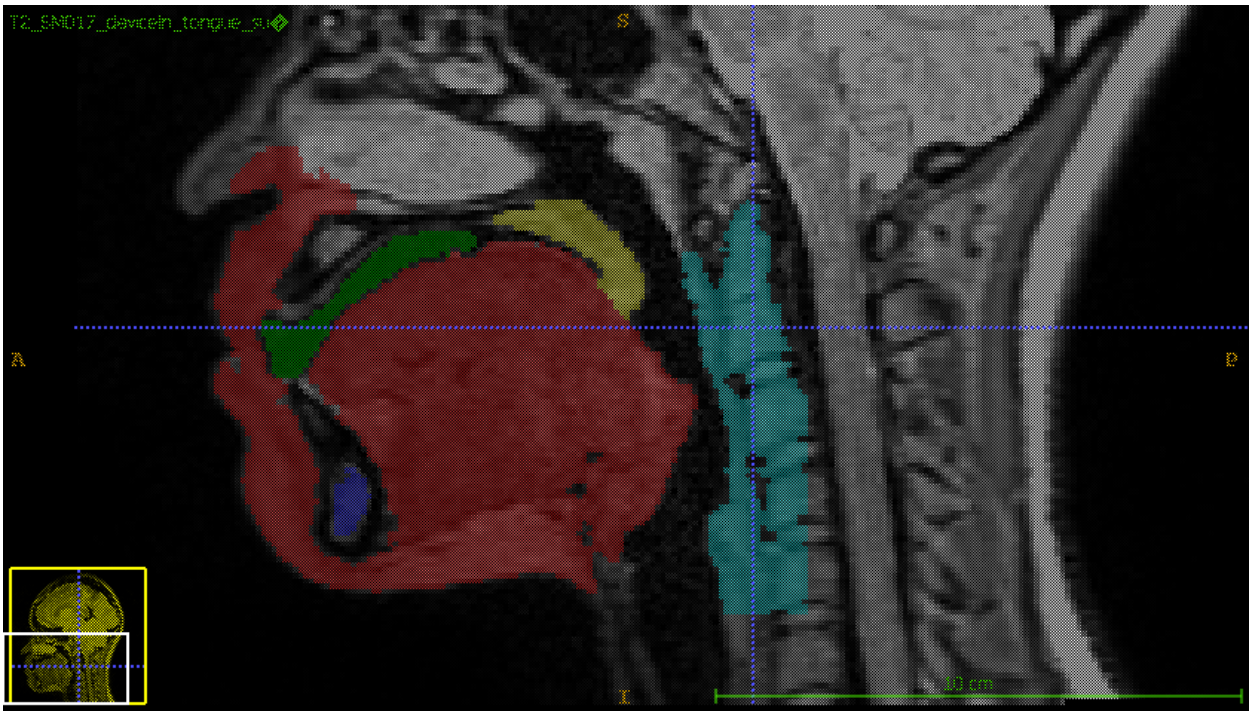

Figure 3-12: Segmented T2 image of Participant A wearing oral device with suction applied to tongue. Oral device is colored green.

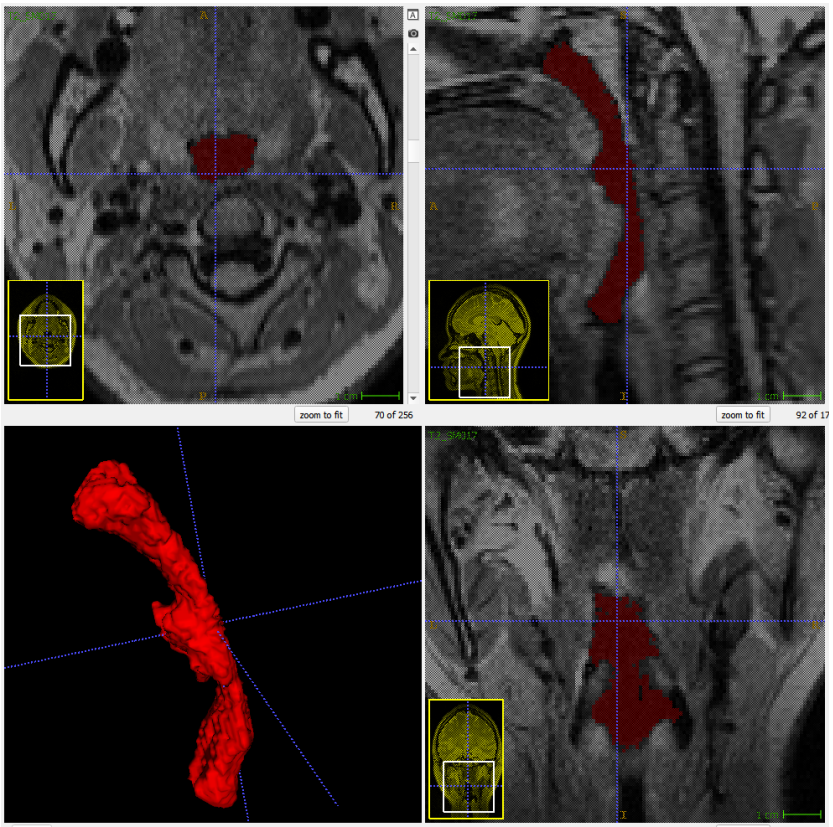

Figure 3-13: the airway of Participant A being segmented with ITK-SNAP using active contour guided segmentation [35]

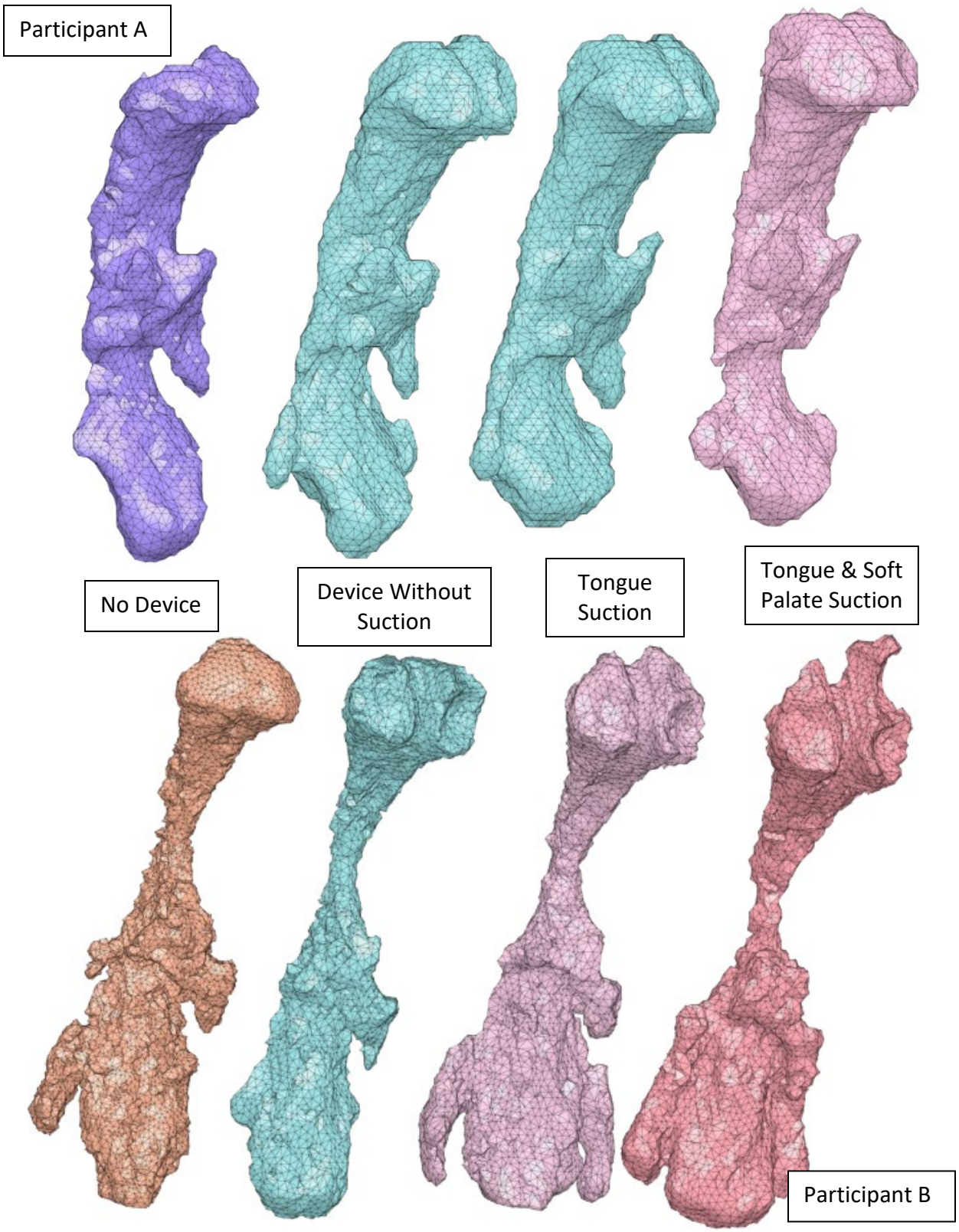

Figure 3-14: Segmented airway of Participant A and B under 4 configurations listed in Section 3.3.2

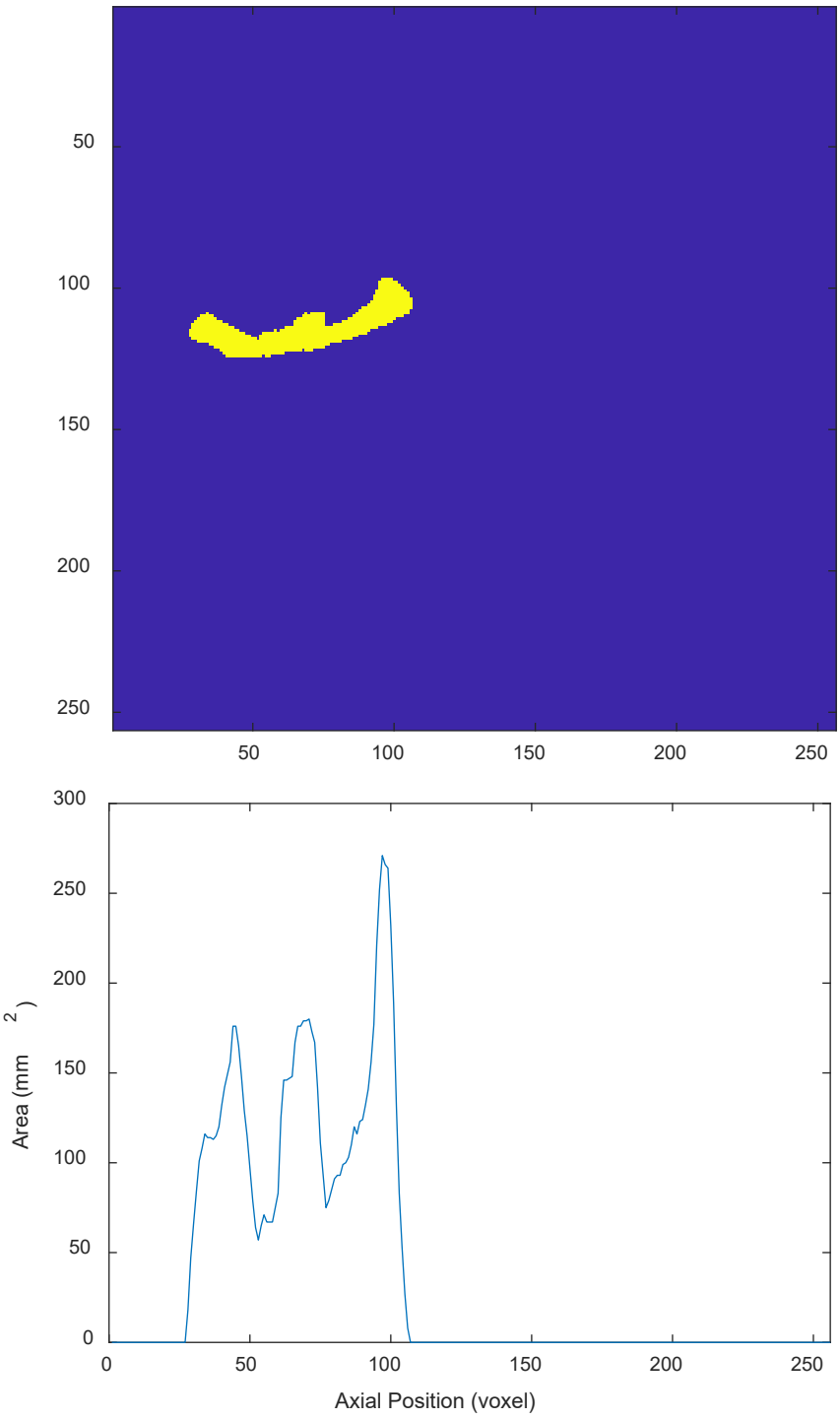

Figure 3-15: Measuring airway cross-sectional area. The top panel shows the sagittal projection of the segmented airway (+X direction is superior; +Y direction is posterior). The bottom panel is the axial cross-sectional area of the airway plotted against the axial slice index. Slice index increases in superior direction.

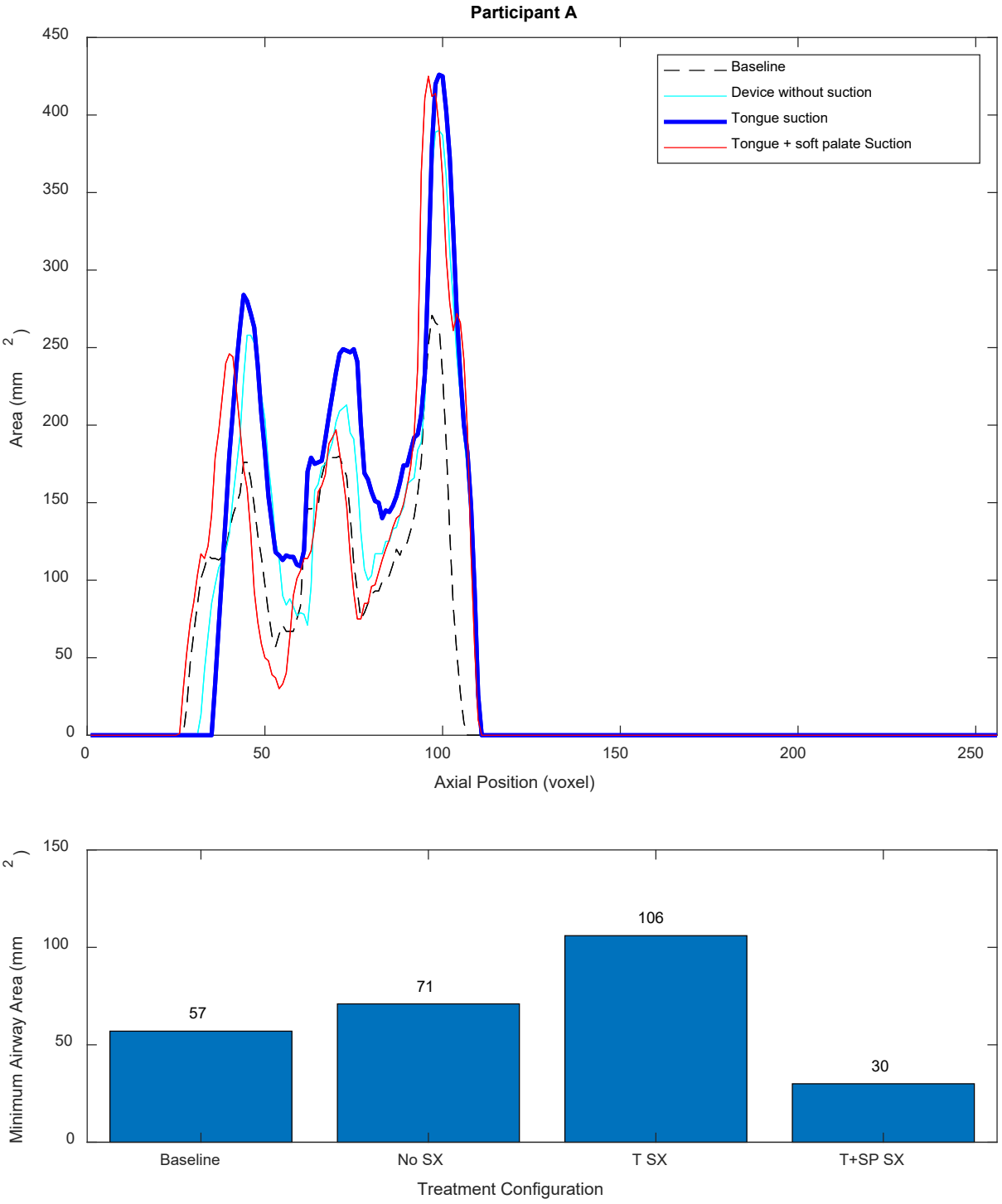

Figure 3-16: Minimum airway cross sectional area of participant A measured with MRI for 4 configurations of treatment defined in Section 3.3.2

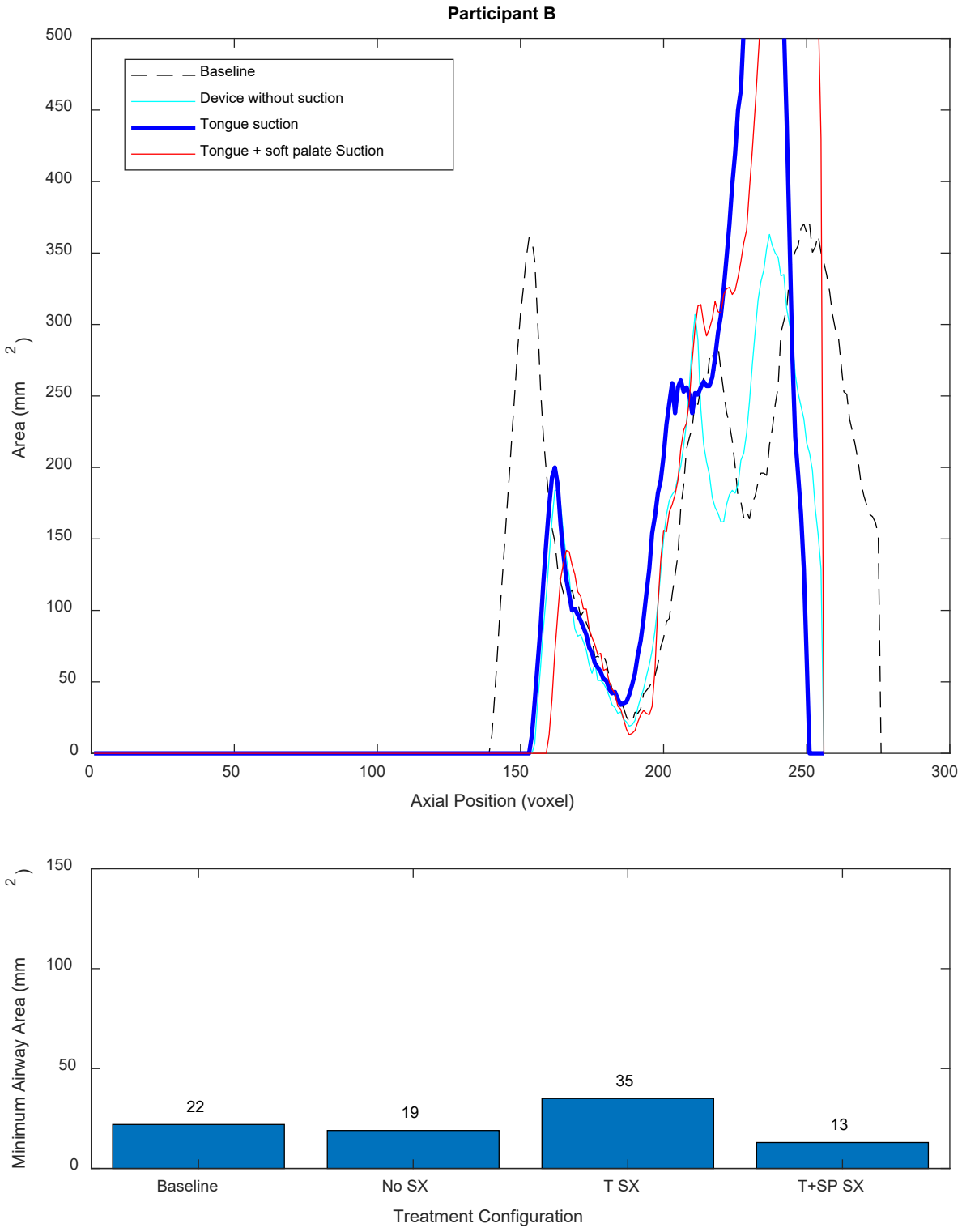

Figure 3-17: Minimum airway cross sectional area of participant B measured with MRI for 4 configurations of treatment defined in Section 3.3.2

3.4 Endoscopic Imaging

This study includes 1 subject (male, age 27 years) wearing a modified oral device with posterior wall removed and an opening under incisor location in order to pass endoscope into the perforated layer (Figure 3-18). The posterior opening exposes soft palate to suction and allows the endoscope to view the soft palate directly. The modified oral device was connected to a pump unit set to -50mmHg. The subject was instructed to swallow in order to make the posterior of tongue contact the soft palate in order to establish a vacuum in the sealed cavity formed by maxillary arch, soft palate and tongue. The digital endoscope is placed in the perforated layer to acquire video.

Using endoscopic imaging, we could visualize the movement of the soft palate. Figure 3-19 shows that the soft palate is drawn forward when a vacuum of -50mmHg is applied to the soft palate with a modified oral device. This endoscopic study demonstrates efficacy of soft palate suction and warrants further exploration in future device iterations.

Figure 3-18: Modified oral device and endoscope

Figure 3-19: Soft palate is drawn forwards by -50mmHg of intraoral vacuum visualized by a digital endoscope.

4 Finite Element (FE) Modeling

4.1 Overview

The framework to model the tongue with finite element method has been established and improved for a long time in context of speech reproduction [36], oncology [37], and general biomechanics [38]. The tongue can be modeled with its general shape and with fiber directions calculated instead of measured with adequate model performance [36]. In recent years, the advancement in Magnetic Resonance Imaging (MRI) technology such as diffusion tensor (DT) MRI, diffusion spectrum (DS) MRI and dynamic MRI, as well as the increase in availability of MRI facilities, have led to the wide usage of MRI data to create high fidelity patient-specific finite element model of the human tongue. The method of acquiring fiber orientation and to some extent, material properties from DT-MRI and DS-MRI have been established [37]–[40].

In the context of sleep medicine, finite element method is widely adopted to model human upper airway in order to simulate OSA [41]–[43] and evaluate treatment devices [44], [45]. At the time of writing, no finite-element study of oral pressure therapy (OPT) devices has been published, nor any of the existing studies focus on the effect of external forces directly applied to the tongue. Therefore, we develop a finite element model of the human tongue and upper airway to study the interaction between OSA and our treatment device.

4.2 Methods

This section describes a finite element model of the tongue, soft palate and a portion of airway in Abaqus. The objective for this model is to simulate OSA and to study the interaction between OSA and our treatment device.

This FE model employs Holzapfel orthotropic hyper-elastic material model [46], [47] for the tongue, and Neo-Hookean isotropic hyper-elastic model for other tissues being simulated. The geometry is derived from T2 image of participant A in the MRI study described in Section 3.3. The material orientations of the simulated tongue are set by muscle fiber orientations derived from DT-MRI image of the same participant. The material properties of tongue muscle were initially set to values presented in [48], then tuned iteratively using inversed finite element method (iFEM) [49] to reproduce the obstruction as seen in the sleep MRI image produced by Volner et.al [50]. Once the simulation of OSA is established, it can be used to study the interaction between OSA and our treatment device.

4.2.1 Derivation of Geometry from T2-Weighted MRI Image

First, the T2 MRI image was segmented using ITK-SNAP (Figure 4-1). The tongue and soft palate were segmented to be modeled. The mandible bone marrow was segmented to locate boundary conditions that represents where the tongue is affixed by the mandible. The posterior of pharynx airway was also segmented so the model can simulate the constriction and dilation of the airway. The segments were exported as surface mesh then imported into Autodesk Fusion for post-processing. The post-processing involves reduction of the mesh count, removal of any dangling mesh nodes and conversion into solid parts (Figure 4-2). The solid parts were exported into IGES format and imported into Abaqus. Meshing and assembly of parts was performed in Abaqus. (Figure 4-3) In preparation of the subsequent assignment of material orientations[2] to the tongue, the FE mesh of the tongue was written to an Abaqus Input file in plain text format.

[2] Geometry can also be derived DTI image directly to avoid registering T2 to DTI. In this model, segmentation from T2 is preferred since T2 has much higher spatial resolution and contrast than DTI, making it easier to segment as well as producing a more accurate anatomical representation.

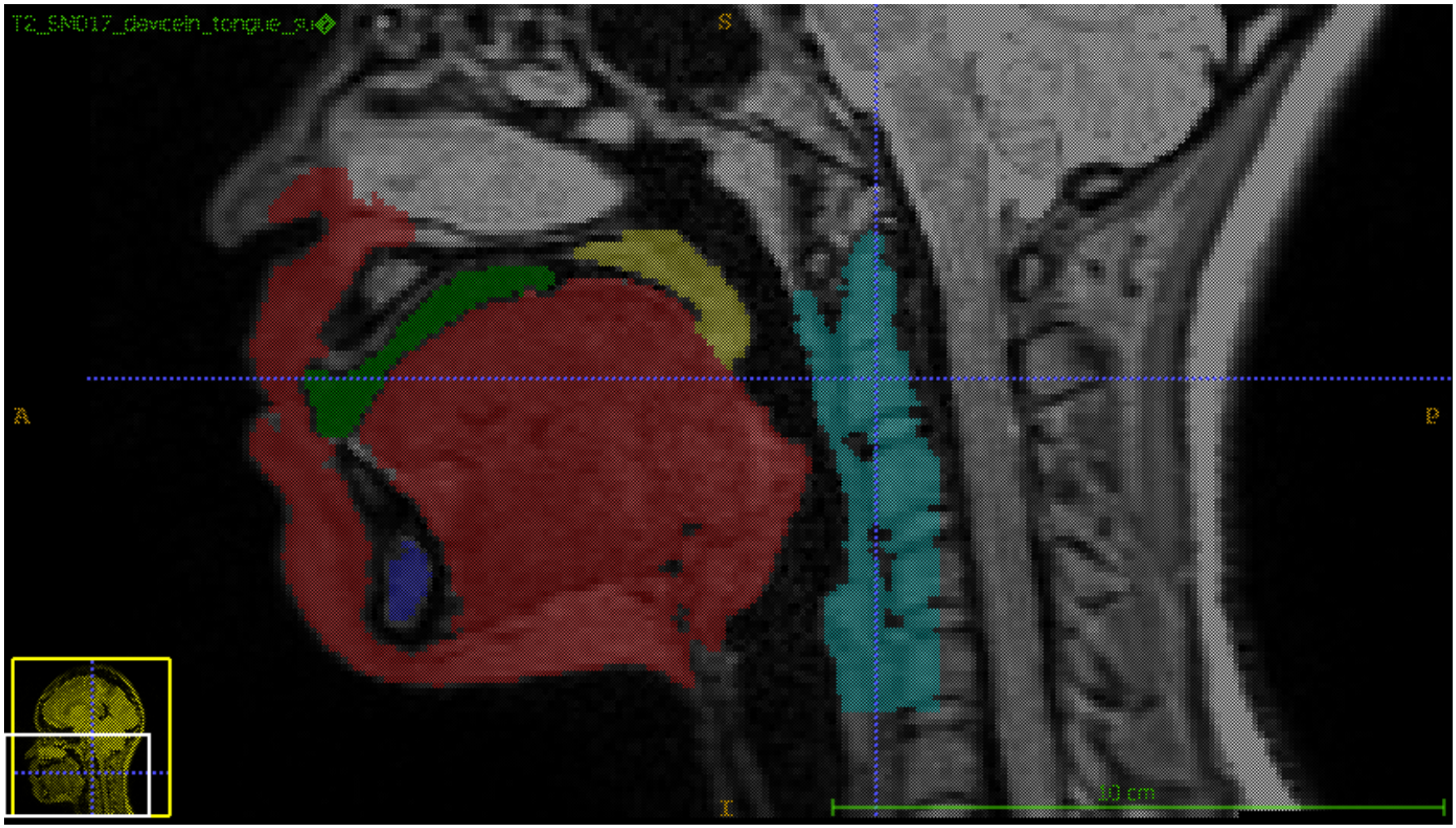

Figure 4-1: Segmentation of tongue (red), soft palate (yellow), oral device (green) and a portion of airway (cyan).

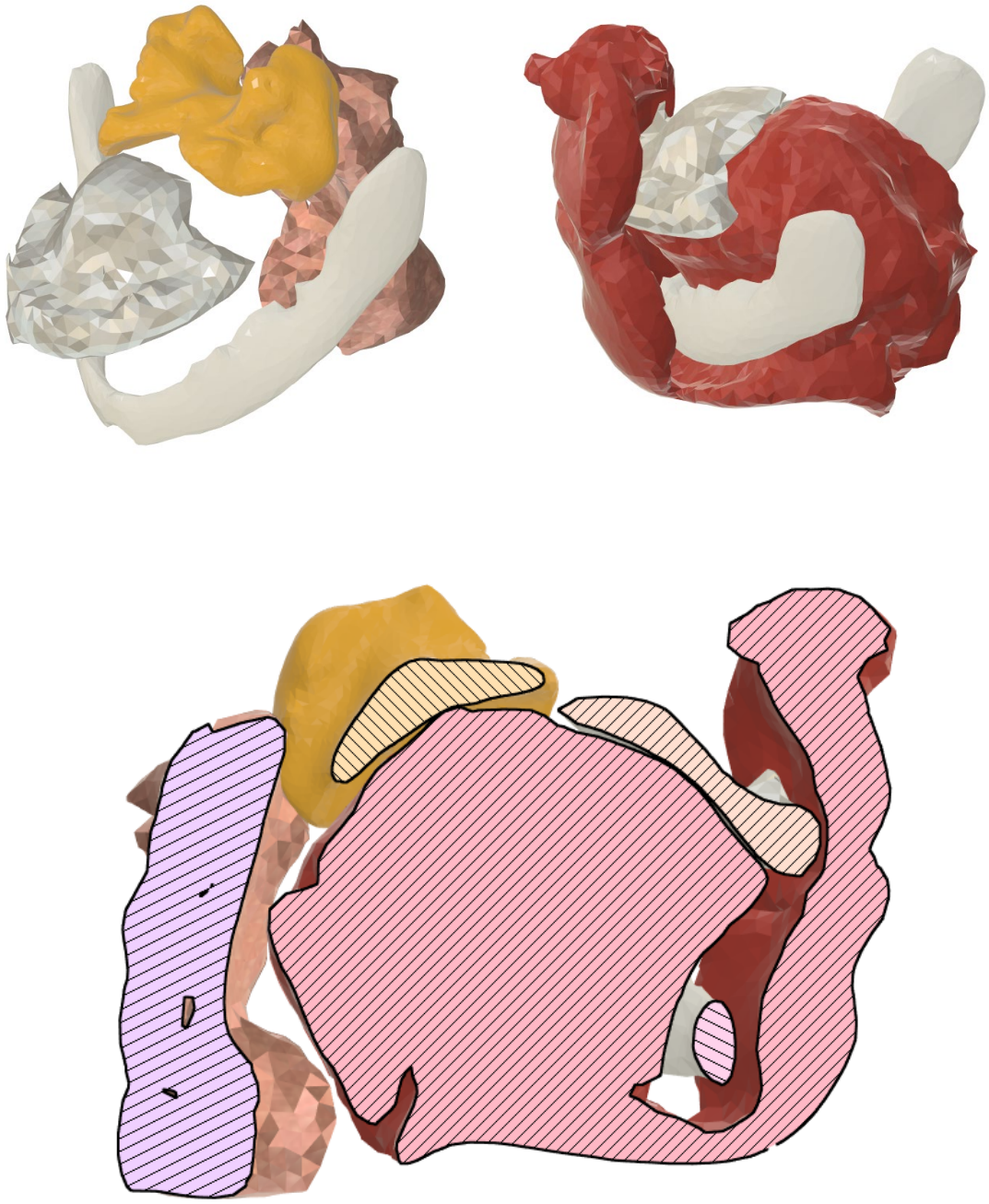

Figure 4-2: Solid representation of tongue (red), soft palate (yellow), posterior of the pharynx space (copper), bone marrow of the mandibular bone (white), and oral device (silver). Bottom panel shows a center-sagittal cross-sectional view.

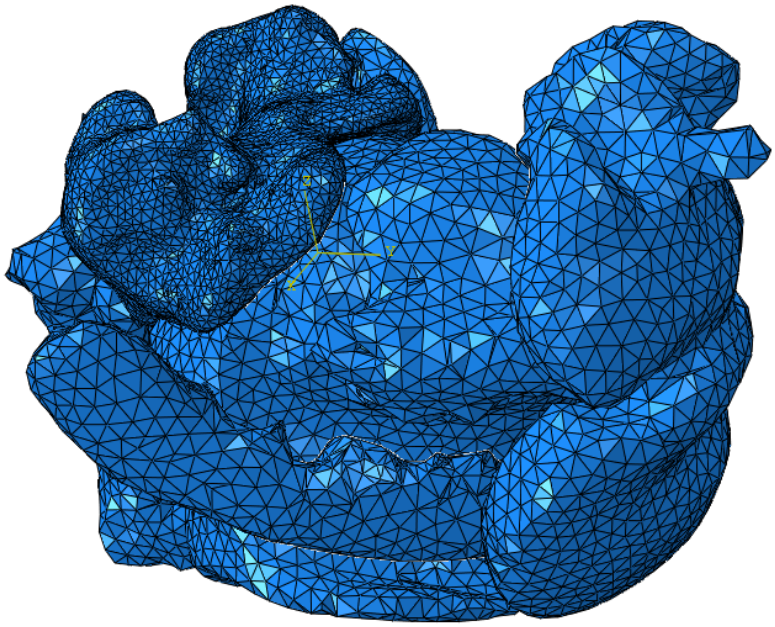

Figure 4-3: The anatomical solid representation of tongue is imported into Abaqus and meshed.

4.2.2 Assignment of Material Orienation from DT-MRI Image

First, DT-MRI image was affinity-registered onto T2 image (that provided anatomical geometry) to correct misalignment and distortion caused by patient movement between T2 and DTI sequence. Then, the eigenvectors and eigenvalues of the DT-MRI image were read into MATLAB, and dominates eigenvectors (Figure 4-4) were extracted since they represent the fiber orienation of the tongue. The obtained fiber orienation (Figure 4-5) was compared against tractography (Figure 4-6) obtained with TrackVis Diffusion Toolkit [51] for a sanity check[3].

Then, the FE mesh of the tongue was read into MATLAB from the Abaqus Input file generated in Section 4.2.1.1. The orientation of each Abaqus element was calculated from the DT-MRI eigenvectors using nearest-neighbor interpolation. If one element spans multiple voxels,

[3] One may also use tractography to set material orientation. However, in this thesis, the raw DT data is used for the sake of simplicity.

the orientation of the closer voxel is used. Every element now has its orientation assigned (Figure 4-7).

Finally, the material orientation data was written back into the Abaqus input file. This input file was imported into Abaqus so that the resulting tongue model with material orientation is ready to be manipulated. The material orientation as viewed in Abaqus is shown in Figure 4-8.

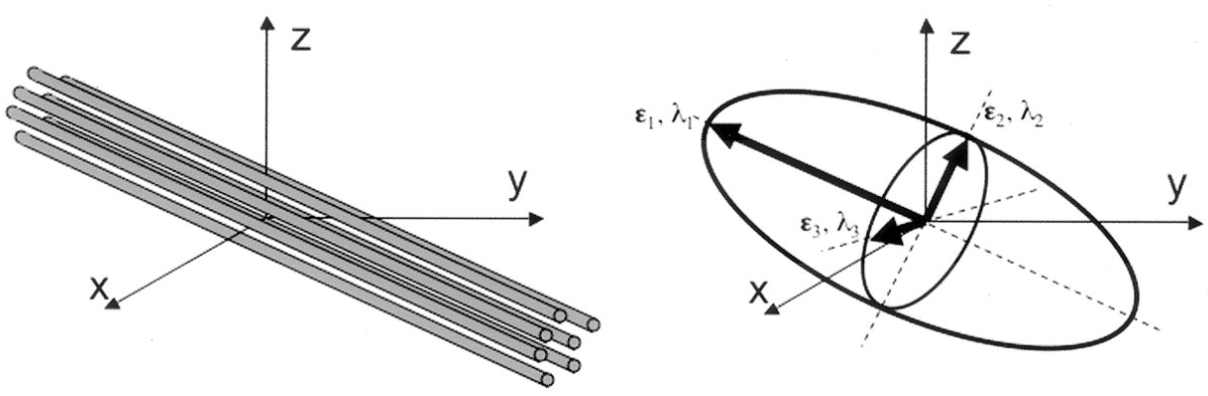

Figure 4-4: Definition of eigenvector and eigenvalues of processed DT-MRI image [52].

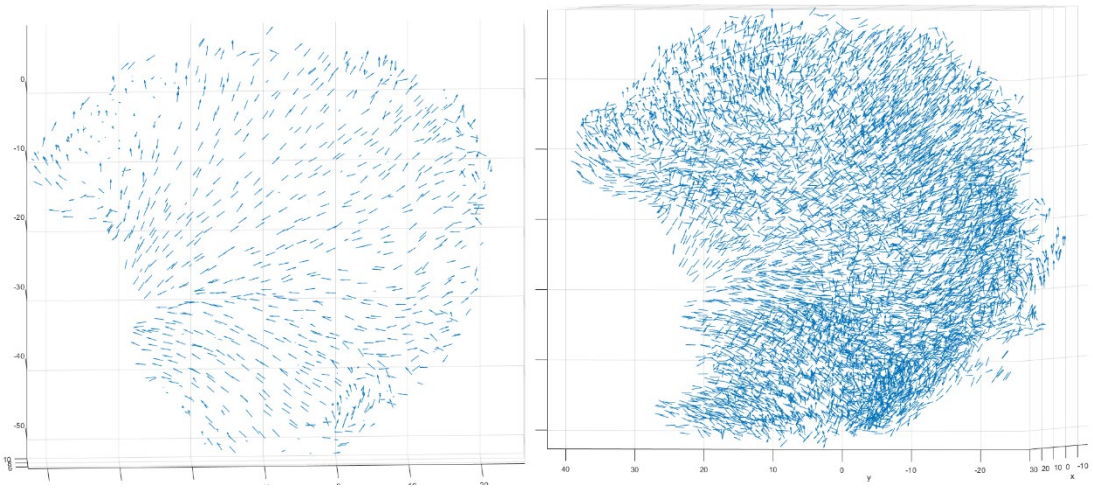

Figure 4-5: Dominate eigenvectors of the human tongue. Left panel shows a single sagittal slice and right panel shows the whole tongue.

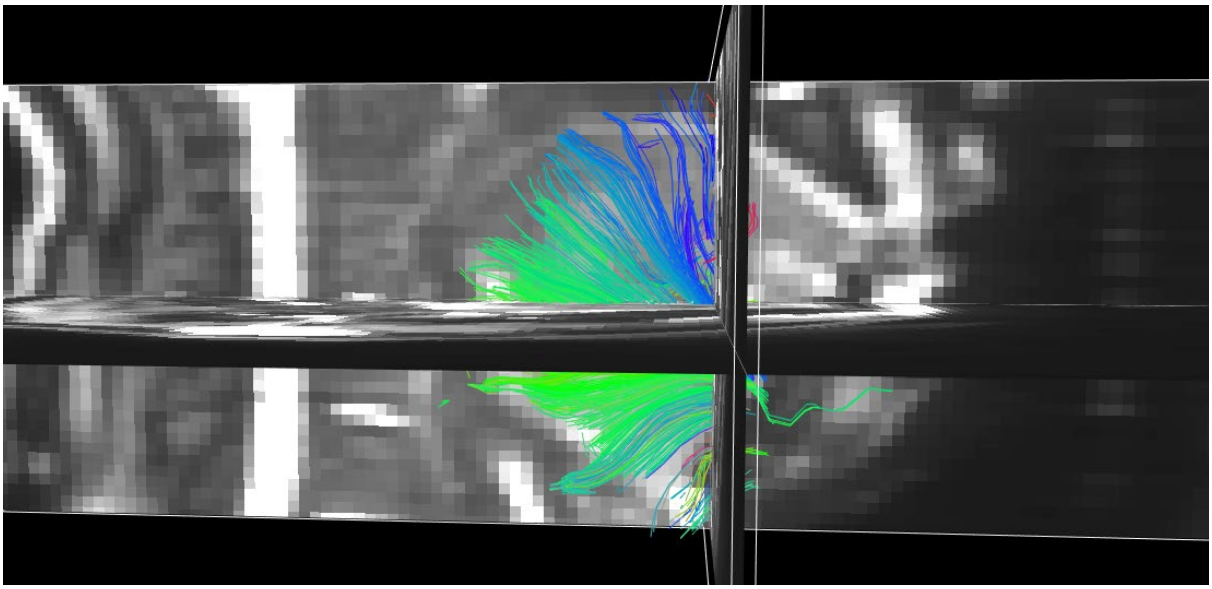

Figure 4-6: Tractography of tongue.

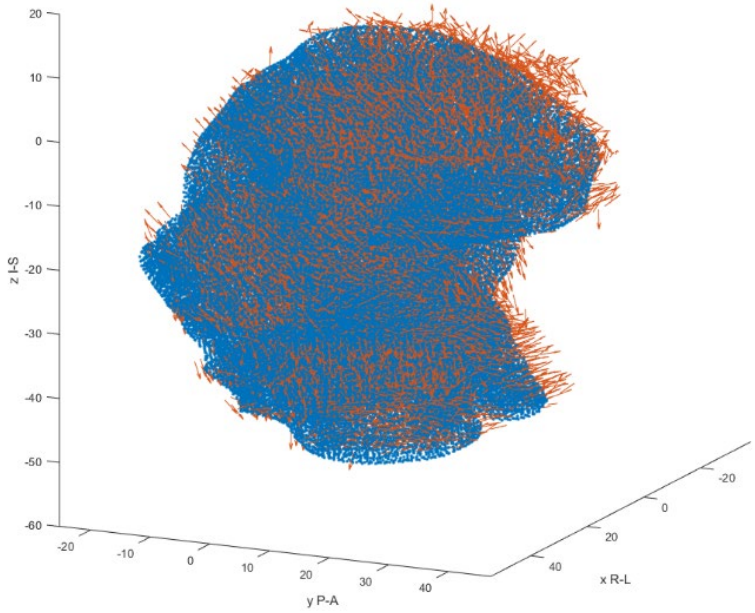

Figure 4-7: Fiber orientation assigned to tongue, plotted as vector arrows.

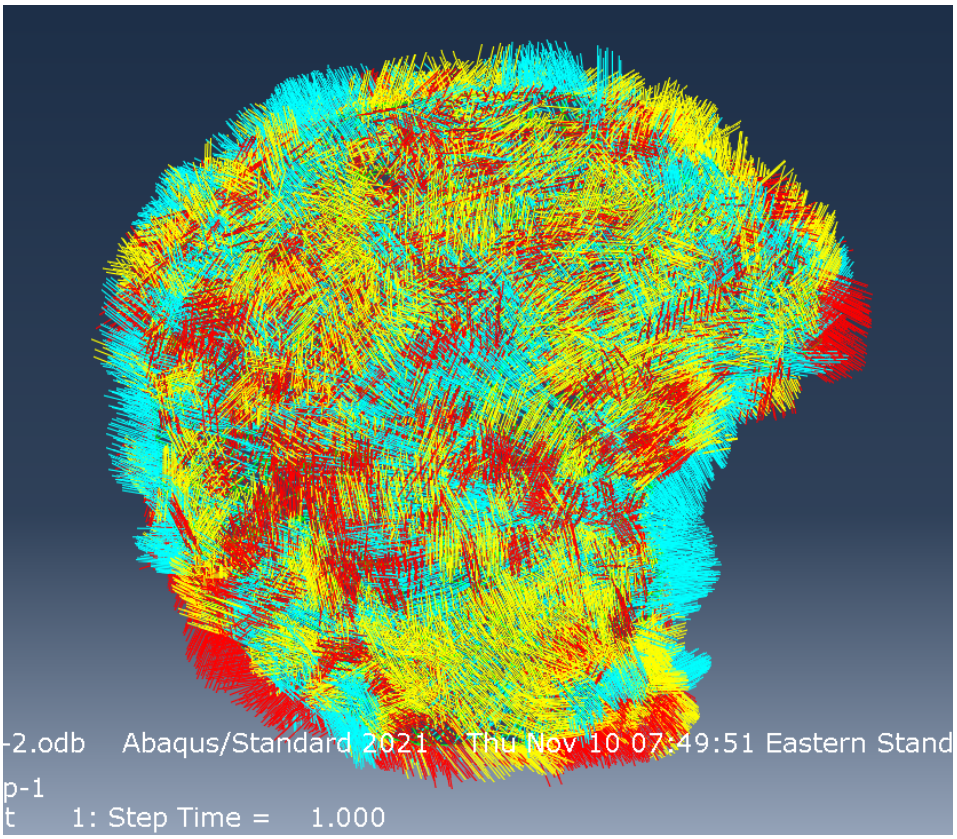

Figure 4-8: Material orienation of the tongue model as viewed in Abaqus.

4.2.3 Loads and Boundary Conditions

A gravity load of 1G was applied globally. An inspiration pressure of –30 mmHg [53] was applied to the posterior of tongue as a worst-case load without nasal obstruction. The boundary conditions representing the mandible and maxilla is shown in Figure 4-9. The inspiration pressure load is shown in Figure 4-10.

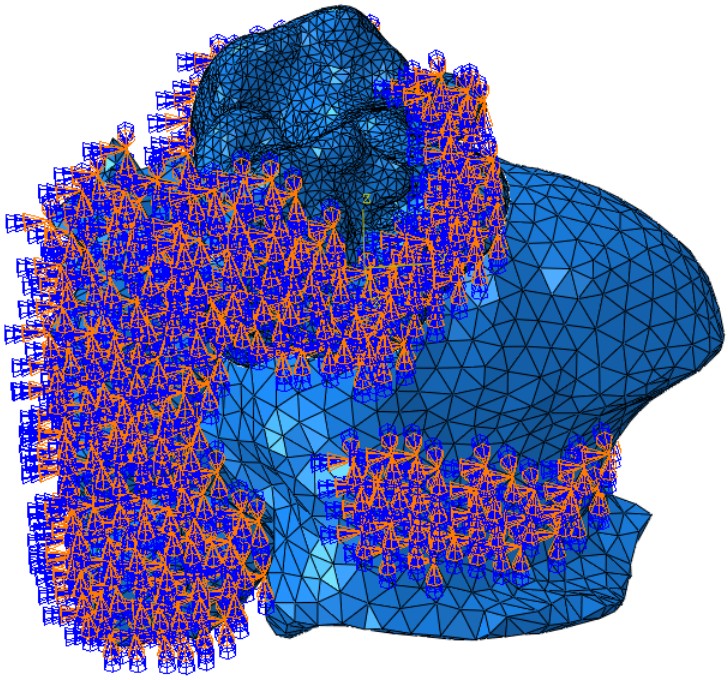

Figure 4-9: Boundary conditions (BC's) representing the mandible is applied to the tongue. BC's representing the maxillary bone is applied to the soft palate, The posterior of the airway section is encastred immobile by another group of BC's.

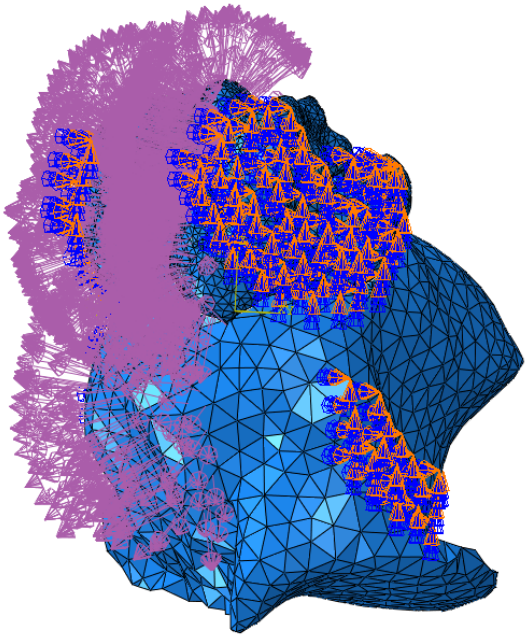

Figure 4-10: Inspiration pressure is represented as purple arrows. Gravity is not shown.

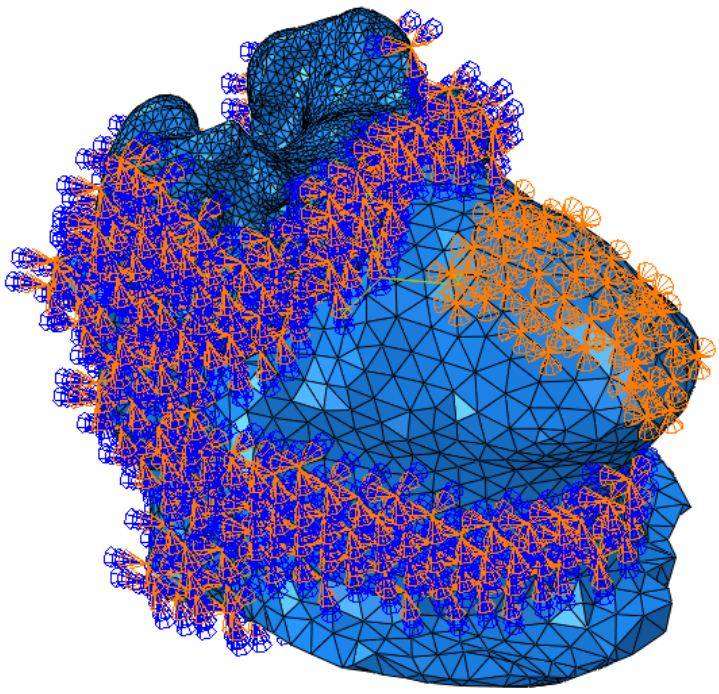

Figure 4-11: The treatment device is simulated as the boundary conditions shown in orange.

4.2.4 Tuning and Simulation

Inverse finite element method was applied here to find the correct set of material properties that leads to the realistic simulation of apneic episodes. Simulation was executed repeatedly with material properties adjusted manually between each iteration, until the result is comparable to the reference apneic episode imaged with sleep MRI. (Figure 4-12b). The material properties found and the simulated OSA is reported in Results section. The simulated apneic episode is reported as 'No Treatment' case. At this stage, a patient-specific OSA simulator was established and ready to be used to evaluate our treatment device.

To simulate treatment, an additional boundary condition was applied to the 'No Treatment' case to simulate the oral device. The node on the surface of tongue contacting the treatment device was encastred (rendered immobile) as shown in Fig 4-11. The simulation was executed and the result is reported in Results section as 'Treatment' case.

4.3 Results

A finite element model of the tongue, soft palate and a portion of the airway was developed to further understand and characterize the tissue/device interaction and to guide the design of the device.

Figure 4-12a shows the original tongue without any load. Figure 4-12b is a sleep MRI image of a patient having an apneic episode. The image is produced by Volner et.al [50] and used here as a reference to be reproduced by our model.

Figure 4-12c shows the model successfully reproduced the airway obstruction caused by tongue and soft palate falling posteriorly when subjected to gravity and respiratory pressures. To match the model response to actual OSA cases, the material properties of the Holzapfel hyper-elastic tongue model is tuned to $C_{10} = 800$ Pa, $D = 18$ MPa-1, $k1 = 1200$ and $k2 = 0.1$. This number fall within range of human muscle. [54]

The displacement of the posterior of the tongue is 7.9mm under gravity of 1G and inspiration pressure of –30 mmHg, without treatment.

Figure 4.12d shows a simulated OSA treatment using our oral device described in Section 2. The oral device is modeled as a boundary condition constraining surface nodes in the treatment area. The boundary condition created a reaction force of 1.02N in the anterior direction and 0.21N in the superior direction. The simulated treatment is successful as tongue does not obstruct the airway. The displacement of the posterior of the tongue is reduced to 1.2 mm.

Figure 4-13 shows the axial cross-sectional view of the narrowest part of the airway of the no-OSA, simulated untreated OSA and simulated treated OSA in order to illustrate the size of the airway. Figure 4-14 shows non-loaded geometry superimposed onto untreated and treated geometry to illustrate the predicted efficacy of our oral device.

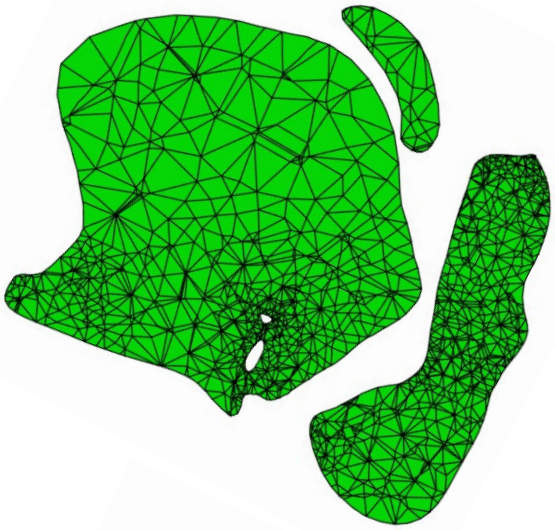

(a) No load applied

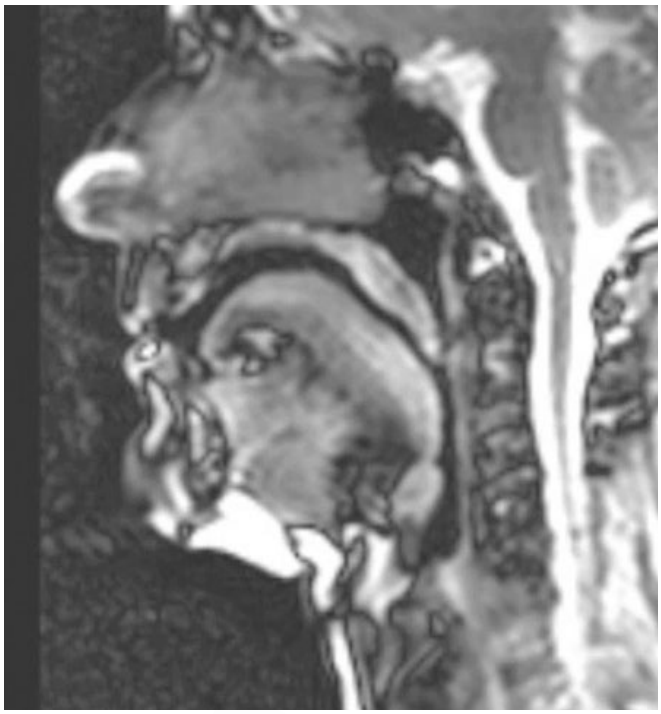

(b) Sleep MRI showing apneic episode

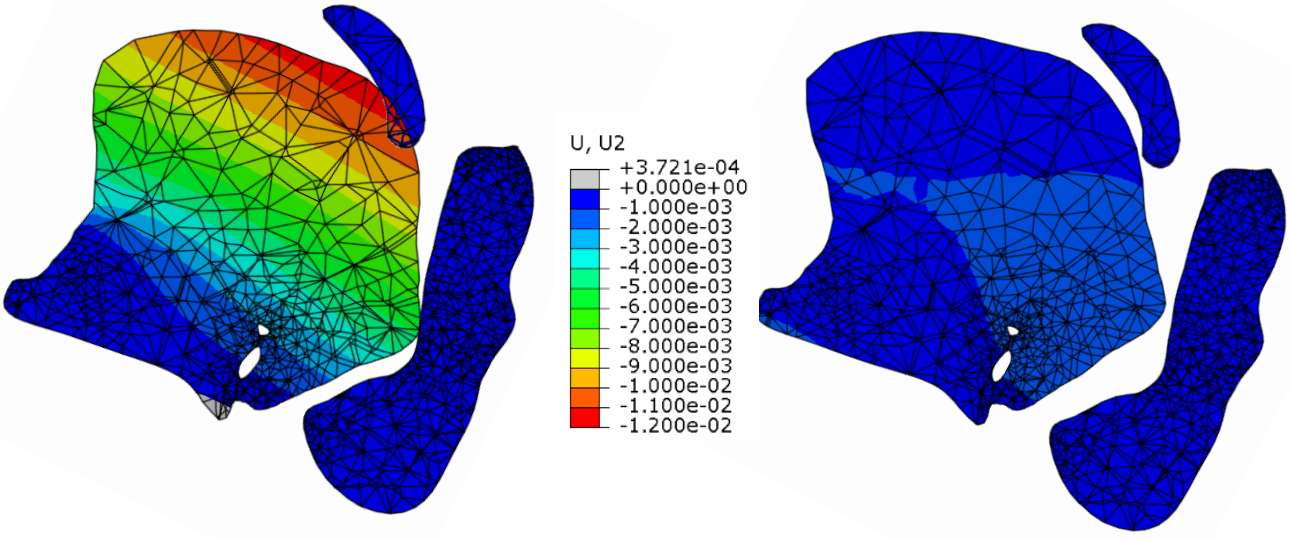

(c) Simulated apneic episode

(d) Simulated treatment applied

Figure 4-12: Simulating OSA and treatment with our oral device. (Center sagittal slice). Color indicates displacement in Y direction (+Y is anterior). Color scale is in meters. Panel (c) and (d) are plotted with the same color scale. Color scale is not applcable to (a).

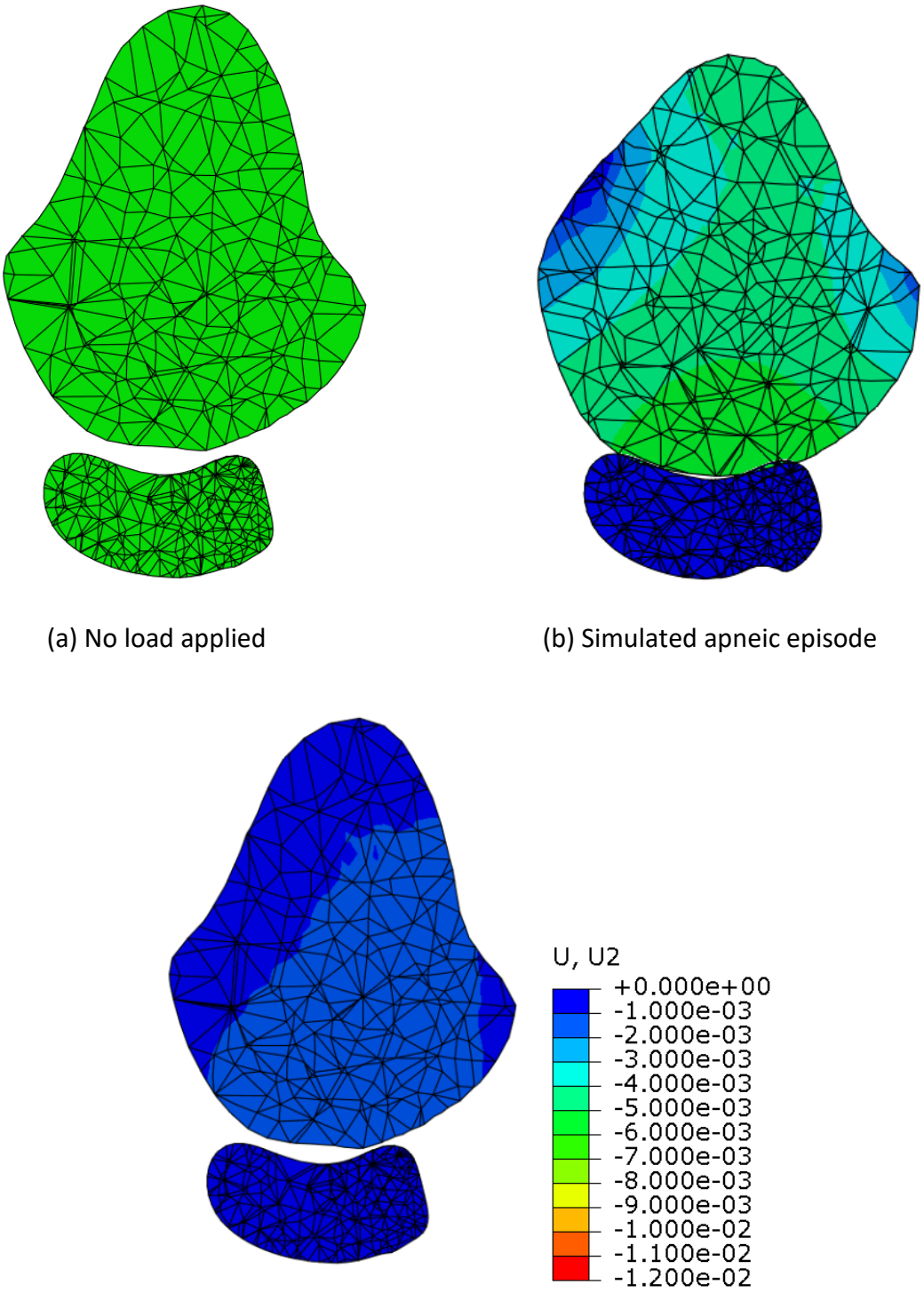

(a) No load applied

(b) Simulated apneic episode

(c) Simulated treatment applied

Figure 4-13: Axial cross-sectional views sliced at the narrowest site of airway. Color indicates displacement in Y direction (+Y is anterior). Color scale is in meters. Panel (b) and (c) are plotted with the same color scale. Color scale is not applcable to (a).

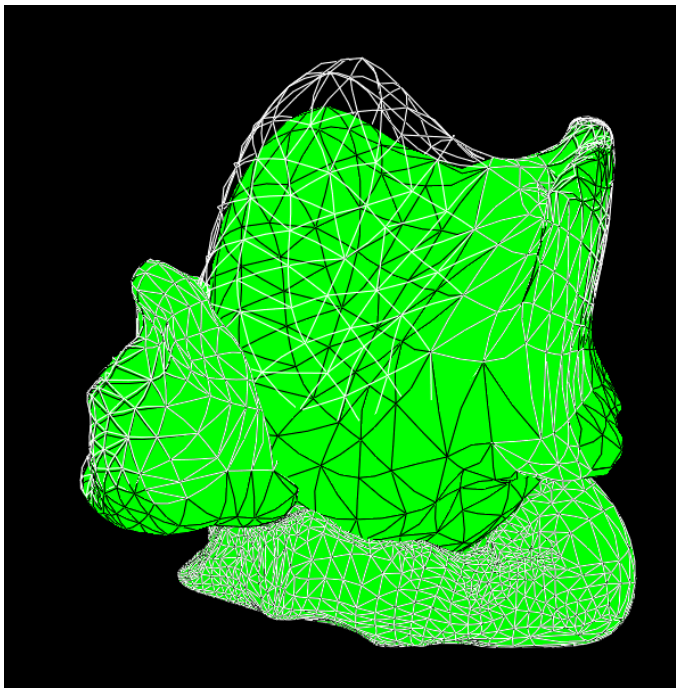

(a) Untreated

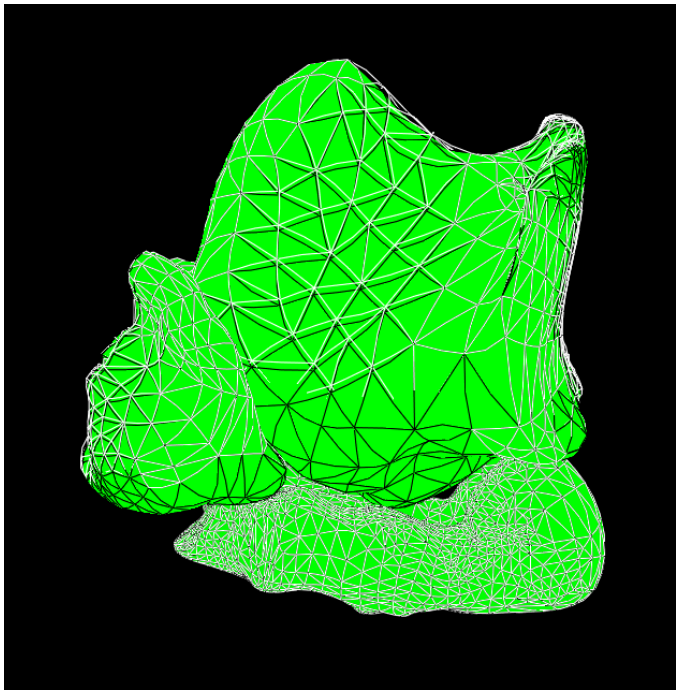

(b) Treated

Figure 4-14: Superimposed plot of treated simulation versus untreated simulation. White wireframe plot represents non-loaded geometry corresponding to awake position.

5 Discussion

In this thesis, we report a novel device for obstructive sleep apnea, and characterize the mechanism of action with a finite element model and endoscopic study. Further, we demonstrate safety and efficacy of the device with a 5-subjects clinical study. We report that the device is capable of stabilizing the tongue for >90% of the time when the device is worn.

During sleep, the tongue moves, and this device stabilizes the tongue in its natural resting position as opposed to fixing it securely. This stabilization combined with adequate suction control makes the tongue instantly re-latch to the oral device upon temporary unlatching.

OSA episodes typically occur when there is no signal in the hypoglossal nerve, the tongue is relaxed and falls posteriorly under the combination of gravity load and respiratory pressure and causes obstruction. In this case, the tongue would have a lower tongue muscle force acting against the device that what we observed in healthy volunteers with intact hypoglossal nerve stimulation. In OSA patients, the device would need to work against gravity and respiratory pressure, but not against tongue muscle contraction. Based on this hypothesis, we performed computational modeling on a relaxed tongue and set the treatment pressure to be adequate to hold a relaxed tongue in place.

Re-positioning of tongue to the stabilized position was demonstrated by the tongue stabilization study. Other tongue retention devices require a complex recovery process if the tongue becomes unlatched – for example, manually pushing the tongue back into a chamber hanging outside of the patient's lip, or swallowing with the tongue in the correct position to re-engage whole-mouth suction. Conversely, our device takes advantage of the tendency of the wearer to reposition the tongue into its resting position, thus ensuring a high percentage of successful treatment recovery or relatching. In the sleep study, we proved that our device would not cause additional obstruction by proving the statistically insignificant change in AHI on healthy volunteers who have an AHI less than 10.

In the MRI study, we showed that the device enlarges the airway. Since healthy and awake patients are used in the study, this airway enlargement is not related to the prevention of tongue falling posterior, as would be the case in OSA patients. There are two factors contributing to airway enlargement; first, the nightguard provides a 1.2-1.5mm thickness between the upper and lower molars. This effectively jacks the mouth open by several degrees and changes the geometry of the mouth so that the tongue is moved anteriorly and caudally, and surrounding oral tissue is also moved anteriorly, resulting in dilation of pharynx cavity. Second, as airway enlargement is more pronounced when suction is applied, we hypothesize that suction suspends the tongue against the device so the patient does not have to contract the tongue or exert a force to maintain the tongue in the resting position. This causes the tongue to relax and may affect the strain distribution around the pharynx or lingual tonsil, indirectly causing the airway to dilate.

The endoscopic study allowed us to visualize the anterior movement of the soft palate with a modified oral device, but we did not observe the same movement in the MRI study. Instead, the posterior aspect of the tongue moved upwards and obstructed the posterior opening of the oral appliance. We hypothesize that in the endoscopic study, the volunteer can see the video feed and subconsciously kept their tongue down allowing the soft palate to be exposed to suction and moved forward. In contrast, in the MRI study the volunteer did not have visual feedback of their oral cavity and did not maintain the tongue in that position. During use, the participant would not have visual feedback. Thus, the endoscopic study proves that the mechanism of using suction to move soft palate forwards is valid, but we have primarily focused on tongue stabilization, without soft palate suction. We posit that tongue suction is superior to tongue and soft palate suction due to the ease of latching of the tongue to the oral device. In the future, if the anatomy of the patient is more suitable for soft palate suction – for example, a patient with a large soft palate that causes obstruction – a device optimized for soft palate suction can be designed.

Finally, for the finite element model of the tongue and airway, we reproduced obstruction similar to sleep MRI data produced by Volner et al [50] by tuning the tongue material properties. Next, we showed that our device can treat this condition by stabilizing the tongue in the rest position. Our model assumes that the tongue is in a ‘zero-gravity’ condition when the person is

awake since the muscle actuation force balances out any gravity load or respiratory pressure. Thus, the rest shape and position of the tongue becomes the no-load shape of the tongue. Subsequently, gravity, respiratory pressure and treatment boundary conditions are applied. The suction from the oral device was applied as a boundary condition since the objective of our model was to measure the force required to stabilize the tongue. The model may require refinement with the passive tongue properties of a patient with OSA, but serves as a good proof-of-concept to guide the device design. The force predicted by the model was demonstrated to be efficacious in the clinical study.

6 Future Work and Outlook

Currently, the perforated layer of the oral device is a hand drawn spline that we deemed fit for patient using trial and error. The computational model can be further explored to optimize the shape of the perforated layer to achieve maximum traction with minimum pressure thus improving comfort and efficacy.

The shape of the opening on the perforated layer is currently a hexagonal mesh with size determined by trial and error to achieve acceptable traction and comfort. In the future a viscoelastic model of the tongue should be made to interact with the treatment device to determine the optimal shape and size of the openings in the perforated layer to achieve maximum traction with minimum pressure and minimum local tongue deformation, thus improving comfort and efficacy.

A clinical trial with OSA patients is planned to commence in Summer 2023 at the Veterans Affairs hospital in Boston. This study with OSA patients, instead of healthy volunteers, is absolutely necessary to prove the efficacy of this device to reduce AHI and improve quality of sleep for OSA patients. If successful, this could change the paradigm of treatment for those suffering from OSA with a discrete oral device replacing a cumbersome, bulky CPAP device.

Appendix A: Design and Manufacture of the Oral Device

Renderings and a photograph of the oral device are shown in Figure 2-3. The oral device consists of a dental interface and a perforated layer. The oral device can be manufactured with dental interface and perforated layer as one body or as an assembly.

The dental interface takes the form of a dental device such as nightguard, retainer or aligner. The dental interface affixes the oral device to patient's upper palate (maxillary arch) and could serving dental purposes such as preventing damage from bruxism, or aligning teeth.

The perforated layer directs externally provided suction towards tongue and/or soft palate through a number of opening at various locations to stabilize the tongue and/or soft palate to prevent them from obstructing the airway. The form and location of perforated layer might vary from patient to patient based on patient condition, oral geometry, and required intensity of treatment.

A suction tube and a sensing tube are connected to the perforated layer, routed out of patient's mouth, and connected to the pump unit. Separate suction and sensing tubes are used in order to measure the pressure within the perforated layer without being affected by the pressure drop in the length of tubing.

A.1 Form and Construction

The current iteration of oral device employs a patient-specific upper-jaw bruxism nightguard as the dental interface. The perforated layer is a configurable suction chamber that can deliver suction to tongue, soft palate, or both.

The tubing in the current iteration is of biocompatible Tygon® material, with internal diameter of 1/16 inch, and of 6 feet length to accommodate the bedside pump unit.

The current iteration of oral device is constructed using the following steps:

- Oral scan with 3Shape TRIOS® dental 3D scanner using standard nightguard protocol. The 3D scan captures patient's upper jaw, lower jaw and bite occlusion. (Figure A-1)

- The scan is pushed to 3Shape Automate® platform to automatically generate a patient-specific nightguard (Figure A-2).
- The perforated layer is designed in Autodesk Fusion with tongue-facing surface approximates the at-rest tongue shape (Figure A-3), and palate-facing surface match the shape of hard palate obtained from upper jaw scan (Figure A-4).
- Connectors and channels for tubing are designed in Autodesk Fusion. The location and shape of the connector and channel is adjusted per patient to suit oral / dental geometry. (Figure A-5)
- The nightguard, connectors, channels and perforated layer are merged into one body (Figure A-6) and printed in one single piece of material with Formlabs Dental LT V2 resin.

This method of oral device design is suitable to be automated in later stages.

Figure A-1: Illustration of oral scanning and acquired scan. Photo by 3Shape [55]

Figure A-2: Patient specific nightguard generated by 3Shape Automate®. Perforated layer is not yet added by us.

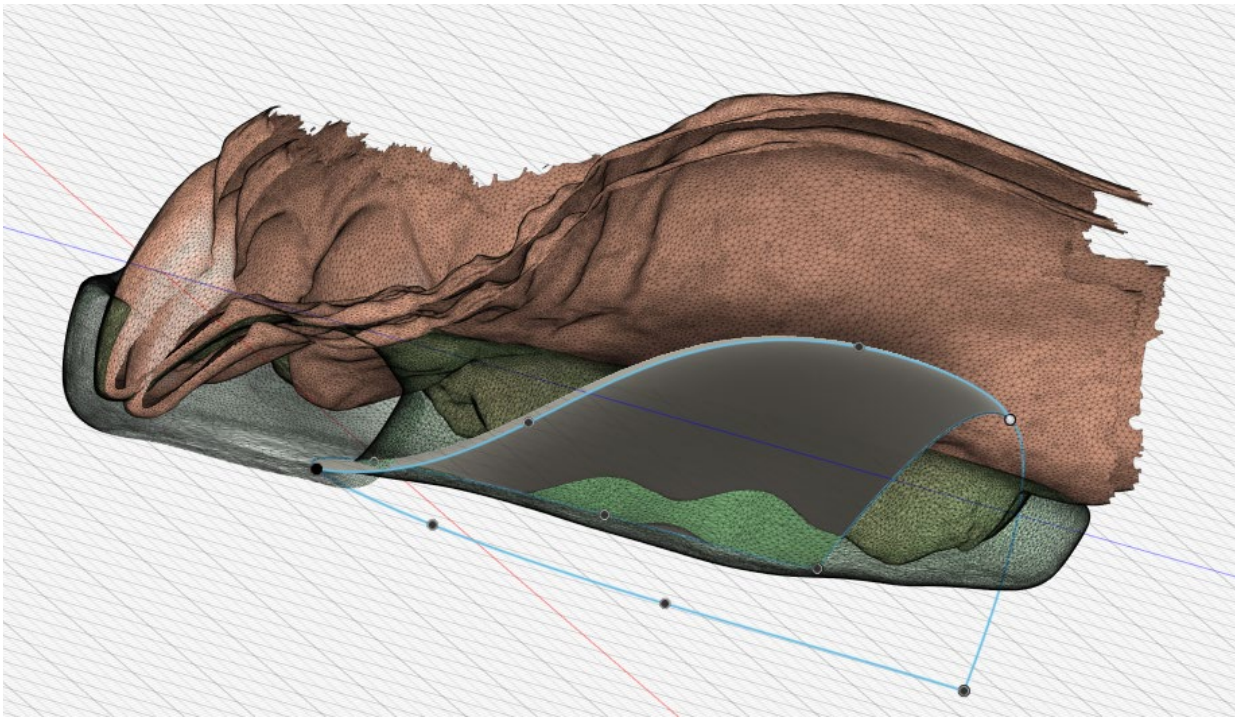

Figure A-3: The tongue-facing surface (grey) is generated from the curve shown in blue. Scan of the upper jaw is shown in tan.

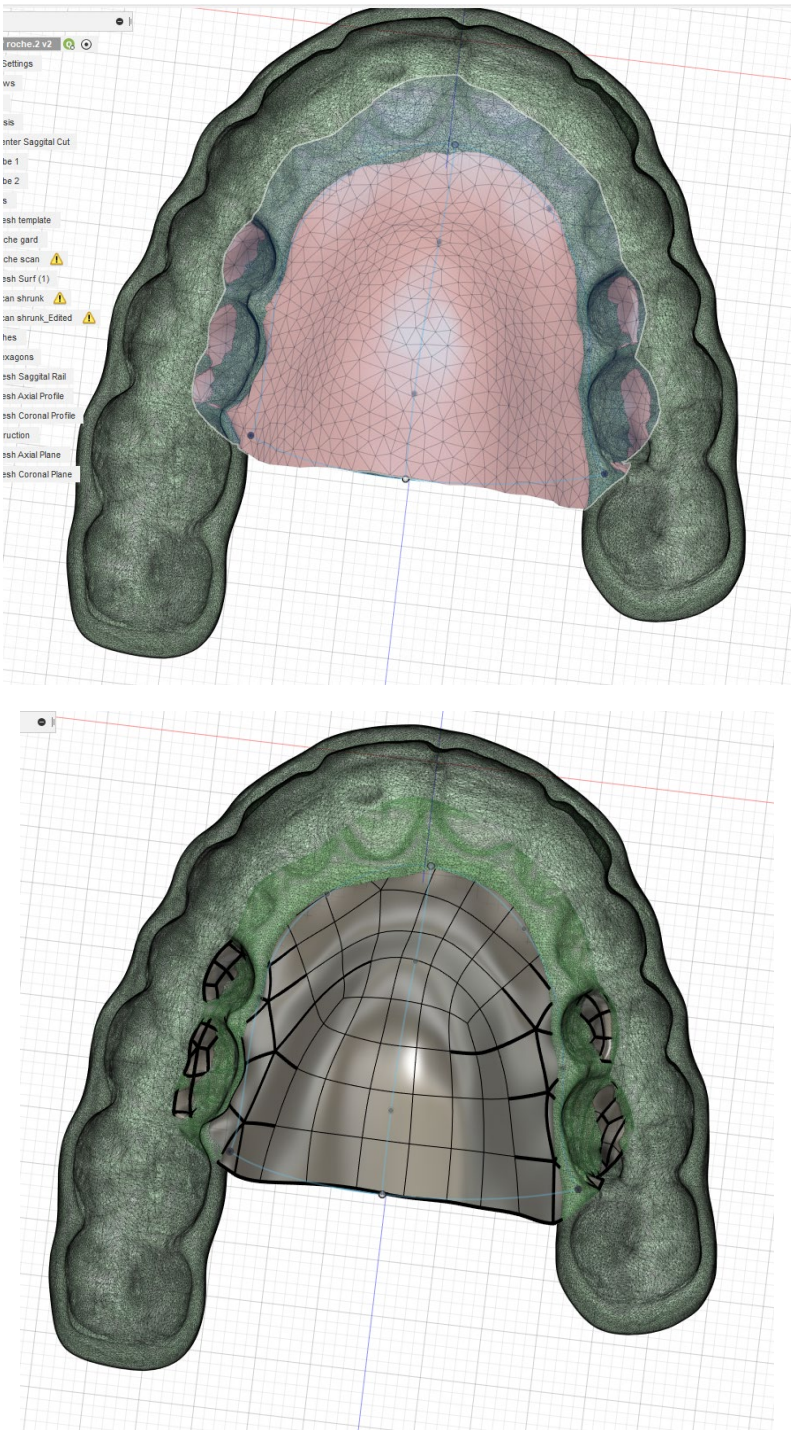

Figure A-4: Upper jaw geometry of the patient is taken from scan, offset, smoothed (top panel) and fitted to a parametric representation shown in bottom panel.

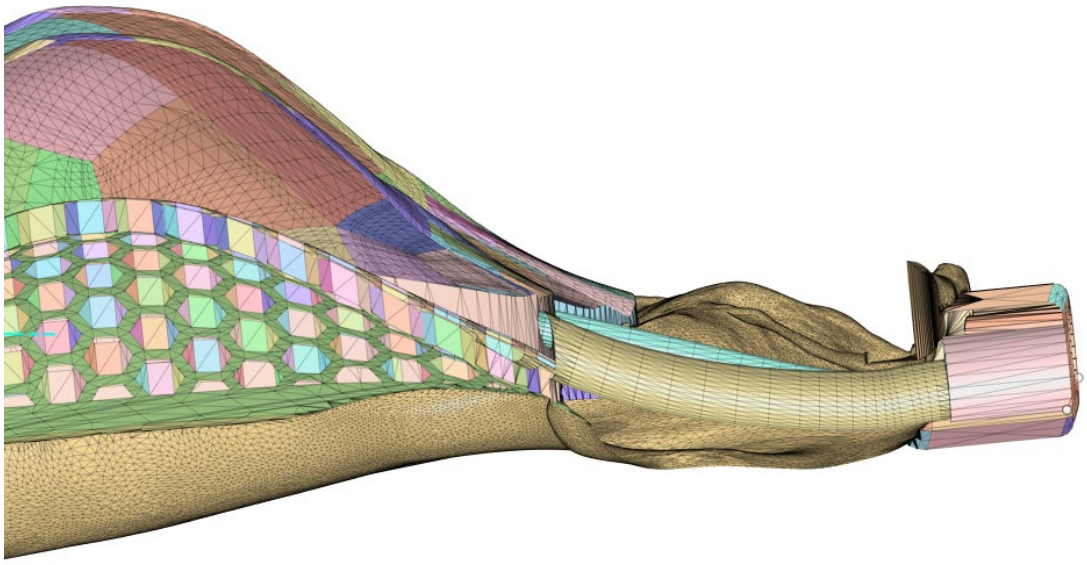

Figure A-5: Embedded channel and socket connectors of the oral device can be seen in this cross sectional view.

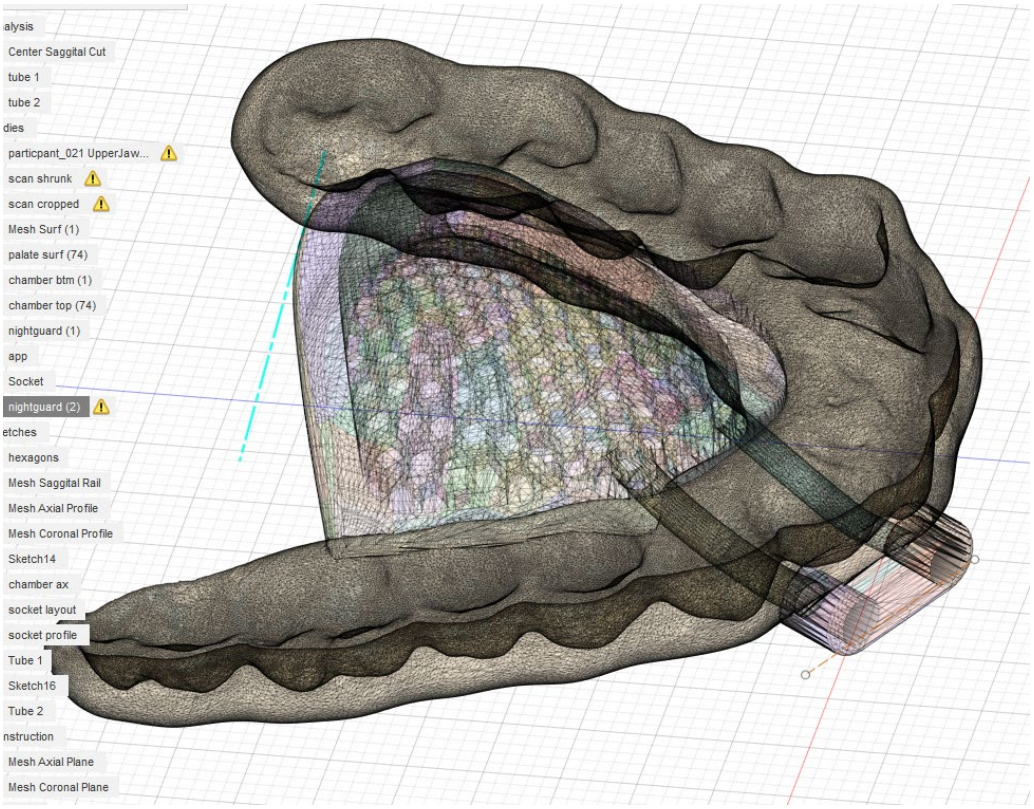

Figure A-6: Oral device ready to be printed. Hexagonal mesh is visible.

A.2 Treatment Delivery

As mentioned in section form and construction, the perforated layer directs suction towards tongue and/or soft palate through a number of openings. The location of opening depends on the treatment type: tongue suction, or tongue-and-soft-palate suction.

When the oral device is worn correctly, the suction is engaged by the creation of a sealed cavity, referred to as ‘latching’. The disengagement of suction caused by the voluntary or involuntary opening of such sealed cavity is referred to as ‘unlatching’.

A.2.1 Latching

Latching is the creation of an intra-oral sealed cavity. Depending on the treatment type the sealed cavity is formed by different tissue.

For tongue-only suction, the sealed cavity is formed by the tongue pressing against the mesh opening of the perforated layer and being affixed by vacuum inside the perforated layer. The tongue is thus prevented from moving posterior and obstructing the airway. The oral device used for this type of treatment is shown in Figure 2-3.

For tongue-and-soft-palate suction, the sealed cavity is formed by tongue, soft palate and the perforated layer. In addition of stabilizing the tongue, the soft palate is being drawn anterior by the vacuum provided by additional opening outside the suction mesh area. In this case, the tongue and soft palate are both prevented from moving posterior and obstructing the airway. Patients are instructed to do a swallow, that moves their soft palate momentarily towards the perforated layer, causing the device to ‘latch’.

Once latched, the pressure in such cavity is maintained by the feedback loop in the pump unit. Any saliva entering the perforated layer is moved through the tubing and being entrapped by the saliva trap in the pump unit.

A.2.2 Unlatching

The disengagement of suction caused by the voluntary or involuntary opening of the sealed cavity is known as ‘unlatching’. Once unlatched, the pressure in the perforated layer is

near atmospheric. The pump unit is capable of decreasing the flow rate in order to avoid excessive saliva extraction, and increase the flow rate again once an attempt of re-latching is sensed.

Appendix B: Design of the Pump Unit

The purpose of the pump unit is to provide a configurable level of suction to the oral device, and to log treatment data and events. A diagram of the pump unit with component callouts is shown in Figure 2-1. A photograph of a working pump unit is shown in Figure 2-6. Figure 2-7 is a simplified hardware-software diagram that illustrates the component and plumbing of the whole system. Figure B-1 shows the internal components of the pump unit.

As shown in Figure 2-1, the oral device connects to the pump unit via two lines. The suction line connects to the saliva trap, which in turn connects to the vacuum pump through hydrophobic filters. Three pressure sensors are implemented at locations shown in Figure B-1 to measure 3 pressures and 2 pressure differentials as tabulated in Table B-1.

The pump unit is protected from contamination by hydrophobic filters at locations shown in Figure 2-1. The components within the box labeled 'disposed between patients' are contaminated by patient and are easily replaceable between patients. Other components of the pump unit remain clean.

Sensor	Pressure Notation	Description
Oral	P_o	Pressure in the perforated layer of oral device
Saliva Trap	P_t	Pressure in the saliva trap of pump unit
Pump	P_p	Pressure of the vacuum pump inlet of pump unit
	$P_{ot} = P_o - P_t$	Pressure-drop from the tubing to oral device
	$P_{tp} = Pt - P_p$	Pressure-drop from the tubing and filter between the saliva trap and vacuum pump

Table B-1: Pressures monitored by the pump unit.

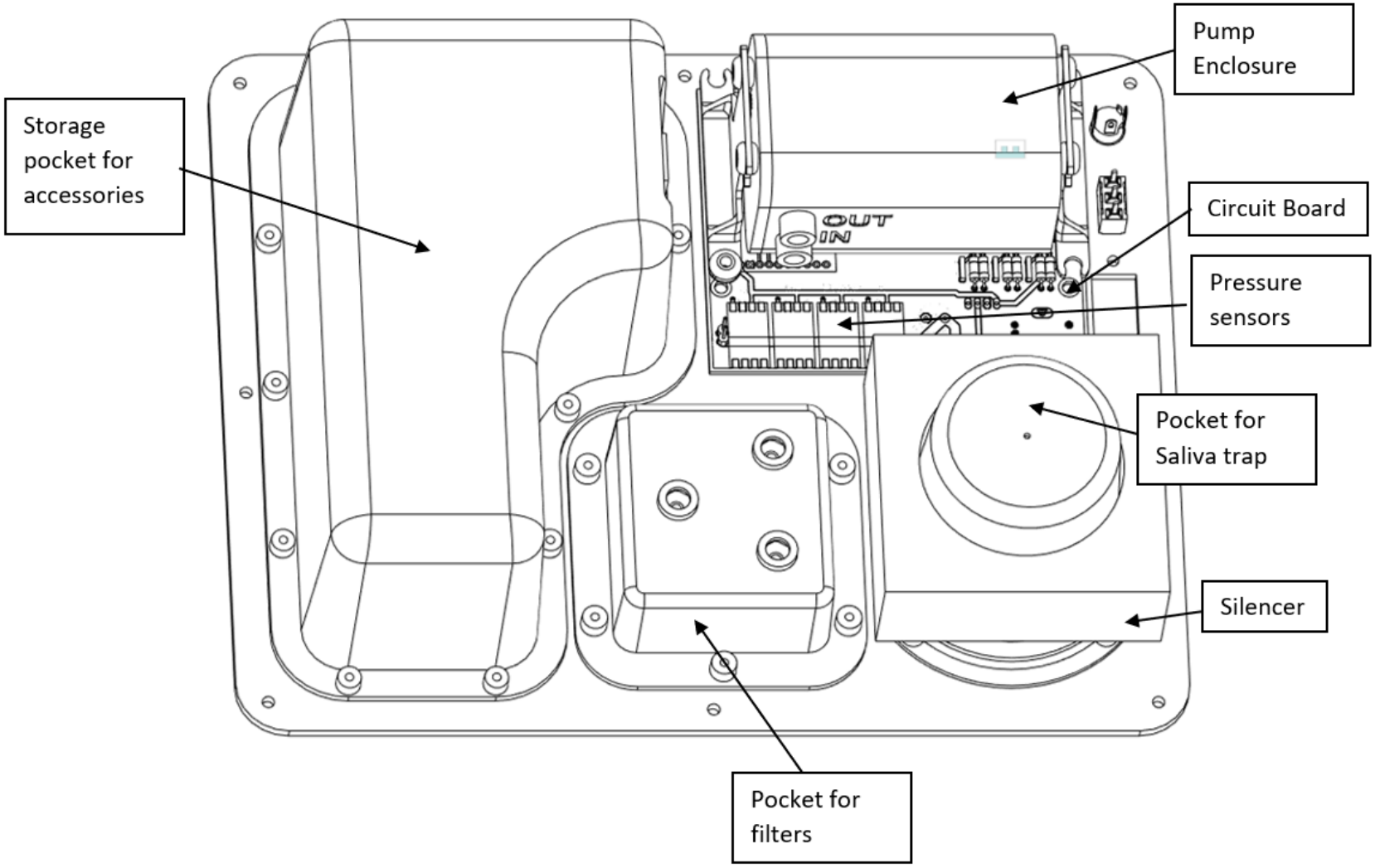

Figure B-1: bottom view of the pump unit with enclosure removed and plumbing omitted

B.1 Functionality & Software

B.1.1 Pressure Control

Pump unit senses and maintains the pressure in the perforated layer of oral device at the set point through feedback control during treatment. The set point is usually determined and set by clinician. The pump unit has capability of allowing or preventing the set point to be adjusted by patient during treatment.

As shown in Figure 2-7, air and saliva are drawn out of the oral device, through the saliva trap and two filters that entraps any saliva and contaminants, by a vacuum pump, then exhausted through a silencer.

Pressure is measured at three points in the system by pressure sensors labeled 'PT' in Figure 2-7. Two pressure differentials are derived from the three pressures. These 5 quantities are fundamental to the control of the pump unit and is tabulated in Table B-1.

The pressure in the perforated layer of oral device, $\mathrm{P_o}$, is maintained by modulating the pumping frequency of the vacuum pump by a PID controller implemented in the software.

The pump unit is capable of detecting whether the patient's tongue is latched or unlatched from the oral device by thresholding $\mathrm{P_o}$ and rate of change of $\mathrm{P_o}$. As the device is latched to patient's tongue, $\mathrm{P_o}$ will rapidly drop to below atmospheric pressure if the vacuum pump is running. Thus, the pump unit is capable of slowing down the pumping frequency to avoid excessive saliva extraction when patient's tongue is not latched onto the oral device, and increase the pumping frequency when the attempt to latch is detected by a rapid drop in $\mathrm{P_o}$ in order to rapidly latch the tongue.

The flow rate through the vacuum pump, $\mathrm{Q_p}$, can be estimated from the pressure at the pump inlet, $\mathrm{P_p}$, and the current pumping frequency. The relationship between $\mathrm{P_p}$, pumping frequency and the flow rate is provided by manufacturer as performance curves. Such curve is translated to a look-up table and embedded into the software to calculate the estimated flow rate on the fly. This flow-rate can be examined to determine whether a leak exists in the system.

The flow rate through the tubing from oral device to pump unit, $\mathrm{Q_t}$, can be estimated from the pressure drop in this tubing, $\mathrm{P_{ot}}$. Fluid equations such as the Darcy–Weisbach equation indicates the pressure drop in tubing is proportional to the volumetric flow rate. Thus, $\mathrm{Q_t}$ can be estimated on the fly by multiplying $\mathrm{P_{ot}}$ by a constant determined by calibrating against a known flow rate. At low-flow condition, $\mathrm{Q_t}$ is less accurate than $\mathrm{Q_p}$ due to sensor resolution. The comparison between $\mathrm{Q_t}$ and $\mathrm{Q_p}$ can be used to determine the location of leakage.

The pump unit is capable of detecting if the tubing from oral device to pump unit, is blocked or crushed. As $\mathrm{Q_t}$ is calculated from the pressure drop within the tubing, a blockage would result in an abnormally high indicated $\mathrm{Q_t}$ exceeding the flow rate through the vacuum $\mathrm{Q_p}$, which is impossible. In this scenario, the pump unit will display an error message.

The pump unit is capable of detecting whether the saliva trap is full by thresholding the pressure-drop from the tubing and filters between the saliva trap and vacuum pump, $\mathrm{P_{tp}}$. When the saliva trap is full, the saliva will saturate the '5u filter' shown in Figure 5. As the filters are hydrophobic, the saturated filter will create a considerable pressure drop. In this scenario, the pump unit will display an error message and shut down the pump until power cycled.

B.1.2 User Interface

As shown in Figure 2-7, the pump unit provides a user interface consists of a lcd screen and a control knob. Through the user interface, parameters such as the set point can be modified during treatment, and the status of the pump unit can be displayed in real time. Please refer to the attached user manual for details of interacting with the UI.

B.1.3 Configuration, Calibration and Datalogging

The pump unit has extensive data logging capabilities and configurability by having a SD card in the data card slot shown in Figure 2-7. The card has the patient-specific pump unit configuration written to it at clinic. During treatment, the pressures, system status and treatment events are is written to the SD card. Configurations loaded are tabulated in Table B-2. Data entries logged are tabulated in Table B-3.

Pressure sensors inside the pump unit are calibrated at manufacture. The calibration parameters are stored in EEPROM in the onboard microcontroller since they are pump-specific and need to be decoupled from SD card.

Field	**Description**
Patient ID	Character Array, Stores patient ID or name.
Default Set Point	The treatment pressure Set Point when pump powers up.
Maximum Set Point	The maximum allowed pressure settable through the user interface, corresponding to minimum suction.
Minimum Set Point	The minimum allowed pressure settable through the user interface, corresponding to maximum suction.
kP	Parameter for the PID controller.
kI	
kD	
Note	Character Array. This field will be carried over to every data file created.

Table B-2: Content of the configuration file.

Field	Frequency	Description
SN	once	Serial number of the pump unit.
Config	once	A copy of the configuration file (Table 2)
Sensor cal	once	A copy of the sensor calibration parameters from EEPROM
Count	20Hz	Count of data entries
Timestamp	20Hz	Unix timestamp of current data entry
Milliseconds	20Hz	Milliseconds since powered on
Millivolts	20Hz	Float array, raw millivolt reading from all pressure sensors
Pressures	20Hz	Float array, pressure from all sensors in millimeter mercury
newSetpoint	20Hz	This entry records how the patient rotates the setting knob in pressure adjustment mode with or without saving the pressure.
Setpoint	20Hz	Pressure setting that are saved and followed by PID controller.
lastTouched	20Hz	The most recent time the patient touched the setting knob. Unit is milliseconds since startup. This number is also used to control the backlight of screen. This number is updated whenever the knob is pushed or rotated, even if the patient is just rotating the knob to turn on the backlight to check on pressure.
Error	20Hz	The difference between the oral pressure and set point.
Error Accum	20Hz	The time integral of error, used by PID controller.
Effort Raw	20Hz	The output of the PID controller, without clamping, nor being affected by various software interlocks.
Vacuum Status	20Hz	Unsigned integer representing the system status. Available states are: Tongue not latched (please put on oral device) Pulling vacuum Tongue latched Vacuum over setpoint Tubing blocked
Saliva Trap Full	20Hz	Boolean. Set when saliva trap is full and cleared by power cycle. If this variable is set, the pump will not run.
Effort	20Hz	The final output to the vacuum pump

Table B-3: Content of each data file.

B.2 Hardware

The hardware components of the pump unit are called out in Figure 2-1 and Figure B-1. The following sub-sections describe each component in detail.

B.2.1 Saliva Trap

Saliva trap retains saliva collected while functions as a vacuum buffer. The saliva trap has 3 ports, namely ‘patient’, ‘sense’ and ‘suction’. One of the two tube from the oral device is connected to the ‘patient’ port in which the air/saliva mixture enters the bucket of the saliva trap. Saliva droplets are entrapped in the bucket by gravity. The top of the saliva trap is connected to the vacuum pump filter. A 5um hydrophobic filter is mounted inside the saliva trap immediately below the outlet. If liquid enters the filter for any reason, such as liquid level inside saliva trap rises above the filter inlet, or the unit is tipped over, the filter will be saturated and create a large pressure differential. As described in functionalities & software, such pressure differential will trigger a ‘saliva-trap full’ event, cause the pump to shut down and prevent any liquid damage. A photograph of assembled saliva trap is shown in Figure B-2.

Figure B-2: Assembled saliva trap

B.2.2 Vacuum Pump

The vacuum pump in the current version of pump unit is a diaphragm pump (Figure B-3, Xavitech Micropumps AB, Härnösand, Sweden) with free flow capacity of 1.5l/min and ultimate vacuum of -350 mbar, which offers some degree of redundancy in case of any leakage. The vacuum pump, along with an exhaust muffler, is placed inside a soundproof enclosure as shown in Figure B-1 and B-5. The pumping frequency of vacuum pump is controlled by a PI controller implemented in software.

Figure B-3: Xavitech VP1500 micropump [56]

B.2.3 Filtration

As shown in Figure 2-1 and 2-7, the patient-facing components are isolated from the rest of the pump unit by three 0.45um filters (Qosina P/N 28211, Qosina Corp., Ronkonkoma, NY) – commonly used to sterilize bio-fluids. The filter used here are hydrophobic thus prevents any droplet from entering the pressure sensors, the vacuum pump, or being vented to atmosphere. Saliva aerosolization is eliminated. When the pump unit is returned from a patient, all contaminated components are discarded and replaced with new ones to eliminate cross contamination.

B.2.4 Exhaust Muffler & Soundproofing

The exhaust muffler attenuates noise emitting from the exhaust of the vacuum pump similar to a car muffler. The exhaust from vacuum pump passes through an acoustic muffler. The acoustic muffler has a number of cascaded expansion chambers with characteristic length ranges from 1 to 1.5 inch. Air flows from one expansion chamber into the next one through expansion holes with much smaller area than the cross-section of the expansion chamber, resulting in attenuation of pressure waves hence noise. The current design shown in Figure B-4 provides at least 40db of sound attenuation.

Likewise, the soundproofing enclosures and suspensions attenuate the noise transmits through the vacuum pump casing in a manner similar to a car's engine bay insulation. As shown in Figure B-5, the vacuum pump is suspended in a hermetically sealed chamber using custom made elastomer suspensions, while having its inlet and exhaust port routed outside. The sealed chamber is then suspended in the outer enclosure by another set of suspension with compliant direction aligned with the stroke direction of the diaphragm pump. This two-stage suspension arrangement takes advantage of the different rigidity of each stage hence provide acceptable isolation of both high and low frequency noise.

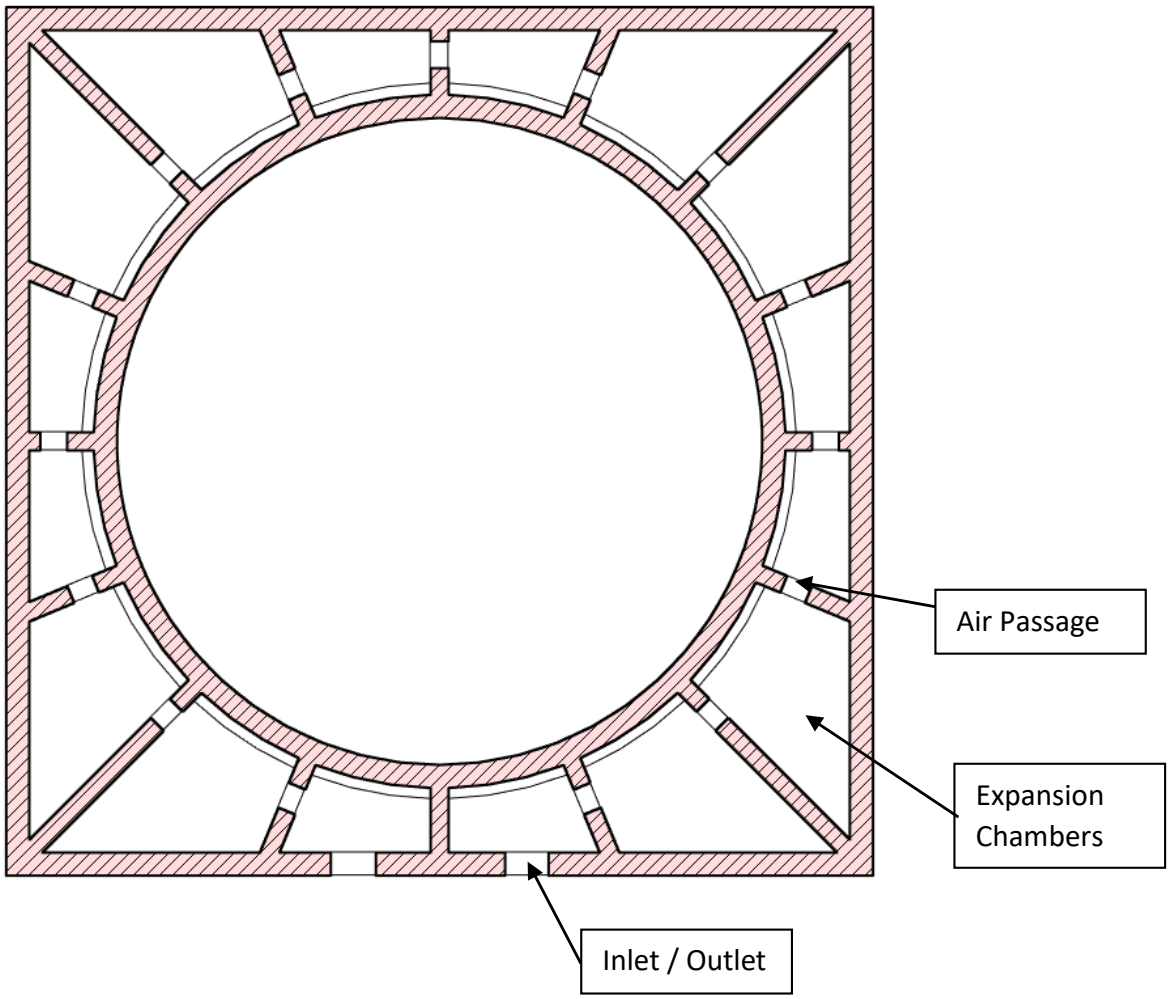

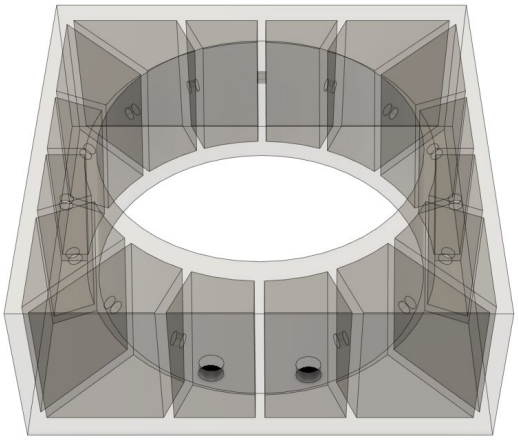

Figure B-4: Top: Cross-sectional view of the silencer. Bottom: semi-transparent perspective view to show internal chambers

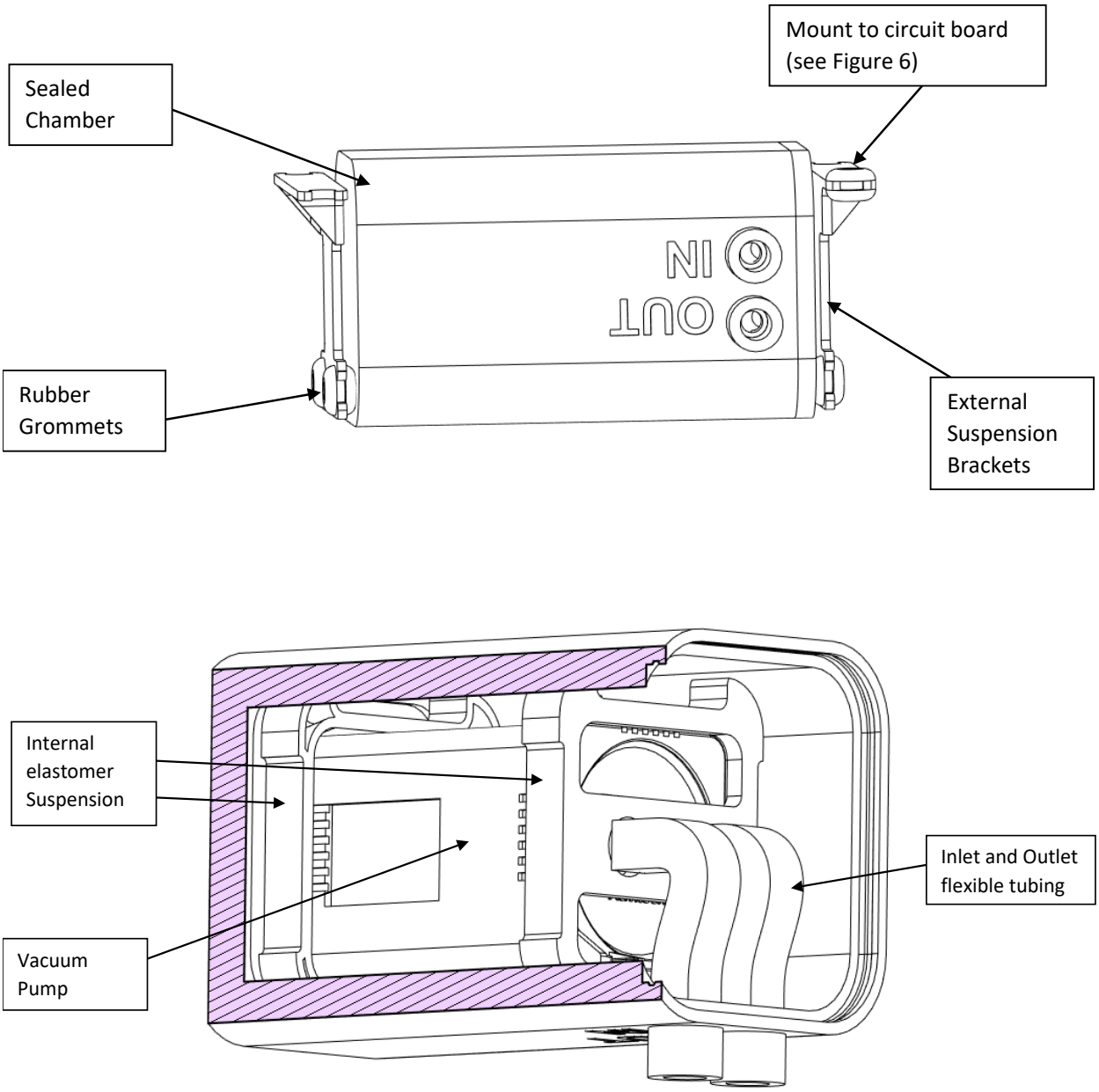

Figure B-5: External and cut-away view of the pump suspension.

B.2.5 Electronics

Electronics are mounted on a printed circuit board. The circuit board carries three of gauge pressure sensors that measures pressures described in Section 'Functionalities & Software'; an analog-digital converter to digitize pressure readouts; a microcontroller that hosts the software and commands the vacuum pump; a SD card reader that stores data; a liquid crystal display and an encoder knob that provides a user interface; a power conditioner; and their supporting passive components. The circuit diagram is shown in Figure B-6 through B-8. The board layout is shown in Figure B-9.

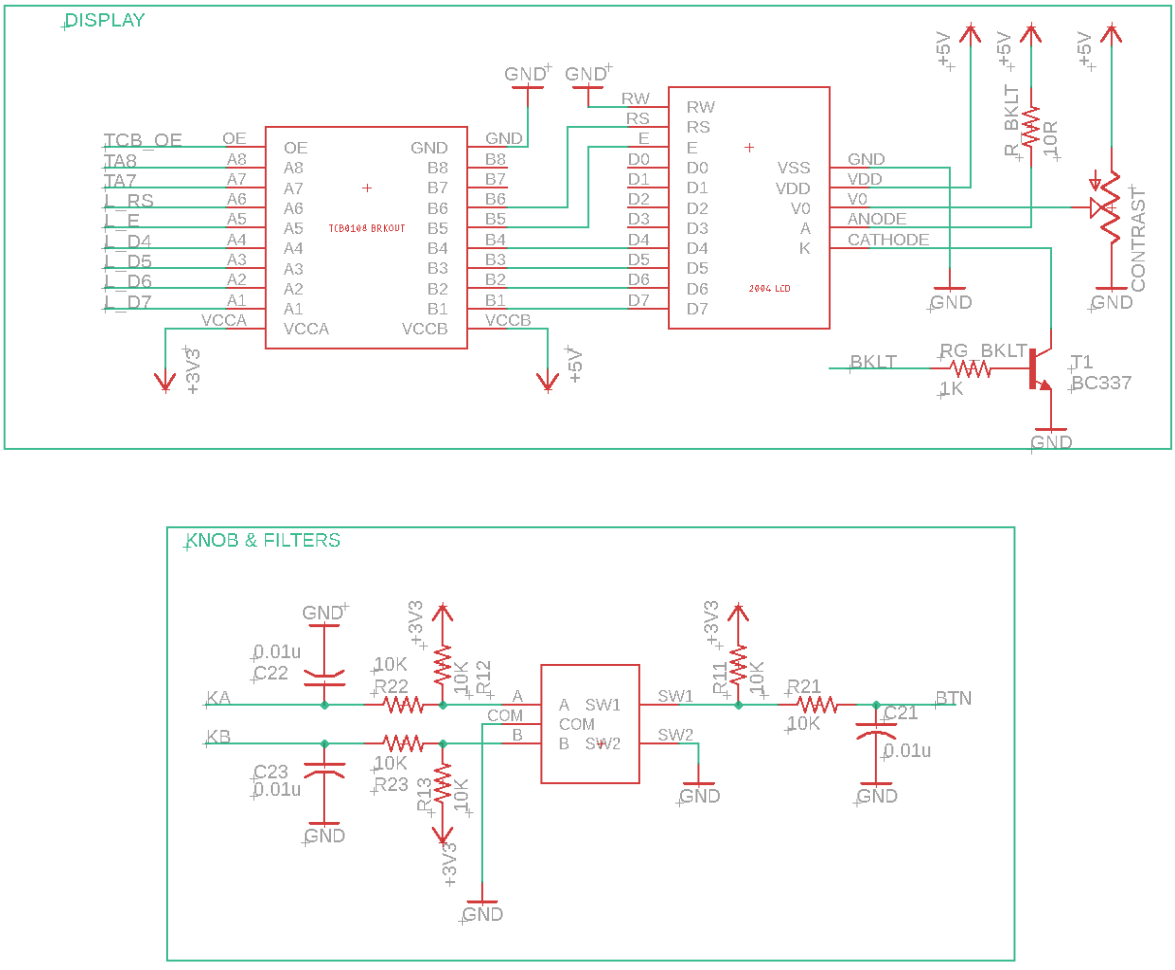

Figure B-6: Circuit diagram of user interface.

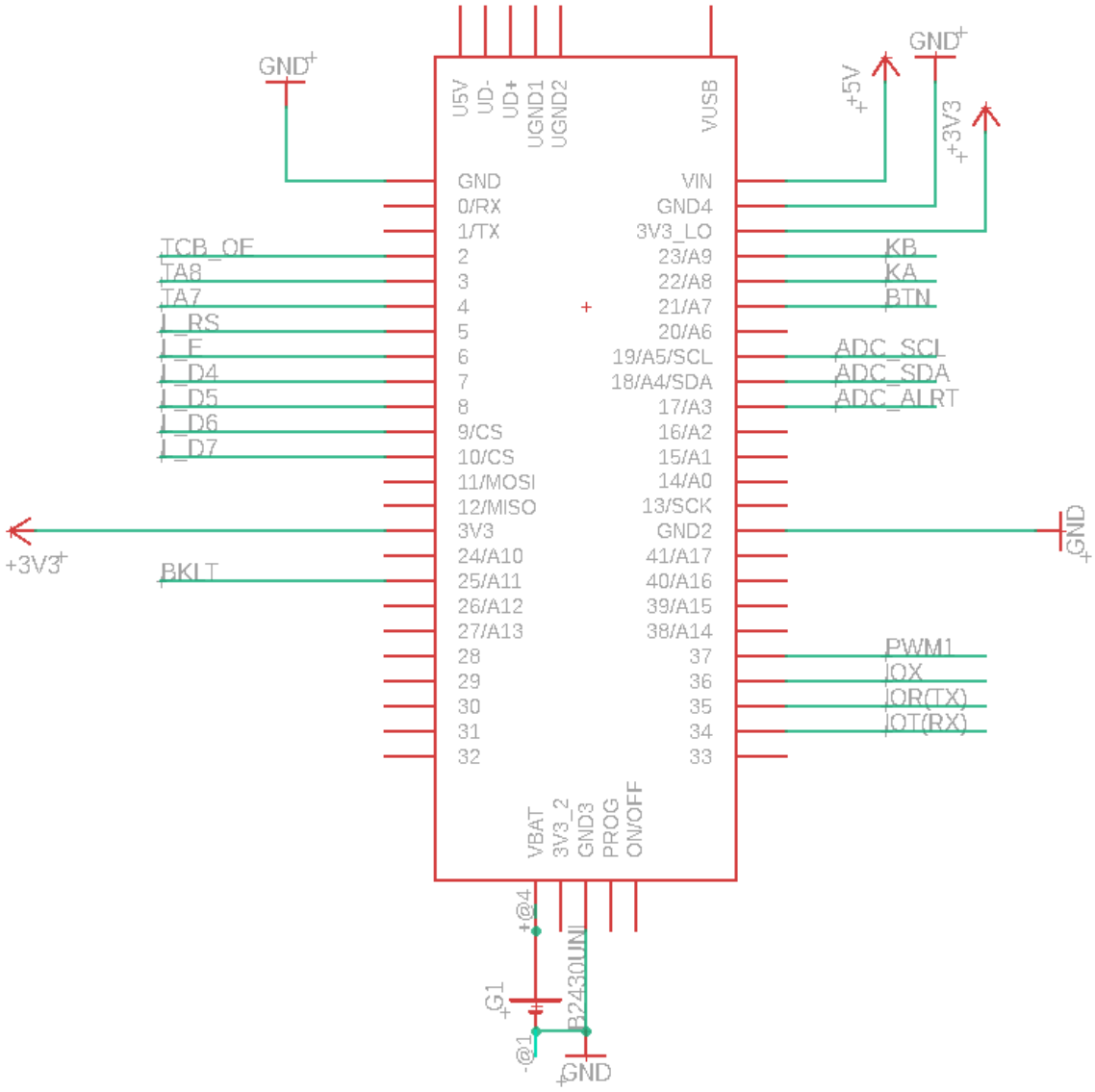

Figure B-7: Circuit diagram of the microcontroller fanout.

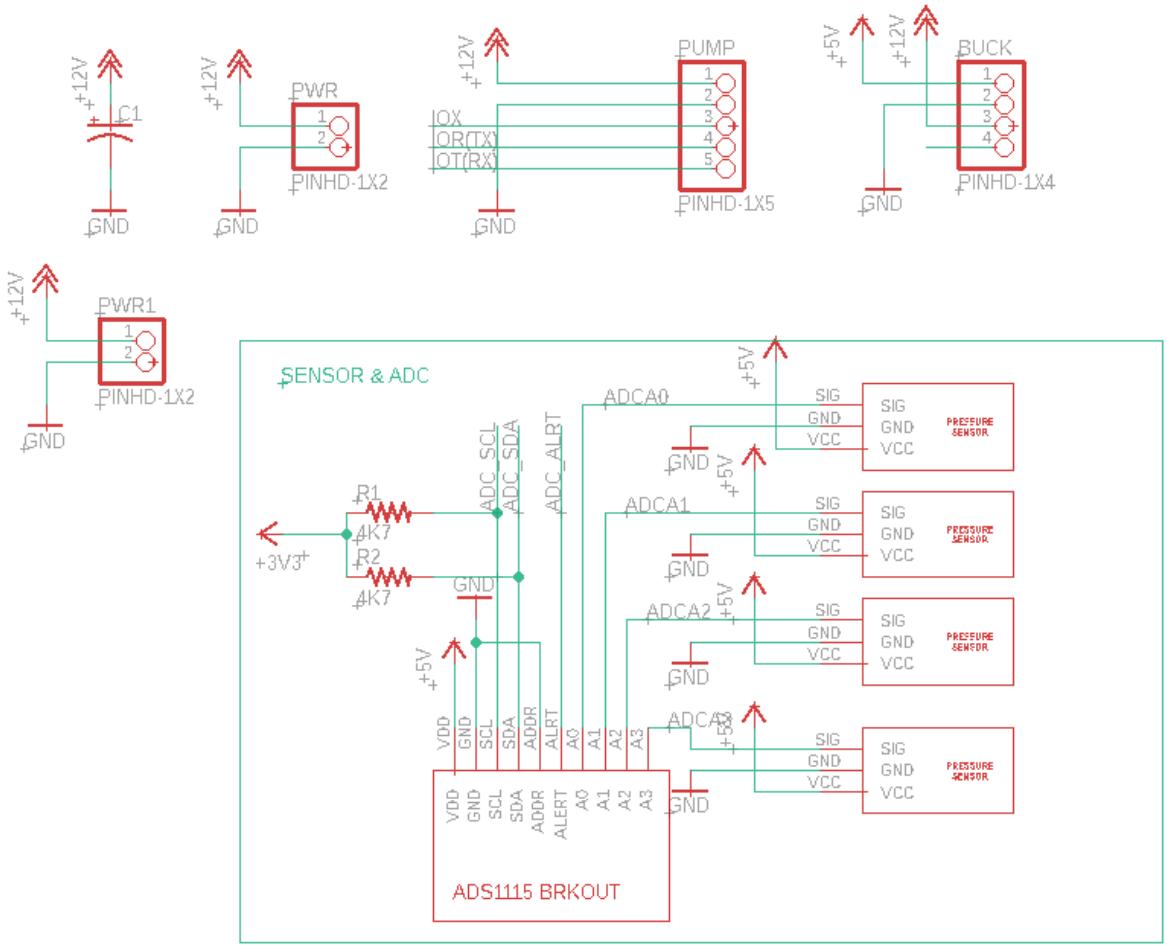

Figure B-8: Circuit diagram of sensors, analog-digital converter, supporting components and off board connectors to pump and power supply.

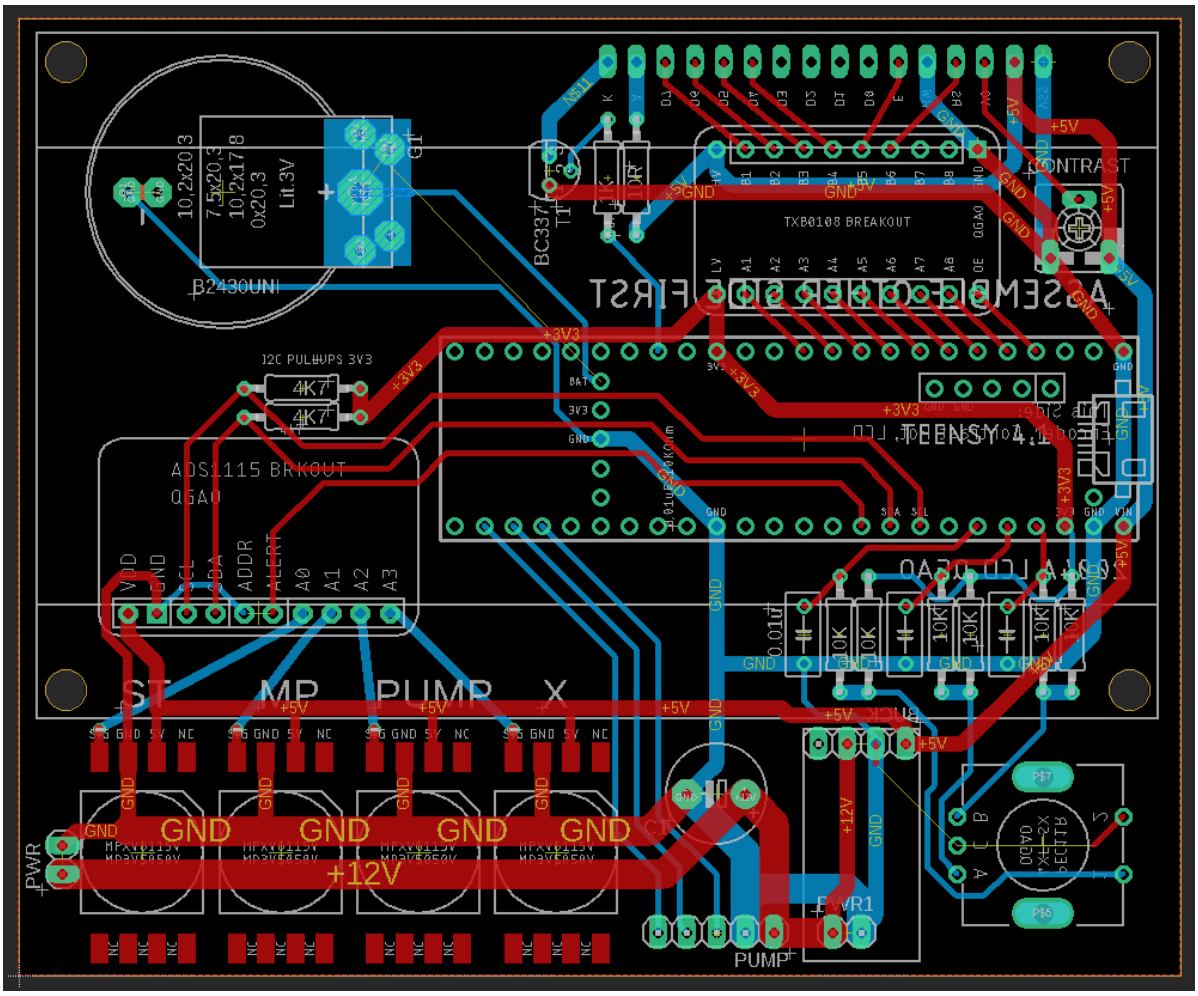

Figure B-9: Printed circuit board layout

Appendix C: Pump Unit User Manual

MIT Obstructive Sleep Apnea Study

Pump User Manual

Hardware V2.3, Firmware V2.3.2, 1 February 2023, Qiyun Gao & Nevan Hanumara
Study Contact OSA-study@mit.edu
Urgent 401-741-5929 (N. Hanumara), 312-730-3983 (E. Roche)

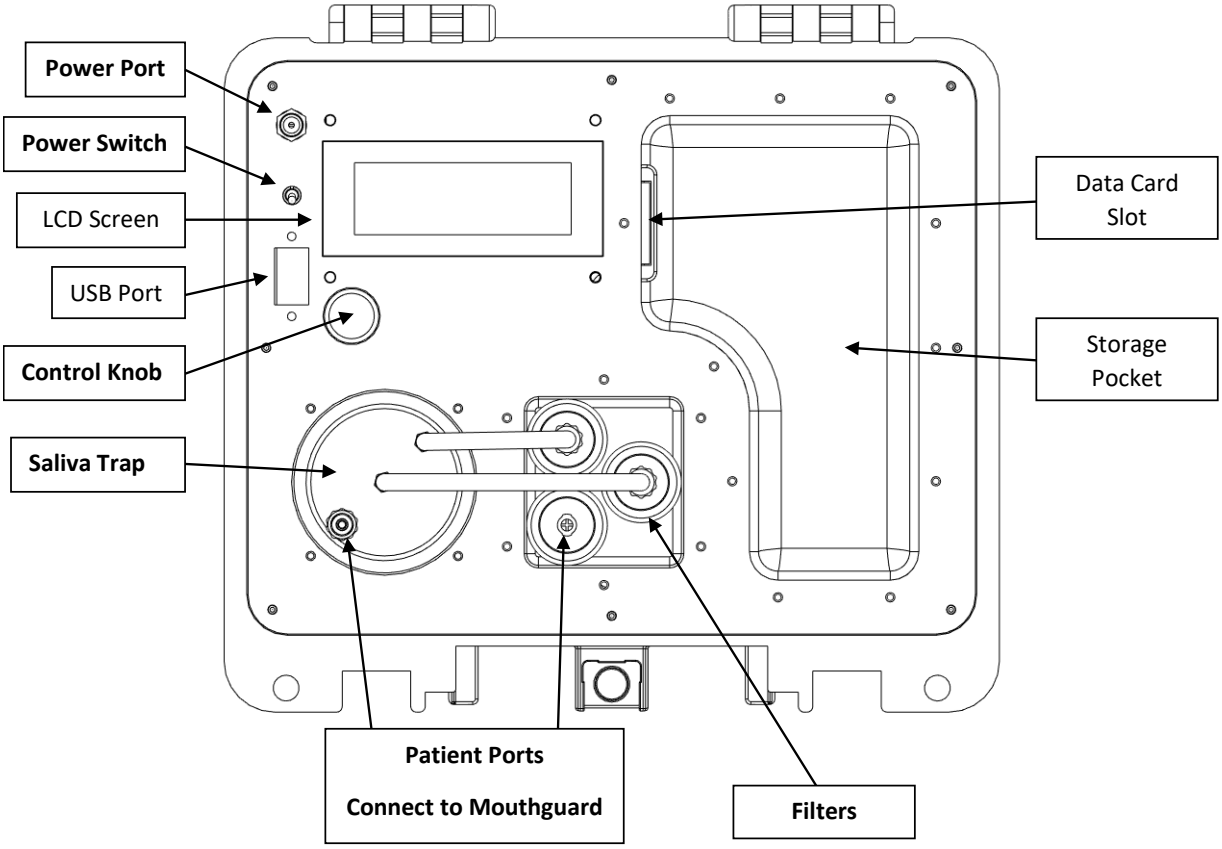

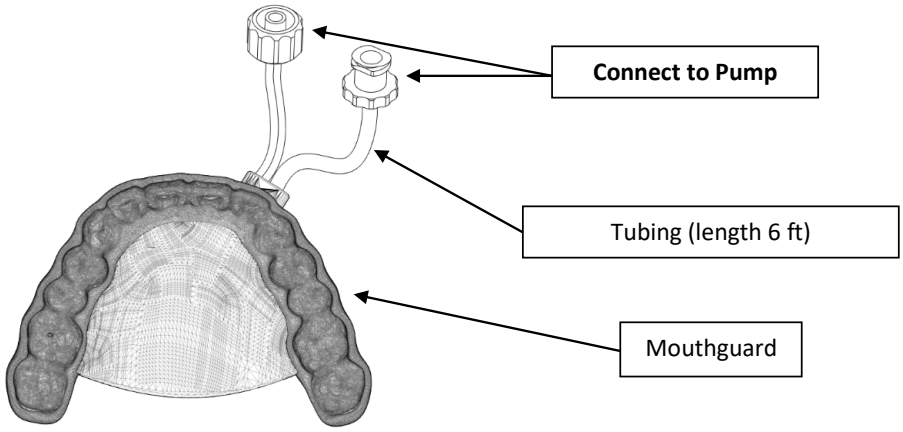

Components

- Pump Assembly, with pre-installed Saliva Trap, Filters and Data Card; Power Adaptor
- Mouthguard with Tubing and Connectors

Using the Pump

- Plug the power adaptor into the wall and connect the other end to the **Power Port**.
  Careful: When shutting the box, unplug the power cable first, to avoid pinching the wire!
- Twist the Luer Lock connectors of the mouthguard tubing into the **Patient Ports**. Hand tighten only.
- Flip the **Power Switch** upwards to the 'ON' position and wait for the self-test to complete.
  - Power-on self-testing lasts approximately 10 seconds.
  - Contact the study team if the screen displays any errors.
- Once the pump is ready, it will display 4 lines of information.
  - Line 1: '**Set Point**' – therapy pressure – user adjustable
  - Line 2: '**Oral**' – suction pressure in your mouth – display only
  - Line 3: Instructions / Status of the pump
  - Line 4: Alternates user ID # and system time

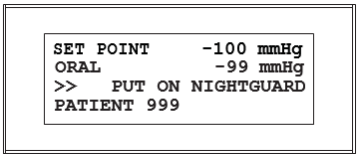

- In the case of another screen displaying, incorrect ID or system time, contact the study team.
- Put on your mouthguard and press your tongue against the suction mesh as trained during fitting. You should feel that your tongue is comfortably secured against the nightguard.
- The pump should display '**VACUUM OK'** on Line 3. You can go to sleep. Counting sheep is optional.
- If you need to get out of bed, you may take off the mouthguard or unscrew the tubes.
- If the Saliva Trap fills up, the pump will shut off and display "Saliva Trap Full." Clean the trap, see below, and turn the system off and on again.

Setting Pressure

- The baseline therapy pressure is pre-set by the research team, but this can be increased within safe limits, if you feel that your tongue is not adequately secured.
- Press the Control Knob once and the Set Point should start blinking.
- Twist the knob to increase the pressure and press the knob again to save the setting.
- If the pump is turned off and on again, the pressure will be reset to the pre-set pressure.

Daily Cleaning

- All part of system must be kept dry except the saliva trap and mouthguard.
- Mouthguard
  - Disconnect the mouthguard's two Luer Locks.
  - Refer to *Mouthguard Daily Homecare Instructions* for cleaning the mouthguard.
  - Rinse the tubing.
- Saliva Trap
  - Unscrew the Luer Lock connectors from the filters. **Do not unscrew the filters.**
  - Pull gently on the tubing and the trap will lift out.
  - Note down the date and amount of saliva, using the graduations on the container.
  - Unscrew the lid, empty and wash top and bottom of the trap with cold/warm tap water and mild detergent. **Do not use hot water.**
  - Screw the lid back on firmly to avoid leakage. Replace the saliva trap and reconnect tubing:
    As shown in the diagram, the **center** tube connects to the rightmost filter labeled with '**Suction.**'
    The **side** tube connects to the top filter labeled with '**Sense'** on the pump faceplate.
  - Ensure that the filters are also tight. Do not overtighten connectors.

References

[1] K. A. Franklin and E. Lindberg, "Obstructive sleep apnea is a common disorder in the population—a review on the epidemiology of sleep apnea," *J. Thorac. Dis.*, vol. 7, no. 8, pp. 1311–1322, Aug. 2015, doi: 10.3978/j.issn.2072-1439.2015.06.11.

[2] A. M. Osman, S. G. Carter, J. C. Carberry, and D. J. Eckert, "Obstructive sleep apnea: current perspectives," *Nat. Sci. Sleep*, vol. 10, pp. 21–34, 2018, doi: 10.2147/NSS.S124657.

[3] T. Ono, "Tongue and upper airway function in subjects with and without obstructive sleep apnea," *Jpn. Dent. Sci. Rev.*, vol. 48, no. 2, pp. 71–80, Aug. 2012, doi: 10.1016/j.jdsr.2011.12.003.

[4] R. Zozula and R. Rosen, "Compliance with continuous positive airway pressure therapy: assessing and improving treatment outcomes," *Curr. Opin. Pulm. Med.*, vol. 7, no. 6, pp. 391–398, Nov. 2001, doi: 10.1097/00063198-200111000-00005.

[5] G. E. de Vries *et al.*, "Long-Term Objective Adherence to Mandibular Advancement Device Therapy Versus Continuous Positive Airway Pressure in Patients With Moderate Obstructive Sleep Apnea," *J. Clin. Sleep Med. JCSM Off. Publ. Am. Acad. Sleep Med.*, vol. 15, no. 11, pp. 1655–1663, Nov. 2019, doi: 10.5664/jcsm.8034.

[6] D. S. Lazard *et al.*, "The Tongue-Retaining Device: Efficacy and Side Effects in Obstructive Sleep Apnea Syndrome," *J. Clin. Sleep Med. JCSM Off. Publ. Am. Acad. Sleep Med.*, vol. 5, no. 5, pp. 431–438, Oct. 2009.

[7] S. Mashaqi *et al.*, "The Hypoglossal Nerve Stimulation as a Novel Therapy for Treating Obstructive Sleep Apnea—A Literature Review," *Int. J. Environ. Res. Public. Health*, vol. 18, no. 4, p. 1642, Feb. 2021, doi: 10.3390/ijerph18041642.

[8] V. Hoffstein, "Review of oral appliances for treatment of sleep-disordered breathing," *Sleep Breath. Schlaf Atm.*, vol. 11, no. 1, pp. 1–22, Mar. 2007, doi: 10.1007/s11325-006-0084-8.

[9] R. B. Berry *et al.*, "Rules for Scoring Respiratory Events in Sleep: Update of the 2007 AASM Manual for the Scoring of Sleep and Associated Events," *J. Clin. Sleep Med. JCSM Off. Publ. Am. Acad. Sleep Med.*, vol. 8, no. 5, pp. 597–619, Oct. 2012, doi: 10.5664/jcsm.2172.

[10] D. E. Jonas *et al.*, "Table 1, Definitions," Jan. 2017. https://www.ncbi.nlm.nih.gov/books/NBK424162/table/ch1.t1/ (accessed May 11, 2023).

[11] "Clinical Guideline for the Evaluation, Management and Long-term Care of Obstructive Sleep Apnea in Adults," *J. Clin. Sleep Med. JCSM Off. Publ. Am. Acad. Sleep Med.*, vol. 5, no. 3, pp. 263–276, Jun. 2009.

[12] A. S. BaHammam, E. ALAnbay, N. Alrajhi, and A. H. Olaish, "The success rate of split-night polysomnography and its impact on continuous positive airway pressure compliance," *Ann. Thorac. Med.*, vol. 10, no. 4, pp. 274–278, 2015, doi: 10.4103/1817-1737.160359.

[13] S. R. Staff, "Is Type-IV Home Testing Enough?," *Sleep Review*, Mar. 09, 2008. https://sleepreviewmag.com/sleep-diagnostics/in-lab-tests/polysomnography/is-type-iv-home-testing-enough/ (accessed May 11, 2023).

[14] M. Goyal and J. Johnson, "Obstructive Sleep Apnea Diagnosis and Management," *Mo. Med.*, vol. 114, no. 2, pp. 120–124, 2017.

[15] “In-home evaluation of efficacy and titration of a mandibular advancement device for obstructive sleep apnea - PMC.” https://www.ncbi.nlm.nih.gov/pmc/articles/PMC2270921/ (accessed May 11, 2023).
[16] E. Tedeschi *et al.*, “Home unattended portable monitoring and automatic CPAP titration in patients with high risk for moderate to severe obstructive sleep apnea,” *Respir. Care*, vol. 58, no. 7, pp. 1178–1183, Jul. 2013, doi: 10.4187/respcare.01939.
[17] N. M. Punjabi, R. N. Aurora, and S. P. Patil, “Home Sleep Testing for Obstructive Sleep Apnea,” *Chest*, vol. 143, no. 2, pp. 291–294, Feb. 2013, doi: 10.1378/chest.12-2699.
[18] R. B. Berry *et al.*, “0463 Validation of a Home Sleep Apnea Testing Device for the Diagnosis of Sleep Disordered Breathing based on AASM 2012 guidelines,” *Sleep*, vol. 42, no. Supplement_1, p. A186, Apr. 2019, doi: 10.1093/sleep/zsz067.462.
[19] “CPAP Machine: What It Is, How It Works, Pros & Cons,” *Cleveland Clinic*. https://my.clevelandclinic.org/health/treatments/22043-cpap-machine (accessed May 11, 2023).
[20] A. L. Rocha, L. E. Wagner, and D. N. Paiva, “Effects of the mandibular advancement device on daytime sleepiness, quality of life and polysomnographic profile of public transport drivers with obstructive sleep apnea syndrome,” *Sleep Sci.*, vol. 14, no. 2, pp. 136–141, 2021, doi: 10.5935/1984-0063.20200058.
[21] P. H. Van de Heyning *et al.*, “Implanted upper airway stimulation device for obstructive sleep apnea,” *The Laryngoscope*, vol. 122, no. 7, pp. 1626–1633, Jul. 2012, doi: 10.1002/lary.23301.
[22] M. Friedman *et al.*, “Targeted hypoglossal nerve stimulation for the treatment of obstructive sleep apnea: Six-month results,” *The Laryngoscope*, vol. 126, no. 11, pp. 2618–2623, Nov. 2016, doi: 10.1002/lary.25909.
[23] P. M. Baptista, A. Costantino, A. Moffa, V. Rinaldi, and M. Casale, “Hypoglossal Nerve Stimulation in the Treatment of Obstructive Sleep Apnea: Patient Selection and New Perspectives,” *Nat. Sci. Sleep*, vol. 12, pp. 151–159, Feb. 2020, doi: 10.2147/NSS.S221542.
[24] T. E. Weaver *et al.*, “Innovative treatments for adults with obstructive sleep apnea,” *Nat. Sci. Sleep*, vol. 6, pp. 137–147, Nov. 2014, doi: 10.2147/NSS.S46818.
[25] “510(k) Premarket Notification.” https://www.accessdata.fda.gov/scripts/cdrh/cfdocs/cfpmn/pmn.cfm?ID=K193460 (accessed May 11, 2023).
[26] G. Nigam, C. Pathak, and M. Riaz, “Effectiveness of oral pressure therapy in obstructive sleep apnea: a systematic analysis,” *Sleep Breath.*, vol. 20, no. 2, pp. 663–671, May 2016, doi: 10.1007/s11325-015-1270-3.
[27] Y.-H. Kuo *et al.*, “Novel Intraoral Negative Airway Pressure in Drug-Induced Sleep Endoscopy with Target-Controlled Infusion,” *Nat. Sci. Sleep*, vol. 13, pp. 2087–2099, Nov. 2021, doi: 10.2147/NSS.S327770.
[28] R. D. Howell, S. Hadley, E. Strauss, and F. R. Pelham, “Blister formation with negative pressure dressings after total knee arthroplasty,” *Curr. Orthop. Pract.*, vol. 22, no. 2, p. 176, Apr. 2011, doi: 10.1097/BCO.0b013e31820b3e21.
[29] “Sleep Apnea - Causes and Risk Factors | NHLBI, NIH,” Mar. 24, 2022. https://www.nhlbi.nih.gov/health/sleep-apnea/causes (accessed May 12, 2023).

[30] Y. Ma, M. Yu, and X. Gao, “The effect of gradually increased mandibular advancement on the efficacy of an oral appliance in the treatment of obstructive sleep apnea,” *J. Clin. Sleep Med. JCSM Off. Publ. Am. Acad. Sleep Med.*, vol. 16, no. 8, pp. 1369–1376, Aug. 2020, doi: 10.5664/jcsm.8556.
[31] Y. Tanaka, J. M. Adame, A. Kaplan, and F. R. Almeida, “The Simultaneous Use of Positive Airway Pressure and Oral Appliance Therapy With and Without Connector: A Preliminary Study,” *J. Dent. Sleep Med.*, vol. 9, no. 1, Jan. 2022, doi: 10.15331/jdsm.7226.
[32] R. Bhattacharjee *et al.*, “The accuracy of a portable sleep monitor to diagnose obstructive sleep apnea in adolescent patients,” *J. Clin. Sleep Med. JCSM Off. Publ. Am. Acad. Sleep Med.*, vol. 17, no. 7, pp. 1379–1387, Jul. 2021, doi: 10.5664/jcsm.9202.
[33] H. Subramanian *et al.*, “Screening for obstructive sleep apnoea in post-treatment cancer patients,” *Cancer Rep.*, vol. 6, no. 3, p. e1740, 2023, doi: 10.1002/cnr2.1740.
[34] “RESMED APNEALINK AIR CLINICAL MANUAL Pdf Download,” *ManualsLib*. https://www.manualslib.com/manual/1990017/Resmed-Apnealink-Air.html (accessed May 11, 2023).
[35] P. A. Yushkevich *et al.*, “User-guided 3D active contour segmentation of anatomical structures: significantly improved efficiency and reliability,” *NeuroImage*, vol. 31, no. 3, pp. 1116–1128, Jul. 2006, doi: 10.1016/j.neuroimage.2006.01.015.
[36] R. Wilhelms-Tricarico, “Physiological modeling of speech production: Methods for modeling soft-tissue articulators,” *J. Acoust. Soc. Am.*, vol. 97, no. 5, pp. 3085–3098, May 1995, doi: 10.1121/1.411871.
[37] K. D. R. Kappert *et al.*, “Personalized biomechanical tongue models based on diffusion-weighted MRI and validated using optical tracking of range of motion,” *Biomech. Model. Mechanobiol.*, vol. 20, no. 3, pp. 1101–1113, 2021, doi: 10.1007/s10237-021-01435-7.
[38] R. J. Gilbert, L. H. Magnusson, V. J. Napadow, T. Benner, R. Wang, and V. J. Wedeen, “Mapping Complex Myoarchitecture in the Bovine Tongue with Diffusion-Spectrum Magnetic Resonance Imaging,” *Biophys. J.*, vol. 91, no. 3, pp. 1014–1022, Aug. 2006, doi: 10.1529/biophysj.105.068015.
[39] S. M. Mijailovich, B. Stojanovic, M. Kojic, A. Liang, V. J. Wedeen, and R. J. Gilbert, “Derivation of a finite-element model of lingual deformation during swallowing from the mechanics of mesoscale myofiber tracts obtained by MRI,” *J. Appl. Physiol. Bethesda Md 1985*, vol. 109, no. 5, pp. 1500–1514, Nov. 2010, doi: 10.1152/japplphysiol.00493.2010.
[40] O. Engwall, “A 3d tongue model based on MRI data,” in *6th International Conference on Spoken Language Processing (ICSLP 2000)*, ISCA, Oct. 2000, vols. vols. 3, 901-904–0. doi: 10.21437/ICSLP.2000-679.
[41] H. Luo, A. Scholp, and J. J. Jiang, “The Finite Element Simulation of the Upper Airway of Patients with Moderate and Severe Obstructive Sleep Apnea Hypopnea Syndrome,” *BioMed Res. Int.*, vol. 2017, p. 7058519, 2017, doi: 10.1155/2017/7058519.
[42] Y. Kajee, “The biomechanics of the human tongue,” Master Thesis, University of Cape Town, 2010. Accessed: May 12, 2023. [Online]. Available: https://open.uct.ac.za/handle/11427/5525
[43] M. Henrik Strand Moxness, F. Wülker, B. Helge Skallerud, and S. Nordgård, “Simulation of the upper airways in patients with obstructive sleep apnea and nasal obstruction: A novel

finite element method," *Laryngoscope Investig. Otolaryngol.*, vol. 3, no. 2, pp. 82–93, Feb. 2018, doi: 10.1002/lio2.140.
[44] M. Caragiuli *et al.*, "A finite element analysis for evaluating mandibular advancement devices," *J. Biomech.*, vol. 119, p. 110298, Apr. 2021, doi: 10.1016/j.jbiomech.2021.110298.
[45] G. Bruno *et al.*, "Comparison of the Effects Caused by Three Different Mandibular Advancement Devices on the Periodontal Ligaments and Teeth for the Treatment of Osa: A Finite Element Model Study," *Appl. Sci.*, vol. 10, no. 19, Art. no. 19, Jan. 2020, doi: 10.3390/app10196932.
[46] Jorgen, "Holzapfel-Gasser-Ogden Model," *PolymerFEM.com*, Jan. 24, 2021. https://polymerfem.com/holzapfel-gasser-ogden-model/ (accessed May 14, 2023).
[47] G. A. Holzapfel, T. C. Gasser, and R. W. Ogden, "A New Constitutive Framework for Arterial Wall Mechanics and a Comparative Study of Material Models," *J. Elast. Phys. Sci. Solids*, vol. 61, no. 1, pp. 1–48, Jul. 2000, doi: 10.1023/A:1010835316564.
[48] J.-S. Affagard, S. F. Bensamoun, and P. Feissel, "Development of an inverse approach for the characterization of in vivo mechanical properties of the lower limb muscles," *J. Biomech. Eng.*, vol. 136, no. 11, Nov. 2014, doi: 10.1115/1.4028490.
[49] A. J. Maree, "The Inverse Finite Element Method: Sensitivity to Measurement Setup," Thesis, Stellenbosch : University of Stellenbosch, 2005. Accessed: May 13, 2023. [Online]. Available: https://scholar.sun.ac.za:443/handle/10019.1/2640
[50] K. Volner, S. Chao, and M. Camacho, "Dynamic sleep MRI in obstructive sleep apnea: a systematic review and meta-analysis," *Eur. Arch. Otorhinolaryngol.*, vol. 279, no. 2, pp. 595–607, Feb. 2022, doi: 10.1007/s00405-021-06942-y.
[51] "TrackVis :: Diffusion Toolkit." https://trackvis.org/dtk/ (accessed May 12, 2023).
[52] "(PDF) Tractography and Neurosurgical Targeting in Deep Brain Stimulation for Parkinson's Disease." https://www.researchgate.net/publication/319059671_Tractography_and_Neurosurgical_Targeting_in_Deep_Brain_Stimulation_for_Parkinson's_Disease (accessed May 12, 2023).
[53] "Respiratory Pressures Sravani Pragna. K 1, Kalyan Chakravarthi. C." https://fayllar.org/respiratory-pressures-sravani-pragna-k-1-kalyan-chakravarthi-c.html (accessed May 12, 2023).
[54] T. T. Dao and M.-C. H. B. Tho, "A Systematic Review of Continuum Modeling of Skeletal Muscles: Current Trends, Limitations, and Recommendations," *Appl. Bionics Biomech.*, vol. 2018, p. 7631818, Dec. 2018, doi: 10.1155/2018/7631818.
[55] "3Shape TRIOS 3 – Proven intraoral scanner technology," *3Shape*. https://www.3shape.com/en/scanners/trios-3 (accessed May 14, 2023).
[56] "Micro pumps from Xavitech with calibrated flow and long lifetime," *Xavitech - Intelligent pumps*. https://www.xavitech.com/micropumps/ (accessed May 14, 2023).